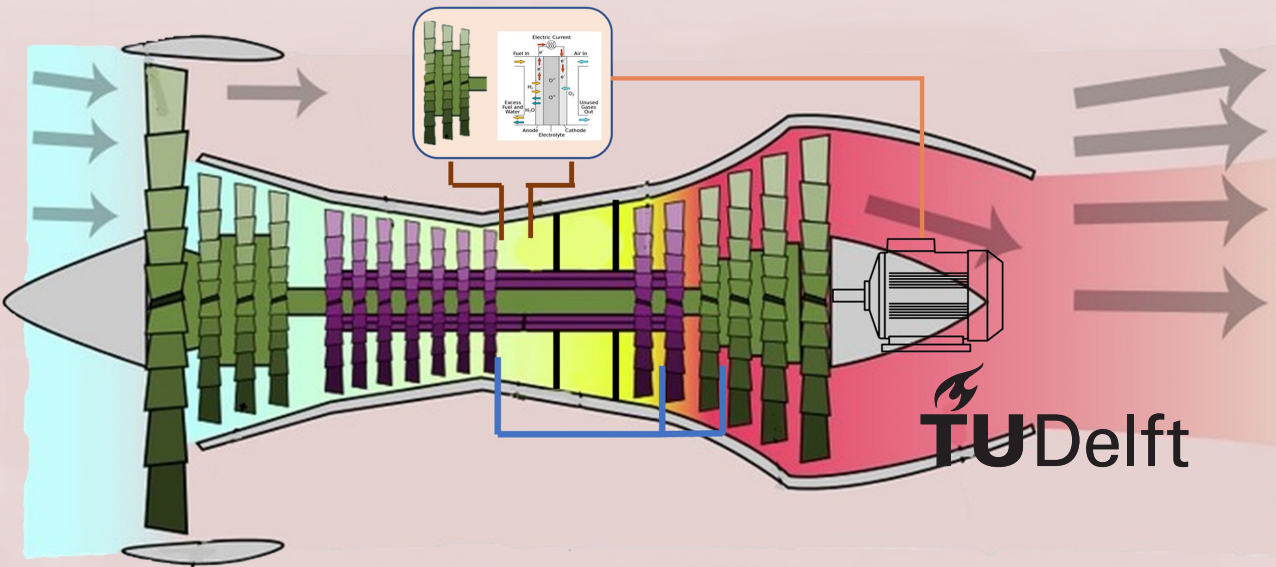


# Techno-Economic feasibility analysis of Solid-Oxide Fuel Cell-Gas Turbine based hybrid propulsion system fueled by Hydrogen

HOW A SOLID-OXIDE FUEL CELL CAN IMPACT THE PERFORMANCE OF THE PROPULSION SYSTEM AND THE ECONOMICS OF THE AIRCRAFT

NAMAN SACHDEVA





# Techno-Economic feasibility analysis of Solid-Oxide Fuel Cell-Gas Turbine based hybrid propulsion system fueled by Hydrogen

by

Naman Sachdeva

in partial fulfilment of the requirements for the degree of

## Master of Science in Aerospace Engineering

at the **Delft University of Technology**, to be defended publicly on  
Thursday, May 19, 2022 at 14:00

Student Number: 5052297

Supervisors: Dr. Victor Scholten, Dr. Carlo De Servi & Mr. Carlos Mourao

### **Thesis Committee:**

Chair: Dr. Gianfranco La Rocca, TU Delft

Examiner: Dr. Fabrizio Oliviero, TU Delft

Examiner: Dr. Victor Scholten, TU Delft

Examiner: Dr. Carlo De Servi, TU Delft

Examiner: Mr. Carlos Mourao, Embraer

Place: Faculty of Aerospace Engineering, TU Delft

Project Duration: November, 2021 - May, 2022

This research project has been done with the support of Embraer. Embraer does not own the copyright of the contents of the report and the models developed for this research.



# DEDICATION

*"To each and every living being who has, does, or will ever exist and has never given up  
on their dreams,*

just like my grandparents and my parents who have done everything in their lives to  
give the best possible opportunities to their grandchildren and children.

Not sure if this is dedication, stubbornness, ego, or passion to just go for things when it  
does not matter if someone support you or not. But one thing that I am sure of is, that it  
does feel like freedom. To do what you want to do, is, True Freedom."



# ACKNOWLEDGEMENT

When I was thinking of working on this project for which I had little prior knowledge, my friends told me that I should consider a thesis that is in my domain of knowledge so that I can graduate early. However, I really wanted to work on this topic because I wanted to take on a challenge and one of the biggest reasons I was able to do it is because of my parents. They have always supported me in my decisions and gave me a privileged life which most of the people in my country have no access to and I feel highly lucky for that. I hope I will make them proud of all the sacrifices they have and will make for me.

Second, I would like to thank my academic mentors, Dr. Victor Scholten and Dr. Carlo De Servi for helping when I needed them the most. There have been many instances when I doubted myself but they have always believed in me which helped me to stand up every time I was faced with a challenge. Also, I would like to thank Prof. L. van Biert for helping me to understand fuel cells better and answering my curious questions. I would also like to thank my company mentors, Mr. Carlos Mourao, Mr. Raphael Felipe Gama Ribeiro, and Ms. Luciana Ribeiro Monteiro who have helped me by providing a more realistic perspective on the problem. I would also like to thank Dr. Keiichi OKAI who discussed his paper with me and told me about his experience on the project.

Last, I would like to thank my friends, without whom I would have never even been able to imagine myself at Delft. To all my friends-

Kiran, Gagandeep, Vasu, Parv, Aditya, Apoorv, Ascharya, Aryan, Yamini, Arihant, Ravi, Kaushal and Shreejit Bhैया; who has always been in my side when I was right and highly critical when I was wrong. They helped me to become a more unbiased version of myself who can, to some extent, improve by critically analyzing my own actions. In the end, it's all about the relationships you build and the people you find who push you to become the best version of yourself when you need it and help you to slow down when required.

A special thanks to Anand for thoroughly discussing about multiple technical topics and listening to all the good and bad ideas which I came across during this research and to my big brother, Ninad, who has always supported me in all the things which have gone wrong in my life and shared all the things when they went right.

Without even a single person helping me either academically or personally, I would have not been able to complete this report and move forward with my research thesis. I am happy that I found all of them and I am highly grateful to each and everyone for accepting me into who I am today and helping in change when needed.

*Naman Sachdeva  
Delft, May 2022*



# ABSTRACT

The world is moving towards sustainability and there is immense pressure on Aerospace Industry to reduce its emissions to contribute to a carbon-neutral world. However, maturing gas turbine technology is a big bottleneck towards this goal and hence, this project focuses on the technical and economic feasibility of a new type of propulsion system, called Solid-Oxide Fuel Cell- Gas Turbine or SOFC-GT hybrid propulsion system. SOFC-GT, even though being a low TRL technology, has the potential to reduce fuel consumption, emissions, and operation costs, making it a suitable candidate for a future propulsion system.

This research concludes that in order to achieve the full potential of the SOFC-GT hybrid, engine parameters like BPR, FPR and cooling air requirements need to be changed. The Thrust-Specific Fuel Consumption (TSFC) for the propulsion system has decreased by 6.03% and 19.89% for 1 MW and 4 MW fuel cell power output in Off-Design (Cruise) condition. Along with this, core mass flow rate or size, cooling air requirement and Turbine Inlet Temperature has decreased. The emission results show that the  $NO_x$  emissions have been reduced by 29.11% and 78.05% respectively. Sensitivity analysis shows that the thermodynamic efficiency is most sensitive to engine parameters but the impact of fuel cell parameters is increasing as the fuel cell power output is increased.

The economic analysis done in this study shows that the SOFC-GT hybrid is not feasible for the commercially available fuel cell because of the substantial increase in weight of the propulsion system. However, the propulsion system will become feasible at the fuel cell system specific power of 2.30 kW/kg and 2.10 kW/kg for no emission tax and highest emission tax scenario respectively at a fuel price of \$ 6/kg. Along with this, increasing the fuel cell power output leads to the increase in required specific power for fuel cell or has a negative impact on the overall economics. The overall economics of the aircraft is most sensitive to aircraft parameters but increasing the fuel cell power output decreases sensitivity substantially. In the end, the emission has a low impact on the overall economics of the aircraft.

This research shows that it is possible to integrate a SOFC with the turbofan if the fuel cell technology improves in the future. Along with this, the research provides multiple novel methodologies for technical and economic analysis of the SOFC-GT hybrid.



# CONTENTS

<b>List of Figures</b>	<b>13</b>
<b>List of Tables</b>	<b>17</b>
<b>1 Introduction</b>	<b>1</b>
1.1 Maturing Gas Turbine technology	2
1.2 Introduction of Zero-Carbon Fuels	3
1.3 Future Propulsion Concepts	3
1.3.1 Battery Powered Aircraft	3
1.3.2 Parallel-hybrid propulsion system	4
1.3.3 Turbo-electric propulsion system	4
1.3.4 Composite Materials	5
<b>2 Fuel cell</b>	<b>7</b>
2.1 Working Principle of fuel cell	11
2.2 Fuel cell Performance	13
2.2.1 Open Circuit Voltage ( $V_{oc}$ )	13
2.2.2 Activation Losses ( $V_{act}$ )	15
2.2.3 Ohmic Losses ( $V_{ohm}$ )	16
2.2.4 Concentration losses ( $V_{conc}$ )	17
2.2.5 Other losses	19
2.2.6 Fuel cell Efficiency	19
2.2.7 Effect of pressure and temperature on fuel cell	19
2.2.8 Effect of Fuel Utilization	23
2.3 Different Types of fuel cell	24
2.3.1 Low Temperature fuel cell(LTFC)	26
2.3.2 Proton Exchange Membrane fuel cell (PEM FC)	26
2.3.3 High Temperature Proton Exchange Membrane fuel cell (HTPEM FC)	28
2.3.4 High Temperature fuel cell(HTFC)	28
2.3.5 Solid Oxide fuel cell(SOFC)	28
2.3.6 Molten Carbonate fuel cell(MCFC)	30
2.3.7 Selection of fuel cell	30
<b>3 Solid Oxide Fuel Cell-Gas Turbine Concepts</b>	<b>35</b>
3.1 SOFC-GT Concepts for ground applications	35
3.1.1 Shortcomings of SOFC-GT systems for ground and stationary applications	39
3.2 SOFC-GT Concepts for Aerospace Applications	40

<b>4</b>	<b>Research Objectives, Questions &amp; Methodology</b>	<b>47</b>
4.1	Research Gaps . . . . .	48
4.2	Research Objectives & Questions . . . . .	49
4.3	Research Methodology . . . . .	50
<b>5</b>	<b>Fuel Cell Model</b>	<b>53</b>
5.1	Reference Model . . . . .	54
5.2	Solid Oxide Fuel Cell Model . . . . .	55
5.2.1	Verification of SOFC Model . . . . .	57
5.2.2	Sensitivity Analysis of SOFC Model. . . . .	60
5.3	Heat Exchanger . . . . .	62
5.4	Fuel Cell Model verification . . . . .	64
<b>6</b>	<b>Gas Turbine Model</b>	<b>67</b>
6.1	Gas Turbine Tool . . . . .	67
6.1.1	PyCycle . . . . .	68
6.2	Reference Turbofan Model- CFM-56-5B1 . . . . .	68
6.2.1	Turbine Cooling . . . . .	72
6.3	Validation of the Reference Engine Model. . . . .	72
<b>7</b>	<b>Solid Oxide Fuel Cell - Gas Turbine Hybrid</b>	<b>75</b>
7.1	SOFC-GT Hybrid Architecture . . . . .	75
7.2	Verification of SOFC-GT Hybrid Propulsion System. . . . .	79
7.3	Temperature-Entropy (T-s) Diagram . . . . .	80
<b>8</b>	<b>Technical Analysis Results</b>	<b>83</b>
8.1	No Constant Specific Thrust and No Optimum point analysis. . . . .	84
8.1.1	Result 1 . . . . .	84
8.1.2	Result 2 . . . . .	86
8.1.3	Reasons for a reduction in TSFC . . . . .	89
8.2	Constant Specific Thrust and Optimum point analysis . . . . .	91
8.2.1	Constant Specific Thrust and Optimum Point Methodology . . . . .	91
8.2.2	Result 3 . . . . .	96
8.2.3	Result 4 . . . . .	97
8.3	Downsized Engine . . . . .	99
8.3.1	Result 5 . . . . .	99
8.4	Technical Sensitivity Analysis . . . . .	102
<b>9</b>	<b>Emission Analysis</b>	<b>105</b>
9.1	$H_2O$ Emissions . . . . .	106
9.2	Nitrogen Oxide Emissions. . . . .	106
9.2.1	$NO_x$ Emission Analysis Methodology . . . . .	108
9.3	Verification of $NO_x$ Emission Model . . . . .	109
9.4	Limitations of the model . . . . .	110
9.5	Results of $NO_x$ emission analysis . . . . .	111

<b>10 Economic Analysis</b>	<b>113</b>
10.1 Economic Analysis Methodology . . . . .	113
10.1.1 New Design Payload . . . . .	114
10.1.2 Direct Operating Cost . . . . .	115
10.1.3 Indirect Operating Cost . . . . .	119
10.1.4 Total Cost . . . . .	120
10.1.5 Internal Rate of Return (IRR) . . . . .	122
10.1.6 Assumptions for Economic Analysis . . . . .	123
10.2 Economic Analysis Results . . . . .	124
10.2.1 Results (Without Emissions) . . . . .	124
10.2.2 Result 1 . . . . .	125
10.2.3 Result 2 . . . . .	126
10.2.4 Result 3 . . . . .	127
10.2.5 Result 4 . . . . .	128
10.2.6 Economics Sensitivity Analysis (Without Emissions) . . . . .	129
10.2.7 Results (With Emissions) . . . . .	131
10.2.8 Result 5 . . . . .	132
10.2.9 Result 6 . . . . .	132
10.2.10 Result 7 . . . . .	133
10.2.11 Economic Sensitivity Analysis (With Emissions) . . . . .	134
<b>11 Conclusions, Limitations, Contributions &amp; Recommendations</b>	<b>137</b>
11.1 Research Project Summary . . . . .	137
11.2 Conclusion . . . . .	138
11.3 Limitations . . . . .	145
11.4 Scientific Contribution . . . . .	146
11.5 Recommendations . . . . .	147
<b>Bibliography</b>	<b>155</b>
<b>A SOFC-GT hybrid Results (Technical Analysis)</b>	<b>157</b>
<b>B Fuel Weight Calculation (Economic Analysis)</b>	<b>163</b>



# LIST OF FIGURES

1.1	Engine fuel burns over the time	2
1.2	Battery Powered Propulsion Architecture	4
1.3	Parallel-hybrid Propulsion Architecture	4
1.4	Turbo-Electric Propulsion Architecture	5
1.5	NASA STARC-ABL Concept	6
2.1	Solid Oxide fuel cell working principle	11
2.2	Triple Phase Boundary	12
2.3	Energy vs Reaction path	16
2.4	Voltage vs Current density for a typical fuel cell	17
2.5	Voltage vs Current density for different operating pressures	20
2.6	Voltage vs Current density for different operating temperatures	21
2.7	Contribution of different losses in the fuel cell operation	22
2.8	Losses vs Pressure	22
2.9	Losses vs pressure at different temperature	23
2.10	Fuel Utilization vs Efficiency	24
3.1	SOFC-GT system architecture	36
3.2	Entropy generation in different components of SOFC-GT hybrid system	38
3.3	Entropy generation vs compression ratio	39
3.4	The system architecture of SOFC-GT APU	41
3.5	System architecture of engine integrated SOFC-GT power system	42
3.6	$CPO_x$ and SOFC performance for different temperatures of operation	42
3.7	$CPO_x$ and SOFC performance for different pressures of operation	43
3.8	System architecture for SOFC-battery hybrid propulsion system	43
3.9	System architecture for SOFC-GT hybrid-electric propulsion system	44
3.10	Core efficiency vs engine weight vs aircraft range for case 1, hydrogen	45
3.11	Core efficiency vs engine weight vs aircraft range for case 2, hydrogen (SOFC) & kerosene (gas turbine)	45
3.12	SOFC-GT hybrid system architecture	46
4.1	Project Methodology	50
5.1	Fuel Cell Architecture	53
5.2	SOFC Model Architecture	55
5.3	Concentrations of species along the fuel channel	57
5.4	Temperatures of different SOFC components along the fuel and air channels	58
5.5	The SOFC output voltage, losses, and current density along the fuel channel	59

5.6	Comparison between SOFC model and Aguiar model . . . . .	59
5.7	Temperature vs SOFC cell Voltage and losses . . . . .	61
5.8	Pressure vs SOFC cell Voltage and losses . . . . .	61
5.9	Heat Exchanger Architecture Anode . . . . .	62
5.10	Heat Exchanger Architecture Cathode . . . . .	63
5.11	Total energy in and out of Fuel Cell . . . . .	64
5.12	Error in Energy Balance of fuel cell for different fuel cell Power Output for Design Condition . . . . .	65
6.1	Turbofan Nomenclature and station numbers (Adapted from [64]) . . . . .	69
6.2	Block Diagram of CFM-56-5B1 Reference Engine (Adapted from [56]) . . . . .	70
6.3	Reference Engine Validation . . . . .	72
7.1	SOFC-GT Hybrid Nomenclature and station numbers (Adapted from [64]) . . . . .	76
7.2	Block Diagram of SOFC-GT Hybrid Propulsion System . . . . .	77
7.3	Net Fuel Cell Power added to the Low Pressure Shaft . . . . .	78
7.4	Error in Enthalpy Balance of SOFC-GT Hybrid for different Fuel Cell Power Output . . . . .	79
7.5	T-s diagram for reference engine(Left) and T-s diagram for SOFC-GT hybrid engine(Right) (Adapted from [69]) . . . . .	80
8.1	Change in Mass Flow Rate of Air and TSFC for an increase in Fuel Cell Power Output for Design Condition . . . . .	84
8.2	Change in Thrust for an increase in Fuel Cell Power Output for Design Condition . . . . .	85
8.3	Change in Efficiency for an increase in Fuel Cell Power Output for Design Condition . . . . .	86
8.4	Change in Mass Flow Rate of Air and TSFC for an increase in Fuel Cell Power Output for Off-Design Condition . . . . .	87
8.5	Change in TIT and OPR for an increase in Fuel Cell Power Output for Off-Design Condition . . . . .	87
8.6	Change in Core and Bypass thrust for an increase in Fuel Cell Power Output for Off-Design Condition . . . . .	88
8.7	Change in Efficiency for an increase in Fuel Cell Power Output for Off-Design Condition . . . . .	88
8.8	Change in Temperature of HPC Air for an increase in Fuel Cell Power Output for Off-Design Condition . . . . .	89
8.9	Transmission of energy from Core flow to By-Pass flow in gas turbine . . . . .	90
8.10	Transmission of energy from Fuel Cell to By-Pass flow in SOFC-GT hybrid . . . . .	90
8.11	Methodology for constant specific thrust and optimum point . . . . .	91
8.12	Changes in power loss and TSFC as FPR is changed . . . . .	95
8.13	Difference in the optimum velocity ratio developed for SOFC-GT hybrid and the method given by Guha . . . . .	95
8.14	Changes in TSFC for different Fuel Cell Power Output for constant Specific Thrust(ST) and constant BPR for Design and Off-Design condition . . . . .	97

8.15	Reduction in TSFC for different Fuel Cell Power Output for constant Specific Thrust(ST) for Design and Off-Design condition . . . . .	98
8.17	Change in TIT and the subsequent cooling air percentage for different Fuel Cell Power Output for Off-Design condition . . . . .	98
8.16	Change in the BPR and reduction in mass flow rate as fuel cell power output is increased . . . . .	99
8.18	Reduction in TSFC for different Fuel Cell Power Output extrapolated to 5.5 MW power output . . . . .	102
8.19	Sensitivity Analysis of Thermodynamic Efficiency for a 1 MW and 4 MW fuel cell power output for Off-Design condition . . . . .	103
9.1	GWP of $NO_x$ and $H_2O$ per kilogram of GWP of $CO_2$ as altitude is increased	105
9.2	Impact on $H_2O$ production as fuel cell power output is increased . . . . .	106
9.3	Temperature of flow at the exit of HPC and the mixture at different fuel cell output power . . . . .	109
9.4	Change in $NO_x$ emissions as equivalence ratio and combustor outflow temperature is changed . . . . .	110
9.5	Impact of increasing the fuel cell power output on $NO_x$ Emissions for Off-Design or cruise condition . . . . .	112
10.1	Complete Overview of the Economic Model Methodology. . . . .	114
10.2	Direct Operating Cost Overview for the aircraft (Adapted from [75]) . . . . .	116
10.3	Methodology to calculate the Internal Rate of Return and evaluate the profitability of the SOFC-GT hybrid . . . . .	122
10.4	Change in fuel cell power vs total lifetime investment vs fuel cell cost . . . . .	125
10.5	Change in required specific power as fuel cell power is changed . . . . .	127
10.6	Reduction in Direct Operating Costs and the change in Internal Rate of Return for Direct Operating Costs as fuel cell power is changed . . . . .	128
10.7	Change in required specific power as the fuel price is increased . . . . .	129
10.8	Sensitivity Analysis of required Specific Power for a 1 MW and 4 MW fuel cell power output in order to breakeven (IRR=0) . . . . .	130
10.9	Change in fuel cell-specific power as fuel cell power output is increased when emission tax is included . . . . .	133
10.10	Change in required specific power as fuel price is increased when emission tax is included for 4 MW power output . . . . .	133
10.11	Sensitivity Analysis of required Specific Power for a 1 MW fuel cell power output in order to breakeven (IRR=0) for different emission scenarios . . . . .	134
A.1	SOFC-GT hybrid nomenclature and station numbers (Adapted from [64])	158
A.2	Data for each station for Design condition (Reference Engine) . . . . .	158
A.3	Data for each station for Off-Design condition (Reference Engine) . . . . .	159
A.4	Data for each station for Design condition (1 MW fuel cell power output) . . . . .	159
A.5	Data for each station for Off-Design condition (1 MW fuel cell power output)	160
A.6	Data for each station for Design condition (4 MW fuel cell power output) . . . . .	160
A.7	Data for each station for Off-Design condition (4 MW fuel cell power output)	161



# LIST OF TABLES

2.1	Comparison of different propulsion technologies . . . . .	7
2.2	Comparison of different fuel cells (Part A) . . . . .	24
2.3	Comparison of different fuel cells (Part B) . . . . .	25
2.4	Comparison of different fuel cells (Part C) . . . . .	26
3.1	Comparison of different SOFC-GT researches . . . . .	37
5.1	Pressure and temperature impact on SOFC OCV, losses and Cell Voltage . . . . .	60
6.1	Parameter Values for the Reference Engine . . . . .	71
6.2	Default Parameter Values for the Reference Engine taken from PyCycle example . . . . .	71
6.3	Parameters for Design (Sea Level Static) and Off-Design (Cruise) Condition . . . . .	72
8.1	Comparison between CFM-56-5B1 (reference engine) and CFM-56-5A3 . . . . .	100
8.2	Results of the analysis of CFM-56-5A3 integrated with a fuel cell to achieve thrust comparable to CFM-56-5B1 . . . . .	101
9.1	Operating condition used for the verification of $NO_x$ emission model . . . . .	109
10.1	Impact of SOFC-GT on the Reference Engine . . . . .	113
10.2	Values of parameters used for the calculation of IRR . . . . .	120
10.3	Summary of the impact of IRR and WACC on overall profitability and Feasibility of the project . . . . .	123
10.4	Values of parameters used for the calculation of fuel cell weight . . . . .	125
10.5	Result of the Economic Analysis for commercially available fuel cell-specific power for 1 MW power output . . . . .	126
10.6	Different scenarios for emission tax considered in this study . . . . .	131
10.7	Result of the Economic Analysis for commercially available fuel cell specific power for 1 MW power output with the inclusion of emission analysis . . . . .	132

# ABBREVIATION

**AC** Alternating Current

**ACARE** Advisory Council for Aeronautics Research in Europe

**APU** Auxiliary Power Unit

**BLI** Boundary Layer Ingestion

**BPR** By Pass Ratio

**CPO<sub>x</sub>** Catalytic Paralytic Oxidation

**DC** Direct Current

**DLR** German Aerospace Center

**DOC** Direct Operating Cost

**DOC** Direct Operating Cost

**DP** Distributed Propulsion

**EU** European Union

**FAA** Federal Aviation Administration

**FAR** Fuel to Air Ratio

**FCC** Fuel Cell Compressor

**FPR** Fan Pressure Ratio

**GdCeO<sub>2</sub>** GadoliniumOxide doped Cerium Oxide

**GT** Gas Turbine

**GWP** Global Warming Potential

**HALE** High Altitude Long Endurance

**HPC** High Pressure Compressor

**HPT** High Pressure Turbine

**HTFC** High Temperature Fuel Cell

**HTPEMFC** High Temperature Proton Exchange Membrane Fuel Cell

**ICAO** International Civil Aviation Organization

**IDOC** Indirect Direct Operating Cost

**IDOC** Indirect Direct Operating Cost

**IRR** Internal Rate of Return

**IRR** Internal Rate of Return

**kg** Kilo Gram

**kJ** Kilo Joule

**LHV** Lower Heating Value

**LPC** Low Pressure Compressor

**LPT** Low Pressure Turbine

**LSCN** Lanthanum Thynacite

**LSM** Lanthanum Strontium Manganite

**LTFC** Low Temperature Fuel Cell

**MCFC** Molten Carbonate Fuel Cell

**MJ** Mega Joule

**MTOW** Maximum Take-Off Weight

**MTOW** Maximum Take-Off Weight

**NASA** National Aeronautics and Space Administration

**NiO** Nickel Oxide

**NPSS** Numerical Propulsion System Simulation

**NPV** Net Present Value

**OCV** Open Circuit Voltage

**OPR** Overall Pressure Ratio

**PEMFC** Proton Exchange Membrane Fuel Cell

**PPM** Parts Per Million

**PPM** Parts Per Million

**PSFC** Power Specific Fuel Consumption

**SLS** Seal Level Static

**SOFC** Solid Oxide Fuel Cell

**SOFC-GT** Solid Oxide fuel cell-Gas Turbine

**ST** Specific Thrust

**TEC** Thermal Expansion Coefficient

**TIT** Turbine Inlet Temperature

**TPB** Triple Phase Boundary

**TRL** Technology Readiness Level

**T-s** Temperature- Entropy

**TSFC** Thrust Specific Fuel Consumption

**YSZ** Yittria Stabilized Zirconia



# NOMENCLATURE

$\alpha$	Charge transfer coefficient	
$\beta$	Mole fraction of oxygen in fuel channel	
$\Delta g$	Change in gibbs free energy	$kJ$
$\Delta h$	Change in enthalpy	$kJ$
$\Delta S$	Change in entropy	$kJ$
$\delta$	Mole fraction of hydrogen in fuel channel	
$\dot{m}_a$	mass flow rate of the air	$kg/s$
$\dot{m}_b$	Bypass mass flow rate	$kg/s$
$\dot{m}_c$	Core mass flow rate	$kg/s$
$\dot{m}_f$	mass flow rate of the fuel	$kg/s$
$\dot{m}_{cold}$	Mass flow rate of cold fluid	$kg/s$
$\dot{m}_{fc}$	Mass flow rate of fuel entering the fuel cell	$kg/s$
$\dot{m}_{reference}$	Mass flow rate of air for reference engine	$kg/s$
$\dot{m}_{SOFC-GT}$	Mass flow rate of air for SOFC-GT hybrid	$kg/s$
$\epsilon$	Effectiveness of heat exchanger	
$\eta_m$	Motor efficiency	
$\eta_n$	Nozzle efficiency	
$\eta_{cc}$	efficiency of the combustion chamber	
$\eta_{fan}$	Fan efficiency	%
$\eta_{fuelcell}$	Efficiency of fuel cell	
$\eta_{is_c}$	Isentropic efficiency of compressor	
$\eta_{is_t}$	Isentropic efficiency of turbine	
$\eta_{shaft}$	Shaft Efficiency	%
$\gamma$	Mole fraction of steam in fuel channel	

$\tau_{an}$	Thickness of anode	$m$
$\tau_{ca}$	Thickness of cathode	$m$
$\tau_{el}$	Thickness of electrolyte	$m$
$A_n$	Area of nozzle	$m^2$
$a_p$	Activity of product	
$a_r$	Activity of reactant	
$C_a$	Initial cost of aircraft	\$
$C_e$	Initial cost of engine	\$
$C_{fc}$	Initial cost of fuel cell	\$
$C_{pa}$	Specific heat capacity of air	$J/kg$
$C_{pe}$	Specific heat capacity of exhaust	$J/kg$
$C_{pg}$	specific heat capacity of exhaust gas	$J/kg$
$C_{pc}$	Heat Capacity of cold fluid	$J/K$
$D_{an}$	Diffusion coefficient of anode	$m^2/s$
$D_{ca}$	Diffusion coefficient of cathode	$m^2/s$
$E^\circ$	Electromotive force	$V$
$F$	Faraday constant	$C.mol^{-1}$
$f_{fc}$	Fuel Cell Power Fraction	
$H_2$	Hydrogen	
$H_{2_{required}}$	Hydrogen required for fuel cell	
$H_{cin}$	Enthalpy of cold fluid going in of heat exchanger	$J$
$H_{cout}$	Enthalpy of cold fluid coming out of heat exchanger	$J$
$H_{hin}$	Enthalpy of hot fluid going in of heat exchanger	$J$
$H_{hout}$	Enthalpy of hot fluid coming out of heat exchanger	$J$
$I$	Current delivered by fuel cell	$A$
$i$	Average current density	$A/m^2$
$i_o$	Exchange current density	$A/m^2$
$k_a$	Heat capacity ratio of air	

$M_{P_{New}}$	New Design Payload	<i>kg</i>
$M_{P_{Ref}}$	Reference Design Payload	<i>kg</i>
$O^{2-}$	Oxide Ion	
$O_2$	Oxygen	
$P$	Pressure	<i>pa</i>
$P^\circ$	Standard pressure	<i>pa</i>
$p_f$	Pressure of fluid at the nozzle exit	<i>pa</i>
$P_{fcC}$	Fuel Cell Compressor Power Input	<i>W</i>
$P_{fcLP}$	Net Fuel Cell Power added to the LP Shaft	<i>W</i>
$P_{fc}$	Fuel Cell Power Output	<i>W</i>
$P_{fc}$	Power output of fuel cell	<i>W</i>
$P_{H_2Otpb}$	Pressure of water/steam at TPB	<i>pa</i>
$P_{H_2O}$	Pressure of Water/Steam	<i>pa</i>
$P_{H_2tpb}$	Pressure of hydrogen at TPB	<i>pa</i>
$P_{H_2}$	Pressure of Hydrogen	<i>pa</i>
$P_{O_2tpb}$	Pressure of oxygen at TPB	<i>pa</i>
$P_{O_2}$	Pressure of Oxygen	<i>pa</i>
$P_{ti}$	Total pressure at inlet	<i>pa</i>
$P_{to}$	Total pressure at outlet	<i>pa</i>
$Q_{fcoutput}$	Heat output from SOFC model	<i>J</i>
$Q_{fcrequired}$	Heat required to increase the temperature of byproducts to $T_{FCout}$	<i>J</i>
$R$	Universal gas constant	$JK^{-1}.mol^{-1}$
$R_a$	Resistivity of the anode	<i>ohm/cm<sup>2</sup></i>
$R_c$	Resistivity of the cathode	<i>ohm/cm<sup>2</sup></i>
$R_{cC}$	Resistivity of the current collector	<i>ohm/cm<sup>2</sup></i>
$R_e$	Resistivity of the electrolyte	<i>ohm/cm<sup>2</sup></i>
$SP_a$	Fraction of spare parts to the cost of aircraft	<i>%</i>

$SP_e$	Fraction of spare parts to the cost of engine	%
$SP_{fc}$	Fraction of spare parts to the cost of fc	%
$T$	Temperature	$K$
$T_{FCin}$	Temperature of inlet products of SOFC	$K$
$T_{FCout}$	Temperature of outlet byproducts of SOFC	$K$
$T_{h_{in}}$	Inlet temperature of hot fluid	$K$
$T_{ti}$	Total temperature at inlet	$k$
$T_{to}$	Total temperature at outlet	$k$
$T_{c_{in}}$	Inlet temperature of cold fluid	$K$
$T_{c_{out}}$	Outlet temperature of cold fluid	$K$
$U_f$	Fuel utilization	
$V$	Aircraft Velocity	$m/s$
$v_{\infty}$	Velocity of aircraft	$m/s$
$v_f$	Velocity of fluid at the nozzle exit	$m/s$
$V_j$	Fully expanded core jet velocity	$m/s$
$V_j$	Jet Velocity	$m/s$
$V_{act}$	Activation loss voltage	$V$
$V_{conc}$	Concentration loss voltage	$V$
$V_{fc}$	Fuel cell voltage	$V$
$V_{jb}$	Fully expanded bypass jet velocity	$m/s$
$V_{ocv}$	Open circuit voltage	$V$
$V_{ohm}$	Ohmic loss voltage	$V$
$W_{fan}$	Total fan power required	$W$
$z$	Number of electrons exchanged per mol of fuel	
$(CO_3)^{2-}$	Carbonate ion	
$CH_4$	Methane	
$CO$	Carbon Monoxide	
$CO_2$	Carbon Dioxide	

---

$H^+$	Hydrogen ion
$H_2O$	Water/Steam
$NO_x$	Nitrogen Oxides
$SO_x$	Sulphur Oxides



# 1

## INTRODUCTION

Climate Change is an important issue and people all around the world have understood the need for a more sustainable and renewable future. Consumers' perspective is changing towards greener solutions or alternatives from every industry in order to reduce their individual carbon emission footprint. Regulators and Governments, due to the pressure from their citizens and the international community, have also started to shift their focus toward more sustainable solutions and invest heavily in disruptive technologies to expedite the transition. The aviation industry is no different. The whole industry is getting constant scrutiny over the emissions that it creates and people are getting more concerned about the way they should be traveling. There have been multiple incidents of flight shaming in the past and other incidents like environmental activist Greta Thunberg using a sailboat to travel to New York while spending 2 weeks in travel time rather than choosing to fly for only 11 hours. This is because of the high amount of emissions per passenger per km(p/km) for the Aerospace Industry as compared to any other mode of transport. According to European Union, a person flying from Lisbon to New York is contributing to as many emissions as their home produces for one whole year of heating[1].

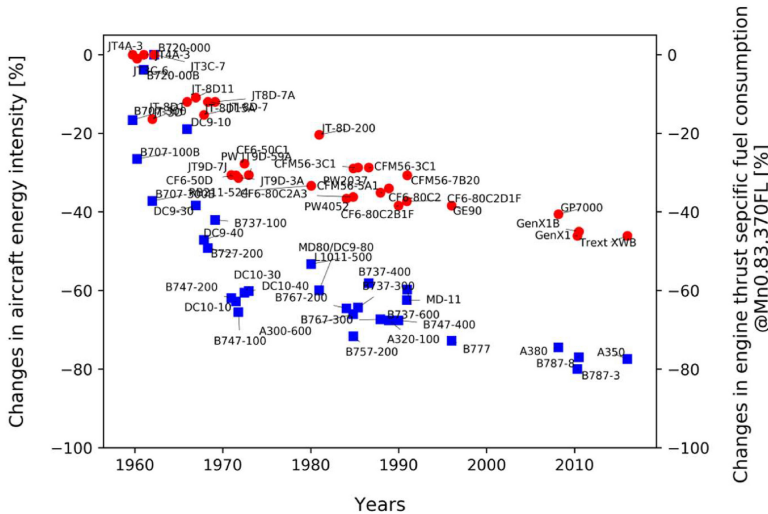
A domestic flight has a direct Carbon Dioxide ( $CO_2$ ) emissions of 133 g/p/km and indirect emissions such as Nitrogen Oxides ( $NO_x$ ), Sulphur Oxides( $SO_x$ ), contrails, etc., of 121 g/p/km compared to a bus of 104 g/p/km and a domestic rail of 41 g/p/km[2]. These emissions not only lead to global warming but also contributes to severe health conditions like respiratory problems. In the EU alone, only aircraft direct emissions contributed to 3.8% of all carbon emissions and 13.9% of transport emissions without considering the indirect impacts, which are quite substantial[1]. Even though the continuous effort from the whole industry has been crucial in reducing the fuel burn per passenger by 24% from 2005 to 2017, which is significant and commendable, it has been outweighed by the increase in air travel by 60% in the same period [1]. This is the reason that the whole Aerospace Industry, as well as the regulators, are pushing hard to reduce their emission footprint. European Union (EU) has built an Advisory Council for Aeronautics Research in Europe (ACARE) flightpath 2050 which aims to reduce the

$CO_2$  emissions by 75 %,  $NO_x$  emissions by 90%, and noise emissions by 65 % by 2050 compared to a new aircraft in 2000. These ambitious goals need to be achieved even though there is a continuous growth in the number of passengers by 4.3% during the pre-COVID-19 times according to International Civil Aviation Organization (ICAO)[3]. The COVID-19 pandemic did have a huge impact on the whole airline industry and as a result, the emissions from the industry reduced significantly. But the industry has already recovered to 70% of the pre-covid level and is hoping to recover to its full potential soon [4]. This means that the number of passengers using the aircraft will also increase steadily in the future. The rate of increase might be lower because of the cultural shift in the business sector and corporate sector which can help in achieving the goals.

This research is a small effort to push this movement forward and contribute to the journey to emission neutral future.

## 1.1. MATURING GAS TURBINE TECHNOLOGY

As mentioned in section 1 in order to achieve the ACARE 2050 Vision, there is a need for radical changes in the aero-engine technology as engine technology is one of the biggest contributors of efficiency improvement and reductions of emissions. But the current gas turbines are approaching technological maturity [5] and this is evident in figure 1.1. The curve for specific fuel consumption is flattening over time which is shown in red and in past 20 years, there is a little improvement in specific fuel consumption. Even the latest GE9X is only 10% [6] more fuel-efficient than its predecessor GE90 compared to GE90's 20% [7] less fuel burn from its predecessor GE CF6. This indicates that gas turbine technology is on the verge of becoming a mature technology which poses a big bottleneck toward emission neutrality.



The data in blue in the figure 1.1 shows the change in aircraft energy requirements over the period and it can be seen that aircraft energy requirements have reduced by approximately 75% since the 1960s. The additional energy savings is due to the improvements in aircraft aerodynamics, structures, and materials. But as the engine improvements have slowed down, so did the improvements in aircraft's total energy consumption as propulsion systems are the biggest contributor to the overall efficiency improvement of an aircraft.

Hence, there is a need for disruptive innovation in propulsion technology in order to meet the ACARE 2050 vision.

## 1.2. INTRODUCTION OF ZERO-CARBON FUELS

Even though the efficiency of aircraft is increasing significantly, the increase in the number of passengers traveling in aircraft is increasing at higher rates. This leads to an absolute increase in aircraft emissions. Hence, researchers have suggested using zero-carbon fuels like hydrogen. One of the current trends in propulsion research is to use hydrogen in the gas turbine just like kerosene.

Using hydrogen in the gas turbines will eliminate carbon and sulfur-related emissions, because of the absence of carbon and sulfur in the fuel, but will still have other emissions like NO<sub>x</sub>, water vapors, etc. Also, the use of gas turbines for hydrogen will have little impact on gas turbine efficiency. The thermodynamic and propulsive efficiency of the engine will improve by a small margin due to the change in the specific heat capacity of the flow, as a result of a change in the composition of the flow because of using hydrogen as a fuel rather than kerosene, after the combustor. But the future scope of improvement is still low because of the maturing of the gas turbine as explained in section 1.1.

Along with this, the combustion process in the combustion chamber is the largest contributor to exergy loss [9]. Using gas turbines for hydrogen will still result in high exergy destruction and hence lower efficiency.

Therefore, it is beneficial to explore other technologies which may perform better than gas turbines for fuels like hydrogen.

## 1.3. FUTURE PROPULSION CONCEPTS

As there is a need of disruptive innovation in propulsion technology, this section talks about potential future propulsion concepts that are being investigated.

### 1.3.1. BATTERY POWERED AIRCRAFT

Batteries have brought a big disruption in the automobile industry and are being researched quite a lot for their application in general aviation. It has proved to be a more efficient and cleaner solution than engines using fossil fuel. Hence, multiple studies have been done to evaluate its possibility for commercial aviation. One of the battery-powered aircraft propulsion architectures by NASA has been shown in figure 1.2. The propulsion system includes the battery which is an energy storage device, an electric motor that converts electric energy into mechanical power, and the propeller which produces thrust. The electric power train is highly efficient (more than 90% [10]) because of

the high efficiency of motors (more than 96% [11]) and power converters (more than 99% [11]) but where this architecture lags is the energy density of batteries. The current state of the art Li-ion battery has an energy density of 150-250 W-hr/kg [12] compared to kerosene of approximately 12000 W-hr/kg, which makes the battery technology significantly heavier than the status quo.

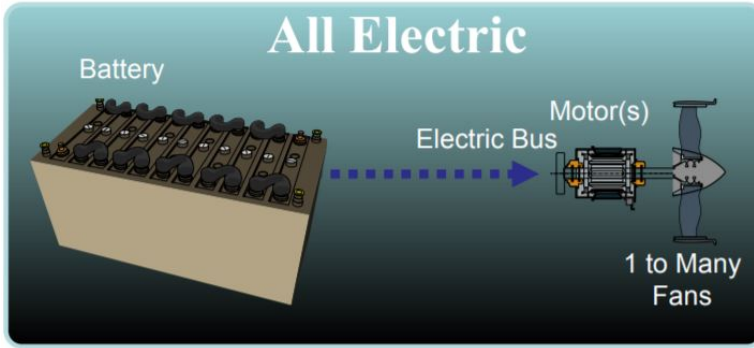


Figure 1.2: Battery Powered Propulsion Architecture

[12]

### 1.3.2. PARALLEL-HYBRID PROPULSION SYSTEM

Another concept is to use a Parallel-hybrid architecture in which a battery is used to aid the turbofan during high power requirement conditions like take-off and climb. As shown in figure

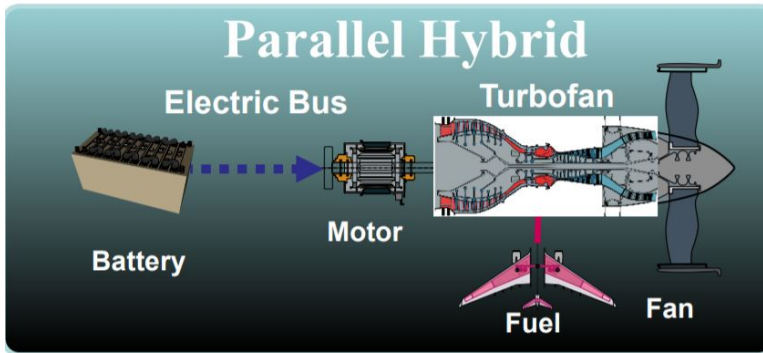


Figure 1.3: Parallel-hybrid Propulsion Architecture

[12]

### 1.3.3. TURBO-ELECTRIC PROPULSION SYSTEM

The turbo-Electric propulsion system is a system in which a Gas Turbine(GT) provides power to motors by converting mechanical power to electric power via a generator. The

turbogenerator provides onboard power by using fossil fuels or hydrogen. Turbo-Electric architecture facilitates the possibility of different aircraft configurations as well as operating the gas turbine at its design point for most of the flight duration, which helps in reducing the fuel burn.

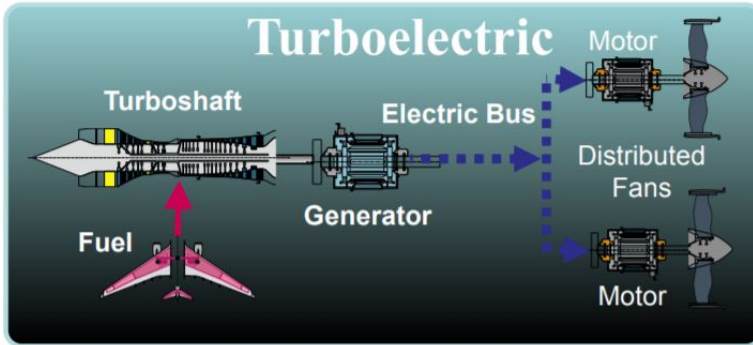


Figure 1.4: Turbo-Electric Propulsion Architecture

[12]

NASA studied a concept named Single-Aisle Turbo-electric Aircraft With Aft Boundary Layer(STARC-ABL) [13], shown in figure 1.5 which incorporated the futuristic technologies like Turbo-Electric propulsion, Distributed Propulsion(DP), and Boundary Layer Ingestion(BLI). The aircraft has two jet engines which power the generator and hence run the propeller. Along with this, a high bypass fan at the end of the tail is also incorporated which is run by electricity generated by turbofan. The tail fan is based on the principle of BLI in which the boundary layer of the fuselage is ingested in the fan which increases the propulsive efficiency of the propulsion system. The analysis of this state-of-the-art futuristic aircraft found that the fuel burn reduction of between 7-12% when compared to the Boeing 737-800 aircraft[13].

Even though the improvements are significant, there are many challenges as well. One challenge of this configuration is the weight of the power train. The current electric power train has a specific power of 2 kW/kg [14] which is substantially lower than a gas turbine. Also, scaling the power train to a megawatts level reduces the specific power by a factor of 4.5[14] because of the increase in rotor mechanical stress and magnetic shear stress in the motor, which makes it much heavier.

#### 1.3.4. COMPOSITE MATERIALS

The operating temperatures of GT have a big impact on its efficiency. Based on the thermodynamics, the higher the Turbine Inlet Temperature(TIT) or the temperature of flow gas after combustor, the higher the energy that can be extracted from the gas at a particular pressure[15]. This means that the core of the gas turbine can be made smaller and the bypass ratio can be increased, hence, increasing the propulsive efficiency of the engine. More explanation has been given in the section 6.



Figure 1.5: NASA STARC-ABL Concept

[11]

Another advantage is the reduction in cooling air requirement. In order to increase the temperature of the combustor flow, the combustor and turbine should be able to continuously sustain that higher temperature so that more energy can be extracted from the flow. Current materials used in combustors and turbines need active cooling as they cannot sustain these high temperatures and this cooling air comes directly from the high-pressure compressor. This means that a fraction of air compressed in the compressor is used for cooling of turbines and combustor rather than being used in the combustor. This reduces the overall engine efficiency.

But using composite ceramic materials, which can sustain high temperatures and do not need much active cooling, can be used in the combustor as well as in the turbine and hence reduce the requirement of cooling. This will lead to higher efficiency as a large fraction of compressor air is put in the combustor, heated to the TIT, and is used to extract the work. The use of composite materials in the combustor and turbine will allow the combustor flow to be at a temperature of about 1950 K [16] by 2050 while reducing the need for cooling air and hence, will help in fuel reduction of 4.25% [17] in the best case scenario.

Along with this, increasing the combustor flow temperature would have a negative impact on the emissions. To increase the temperature of combustor flow, more fuel per kg of air will be injected into the combustor which could lead to an increase in high localized temperature regions in the case of current fuel injectors. These high localized temperature regions will then increase  $NO_x$  as  $NO_x$  is produced when the localized temperature of a region inside the combustor increases above 1700 K. More explanation has been given in section 9.2. Hence, increasing the combustor flow temperature may help in reducing the fuel consumption which will lead to a reduction in  $CO_2$  but will increase the  $NO_x$  emissions..

# 2

## FUEL CELL

As discussed in section 1.3, an electric powertrain or a hybrid electric powertrain, even though very efficient at the vehicle level and have lower emissions, do have multiple disadvantages when compared to a conventional kerosene powered aircraft. Table 2.1 gives an overview of the comparison between the four technologies explained above. It should be noted that the battery-powered aircraft's propulsion system-specific power is not known. It depends on multiple different components like motor, AC-DC converters, cooling systems, control systems etc. Also, for turbo-electric configuration, the specific power of only the electric powertrain is known.

	Battery Powered Aircraft	Turbo- electric with Boundary Layer Ingestion	Composite Materials	Fuel Cell
Efficiency improvement (relative to Airbus A-320)	>100%	7-12%	4-5%	15-20%
Specific Power	-	0.68 kW/kg (electric Powertrain)	>12 kW/kg	>0.5 kW/kg
Emission reduction	100%	7-12%	4-5%	>20%
Noise	Low	High	High	Medium
TRL	Low	Low	High	Very Low

Table 2.1: Comparison of different propulsion technologies

[11][13][17][18]

A thorough explanation of shortcomings is given below:

1. **Power and Energy Density:** It is a very well-known fact that a battery has a very low energy density and hence is unsuitable for commercial aviation. But along with

a low energy density of the battery, the balance of the plant required for electric propulsion is also quite heavy when compared to a kerosene propulsion system. A thorough comparison is given below:-

2

- **Fuel:-**The battery in an electric aircraft is only equivalent to the kerosene in a conventional aircraft and acts as a power source to run the motor. The state-of-the-art Lithium-ion battery has an energy density of 0.72 MJ/kg [19] compared to kerosene which has an energy density of approximately 45 MJ/kg [20], hence 64 times lower. Multiple researches are going on in the domain of battery technology and many new technologies are proposed like Lithium-sulphur battery which has an energy density of 1.8 MJ/kg [21] and an Aluminium air battery which has a theoretical energy density of 29 MJ/kg [20]. But all these new technologies have a very low Technology Readiness Level (TRL) and are still in the research stage.
- **Machine:-**The specific power of the machine used to convert the energy of kerosene fuel into useful thrust, i.e. turbofan is nearly 10 kW/kg compared to a state of the art aircraft grade motor which has the specific power of 5.9 kW/kg [22], without including the weight of the propeller. The latest report from Siemens reveals that the motors with a specific power of 7.6 kW/Kg are being tested [23].
- **Auxiliary systems:-**Electric aircraft need a power converter to convert the Direct Current (DC) of the battery to Alternating Current (AC) and then again to DC for the motor and a gearbox for high torque propellers. All these systems add up to the weight of the system and hence increase the overall weight of the battery-powered aircraft.

Due to the big challenges that electric and hybrid-electric aircraft bring, there is a need to look at other technologies which can take advantage of a highly efficient electric powertrain and complement its disadvantages. One such technology is fuel cells. Fuel cell is an electrochemical cell that converts the chemical energy of a fuel into electricity and heat by the process of chemical reactions. A fuel cell is shown in figure 2.1.

#### **Advantages of the fuel cell are given below.**

1. **High Efficiency:-**fuel cell has an electrical efficiency of 60% [24] and a total efficiency of more than 85% [24] in the integrated system. Compared to a turbofan which has an efficiency between 40-45% or a turboprop which has a maximum efficiency of 50-55%, an increase of 33.3% and 10% from the best-case scenario of turbofan and turboprop respectively only for electrical efficiency perspective.
2. **Lower Emissions:-** As fuel cell works on the principle of oxidizing specific reactants. For example, in the case of SOFC, where electrolyte-doped nickel is used as an anode, only hydrogen and Carbon monoxide can be oxidized to steam and carbon dioxide. This means that all other species like nitrogen, carbon dioxide, etc will not be oxidized as the catalyst used is does not impact the reaction of these species and the operating temperature of the fuel cell is not high enough hence,

these species will leave the fuel cell as they entered. Hence, the emissions from a fuel cell are significantly low compared to a gas turbine as the combustion process in a gas turbine also oxidizes nitrogen to  $NO_x$ . Fuel cells produce no  $NO_x$ , no soot and no  $SO_x$ . For Carbon emissions, it is highly dependent on the fuel used. If any hydrocarbon is used, then fuel cell will still release  $CO_2$  and CO based on the fuel utilization levels but it will still lower than a gas turbine because of the higher efficiency of the fuel cell.

3. **Integrated systems:-** Fuel cells, especially high-temperature fuel cells like Solid Oxide fuel cell (SOFC) or Molten Carbonate fuel cell (MCFC) which operates at high-temperature of 800-1300k and release byproducts which include unutilized fuel, steam, and air. These byproducts contain high exergy which can be used directly in the gas turbine. Also, the pressure losses in the fuel cells are also of a similar order as of the combustion chamber which is approximately 5% [25], hence the pressurized air used for fuel cell operation can be fed directly into the combustion chamber. It should be noted that pressure losses in the piping systems and valves have not been considered and hence, it is a possibility that there is a need of an external compressor to compress the byproducts or the inlet of the fuel cell.

The concept of an integrated system is based upon the complementary nature of two technologies. The high pressure and high-temperature air required by the fuel cell is provided by the gas turbine, hence there is no need for external auxiliary systems to heat or pressurize the inlet air and fuel of SOFC. Afterward, the byproducts of the fuel cell which include unutilized fuel, reaction products, and unutilized air, are at high temperature, because of absorption of the heat generated due to losses in the fuel cell, can be directly used inside the combustor. The unutilized fuel will burn to provide heat and high-temperature air and other products will be part of the combustor flow where they will heat up to the Turbine Inlet Temperature (TIT). Hence, the losses, in the form of heat, of fuel cells is the fuel for gas turbine and the removal of SOFC auxiliary system results in the system efficiency of more than 85% [24] along with the increase in specific power of fuel cell. A more detailed explanation of the concept has been given in section 3.

4. **Efficiency dependency on power output:-** Unlike gas turbines, whose efficiency is highly dependent on the size of gas turbines, fuel cells, to a higher extent, have similar efficiencies for both high power fuel cells as well as the low power fuel cells. This is because of the fact that fuel cell stacks are built by individually connecting the fuel cells together, just like a battery pack. If there is a need for more power, more stacks are added. Although, there are some losses in the transportation of power from cells to the AC-DC convertor the losses are low. Hence, fuel cell efficiency does not depend significantly on the size of the fuel cells.
5. **Lower Noise:-** Fuel cells have almost no moving parts and the reactions inside the fuel cell have much lower noise which results in substantially less noise than gas turbines.

**Disadvantages of fuel cell are given below:-**

1. **Low Specific Power:-** Fuel cell have low specific power as can be seen from table 2.1. Compared to a gas turbine, the specific power is approximately 24 times less for the whole system. There are two reasons for this:-
  - The first reason is the use of an Auxiliary system. The fuel cell, especially PEM and SOFC requires systems like cooling systems, compressors, heat exchangers, and AC-DC converters to support the fuel cell. This increases the weight of system substantially.
  - The second reason is the different applications. The fuel cell has been used for stationary applications. Hence weight is not a priority. But when fuel cell has been researched for transportation like Toyota Mirai, the specific power increased substantially to 2.035 kW/kg [26]. Similar results have been published by NASA which developed a SOFC with a specific power of 2.5kW/kg [27].
2. **Slow Start-up time and transient response:-** The start-up time for fuel cells is very high, especially for high-temperature fuel cells. This is because it takes a lot of time and energy to heat the ceramic electrolyte and electrodes in the high-temperature fuel cell. This impacts the start-up as well as the transient response of the vehicle. According to Yamaguchi et al, the honeycomb structure SOFC can reach a heating rate of up to 100 °C per minute [28]. Assuming this fuel cell, it will take more than 8-10 minutes to just start the fuel cell. At this heating rate, the transient response would also be very slow.
3. **TRL:-**TRL level for PEM fuel cells or low-temperature fuel cells is high but for high-temperature fuel cells for transportation is very low for the same reason as given in point 1. Technology has recently become attractive from the perspective of transportation.

As per the discussion above, all the technologies have their own advantages and disadvantages but the author believes that out of all technologies, fuel cell technology has the most potential and the reason is as follows:

1. First reason is its ability to work as an integrated system which not only increases the efficiency of the system but also reduces emissions.
2. Second reason is the lack of research in this field, especially for aerospace applications. Weight, slow response, and TRL are definitely big constraints for the fuel cell and researchers in past have disregarded the fuel cell technology based on their performance in stationary applications. These stationary applications are purely driven by cost and not on weight and other performance parameters. Both Toyota and NASA have shown that if the technology is explored from the perspective of transportation, there might be a substantial improvement in the technology.
3. Third reason is the parallel use of technology. The fuel cell-GT hybrid can be used along with futuristic technologies like BLI, composite materials, battery-hybrid, etc. The fuel cell will only aid the gas turbine and hence all other technologies can still be used along with fuel cells.

This is the reason that the author is convinced that a fuel cell-GT hybrid propulsion system could be a potential technology alternative for future propulsion systems and hence, is worth researching.

## 2.1. WORKING PRINCIPLE OF FUEL CELL

As mentioned in section 2, the fuel cell is an electrochemical cell that converts the chemical energy of a fuel into electricity and heat by the process of chemical reactions. This section will explain in detail the working principle of the fuel cell and as shown in figure 2.1.

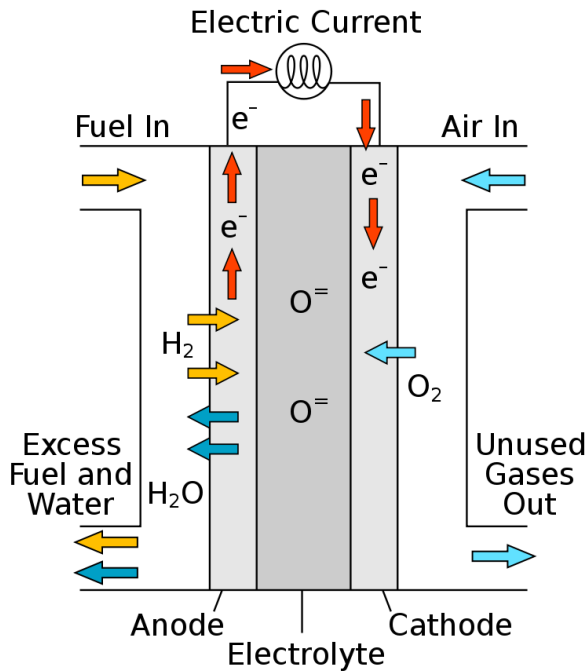


Figure 2.1: Solid Oxide fuel cell working principle

[29]

Fuel cell consists of an anode, a cathode, an electrolyte, and many other supporting parts like an interconnector, current collectors etc. A detailed explanation of each part is given below. In a nutshell, how a fuel cell works is as follows.

The reducer and oxidizer are fed into the anode and cathode of the fuel cell respectively. Then, the catalyst on each electrode converts the reducer and oxidizer into ions, which then travel through the electrolyte to the other side to react and form water. Depending on the type of fuel cell, either the reducer ion or the oxidizer ion can transport to the cathode or anode respectively. For example, in the case of SOFC, the oxidizer ion travels through the electrolyte and reaches the anode where it reacts with the reducer

ion to complete the reaction. When the reaction takes place, the energy released by the reaction is converted to electrochemical potential and heat, hence electrical power is produced.

A more detailed explanation for each process is given below. The following example has used hydrogen as the fuel or reducer and oxygen as the oxidizer.

2

- **Anode:-** Anode of the fuel cell is used to reduce the reducer, in this case, hydrogen to  $H^+$  ion, and conduct the extra electrons and transport them to the cathode. The hydrogen, in presence of an anode or catalyst, converts to  $H^+$  ion as shown in equation 2.1 and then travels on the anode to find a Triple Phase Boundary (TPB) as shown in figure 2.2. A TPB is a location where all the three components necessary for the reaction to take place come together and the reaction takes place at that location. In the case of the anode, the three components are anode (provides  $H^+$ ), electrolyte (provides  $O^{2-}$  or oxidizer ion coming from the cathode), and a current collector (which conducts electron to be transported to cathode), which in this case is anode itself. When these three components meet at TPB, the reaction 2.3 takes place.

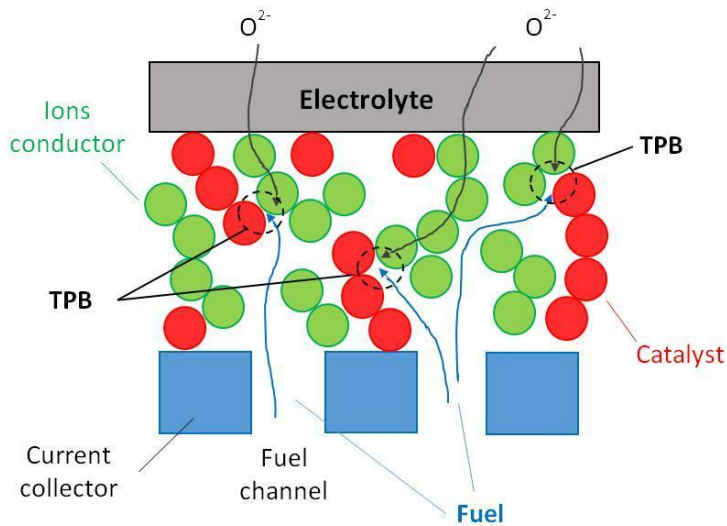
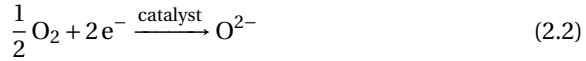


Figure 2.2: Triple Phase Boundary

[30]

- **Cathode:-** Cathode of the fuel cell is used to oxidize the oxidizer, in this case, oxygen to  $O^{2-}$  ion, using the electrons coming from the Anode as shown in equation 2.2. Similar to the anode, oxygen gas oxidizes at the cathode in the presence of a TPB, which in the case of the cathode, consists of the cathode (provides electrons), oxygen (oxidizer), and electrolyte (which conducts  $O^{2-}$ ).



- **Electrolyte:-** Electrolyte of the fuel cell is used to transport ions either from Anode to cathode or from cathode to anode depending on the type of fuel cell used. In figure 2.1, a SOFC is used, and hence an  $\text{O}^{2-}$  ion is transported from cathode to anode through the electrolyte. The mechanism through which ions are transported in electrolytes is by bonding with the molecules of the electrolyte. The  $\text{O}^{2-}$  ion bonds with the electrolyte Yittria based Zirconia (YSZ) and travels through the electrolyte and reaches the anode.
- **Interconnector:-** Interconnector is used to conduct electrons from the anode and transport it to the cathode while also providing the mechanical and structural strength to the fuel cell.

The final fuel cell reaction becomes



## 2.2. FUEL CELL PERFORMANCE

This section explains fuel cell thermodynamics and how to evaluate the performance of fuel cell. The fuel cell delivers a voltage at particular operating conditions like temperature, pressure, fuel utilization, current density, etc. The voltage depends on these conditions as well as the inherent losses that emerge inside the fuel cell. Because of these losses, the fuel cell does not deliver the maximum voltage or the ideal voltage and hence the fuel cell voltage ( $V_{fc}$ ) is less than the maximum achievable voltage,  $V_{oc}$ . Equation 2.4[31] gives the formula to calculate the fuel cell voltage.

$$V_{fc} = V_{oc} - V_{act} - V_{ohm} - V_{conc} \quad (2.4)$$

where  $V_{fc}$  = fuel cell Voltage, V

$V_{oc}$  = Open Circuit voltage, V

$V_{act}$  = Activation Losses, V

$V_{ohm}$  = Ohmoic Losses, V

$V_{conc}$  = Concentration losses, V

It is important to understand these losses because it helps in understanding the working of different types of fuel cells and their characteristics. The upcoming sections explain in detail the open-circuit voltage and each loss that impact the fuel cell.

### 2.2.1. OPEN CIRCUIT VOLTAGE ( $V_{oc}$ )

Open circuit voltage or  $V_{oc}$  is the maximum achievable voltage by a fuel cell at a particular temperature and pressure. This voltage is dependent on the fuel cell temperature and pressure as well as the concentration of reactants and products inside the fuel cell. The open-circuit voltage is derived from the Nernst equation which is represented by equation 2.5

$$V_{oc} = V_{rev} + \left(\frac{RT}{zF}\right) \ln \frac{\sum_i^k a_r(i)^n}{\sum_i^k a_p(i)^n} \quad (2.5)$$

where  $V_{rev}$  is the Electromotive Force (EMF) or the reversible voltage at standard pressure and temperature.

R= Universal Gas Constant,  $JK^{-1}.mol^{-1}$

T= Operating Temperature of fuel cell, K

z= Number of electrons transferred for each molecule of fuel

F= Faraday Constant,  $C.mol^{-1}$

$a_r$ = activity of reactant

$a_p$ = activity of product

n= number of moles reacted per mole of fuel

The EMF or  $V_{rev}$ , which is the voltage at standard pressure and temperature, is derived from the Gibbs Free energy and is calculated using equation 2.6 .

$$V_{rev} = -\frac{\Delta g}{zF} \quad (2.6)$$

where  $\Delta g$  is the change in Gibbs Free Energy.

Change in Gibbs Free Energy ( $\Delta g$ ) is the maximum available energy of a reaction at a particular temperature. This means that if a reaction takes place at a specific temperature, the maximum usable energy which can be used for work is the change in Gibbs free energy. For EMF,  $\Delta g$  is the maximum available energy at the standard temperature. The  $\Delta g$  is derived by the equation 2.7.

$$\Delta g = \Delta h - T\Delta S \quad (2.7)$$

where  $\Delta h$  is the change in enthalpy and  $\Delta S$  is the change in entropy. To understand the EMF, let's take the example of reaction

The z for reaction 2.3 is 2 as it transfers 2 electrons for one molecule of  $H_2$  oxidized. The Faraday constant is a constant which has a value of 96485 C/mol. Hence, the calculated EMF is 1.225 V. Another example of EMF for a cell operating at 800°C (High-temperature fuel cell) would be 0.98 V.

The activity of reactant ( $a_r$ ) or a product ( $a_p$ ) is defined by the equation 2.8.

$$a = \frac{P_i}{P^\circ} \quad (2.8)$$

Where  $P_i$ = Pressure of the reactant or product

$P^\circ$ = Standard Pressure

Using equation 2.5 and equation 2.8 for the reaction

$$V_{oc} = V_{rev} + \left(\frac{RT}{zF}\right) \ln \left( \frac{\left(\frac{P_{H_2}}{P^\circ}\right) \left(\frac{P_{O_2}}{P^\circ}\right)^{\frac{1}{2}}}{\frac{P_{H_2O}}{P^\circ}} \right) \quad (2.9)$$

As standard pressure,  $P^\circ$  is 1 bar, the pressure of reactants and products can be described like

$$P_{H_2} = \delta P \quad (2.10)$$

$$P_{O_2} = \beta P \quad (2.11)$$

$$P_{H_2O} = \gamma P \quad (2.12)$$

where  $P$  is the operating pressure of the system and  $\delta$ ,  $\beta$  and  $\gamma$  are the constants for molar concentrations of reactants and products. The  $V_{oc}$  becomes

$$V_{oc} = V_{rev} + \left(\frac{RT}{zF}\right) \ln\left(\frac{\delta\beta^{\frac{1}{2}}}{\gamma}\right) + \left(\frac{RT}{2zF}\right) \ln(P) \quad (2.13)$$

For example, if a low-temperature fuel cell and a high temperature are operating at  $80^\circ$  and  $800^\circ C$  respectively but at a similar pressure of 20 bar, then the Open Circuit Voltage according to equation 2.13 would be 1.247 V and 1.049 V, respectively. This means that this voltage is the maximum voltage the fuel cell can achieve in the ideal case when there are no losses inside the fuel cell for their respective operating conditions.

### 2.2.2. ACTIVATION LOSSES ( $V_{act}$ )

Activation Losses correspond to the losses during the activation of the reaction. In order for the reaction to take place, a minimum amount of energy needs to be provided to the reactants so that they can cross the energy barrier and form products. This energy is called the Activation energy and is shown in figure 2.3. The energy requirement starts to increase as the reaction moves forward and this energy is supplied by the surroundings to the reactants. Once, enough energy is provided such that the energy barrier can be crossed, the reaction moves forward and forms products. If the reaction is exothermic, as in the case of reaction 2.3, more energy will be released than reactants consumed from the surroundings.

The activation energy consumed by the reactants comes from the surroundings or in this case, from the fuel cell. The part of the energy which is supposed to be used for creating the potential is being used to cross the energy barriers by the reactants. This leads to a loss in voltage and is hence called the Activation loss or Activation Over potential. Equation 2.14 [31] provides the relation to calculate the activation loss.

$$V_{act} = A \sinh^{-1}\left(\frac{i}{i_o}\right) \quad (2.14)$$

where  $A$  is a constant,  $i$  is the operating current density, and the  $I_o$  is the exchange current density.

$$A = \frac{RT}{2\alpha F} \quad (2.15)$$

where  $\alpha$  is the charge transfer coefficient.

The exchange current density ( $I_o$ ) is the current density when the reaction is at equilibrium. During equilibrium, the rate of exchange of current does not go to zero, which means that the reaction is still taking place but the rate of forwarding and backward reaction is the same. When a reaction moves forward, it means that the rate of exchange current is more for the forward direction than the backward reaction but at equilibrium, these rates are the same.

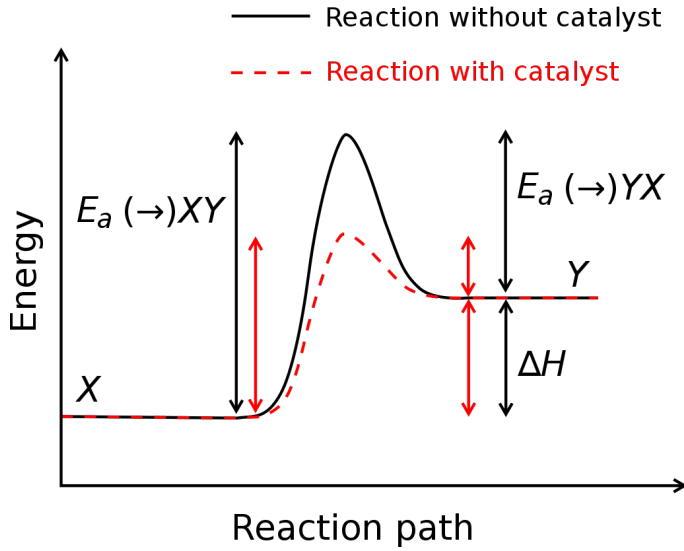


Figure 2.3: Energy vs Reaction path

[32]

The exchange current density depends on the temperature and the type of catalyst used for the reaction. Both temperature and catalyst increase the exchange current density which reduces the activation energy required to cross the energy barrier and hence reduces the activation losses. As can be seen from figure 2.3, the use of catalyst has reduced the activation energy.

Figure 2.4 shows the behavior of cell voltage when the current density is increased. The sudden dip in the voltage as the cell starts to deliver the current (at the current density of  $1\text{-}30\text{ mA cm}^{-2}$ ) is because of the activation losses. Activation losses are dominant in the low current density region as other losses are negligible.

### 2.2.3. OHMIC LOSSES ( $V_{ohm}$ )

Ohmic losses ( $V_{ohm}$ ) are the losses that are due to the resistance to moving charges inside the fuel cell. As explained in section 2.1, the electrons transfer from the anode to the cathode via current collectors, and oxygen ions travel from cathode to anode via the electrolyte. This movement of charges experiences the resistance through the medium in which they travel which leads to loss of potential. This potential loss is called the ohmic loss or  $V_{ohm}$  and is being represented in equation 2.16 [31]

$$V_{ohm} = i(R_c + R_a + R_{cc} + R_e) \quad (2.16)$$

where  $i$  = current density;  $A/cm^2$

$R_c$  = Area specific Resistance of Cathode;  $ohm/cm^2$

$R_a$  = Area specific Resistance of Anode;  $ohm/cm^2$

$R_{cc}$  = Area specific Resistance of Current Collector;  $ohm/cm^2$

$R_e$  = Area specific Resistance of Electrolyte;  $ohm/cm^2$

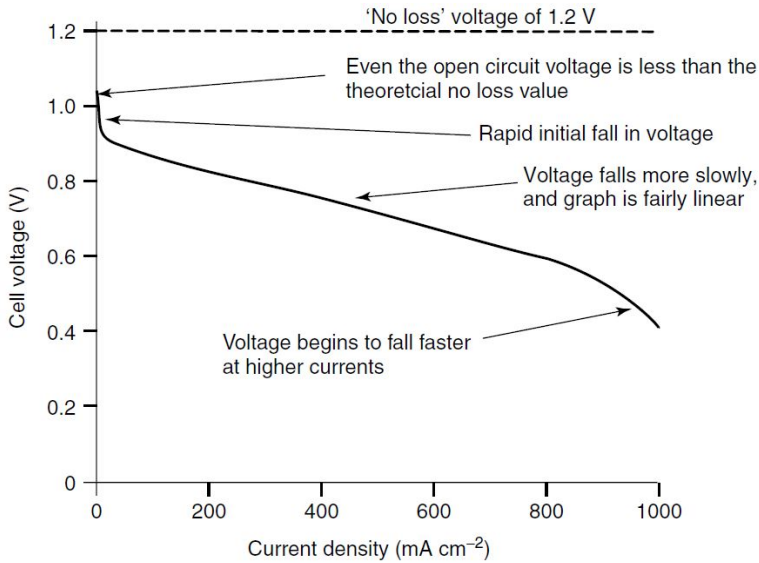


Figure 2.4: Voltage vs Current density for a typical fuel cell  
[31]

Figure 2.4 shows that as the current density increases, the voltage drop is linear and this voltage drop is because of the ohmic losses. An increase in current density increases the movement of electrons and ions in the fuel cell and makes Ohmic losses as the dominant losses.

The temperature has a direct impact on the ohmic losses. The electronic conductivity decreases as temperature increases because the resistivity of metal increases with temperature. The vibrations of molecules in the metal increase with temperature which restricts the movement of electrons and hence, increases the resistivity. But the ionic conductivity increases with temperature as ions are transported through the electrolyte using the chemical reactions. So, with temperature, the rate of reaction increases which increases conductivity.

The effect of ionic conductivity is much higher than electronic conductivity because of the size of the ions. The size of  $O^{2-}$  is higher which leads to higher ohmic losses than the movement of electrons. Hence, even though, the electronic conductivity decreases with increasing temperature, the ionic conductivity increases, and hence, the overall ohmic losses decreases.

#### 2.2.4. CONCENTRATION LOSSES ( $V_{conc}$ )

Concentration losses are the losses that happen when maximum diffusion rates of gases reach the electrodes. As explained in section 2.1, the reaction at anode and cathode happens at a geometrical location called TPBs. The reactants (both  $H_2$  and  $O_2$ ) reach the TPB by the process of diffusion. As the demand for current increases, more and more

reactants need to diffuse to electrodes so that a more number of reactions can take place and more current is produced. But when the maximum diffusion rate is reached and no more reactants can be supplied to electrodes, the concentration of reactants significantly decreases near the electrodes. At the same time, due to an increase in a number of reactions, the concentration of products increases near the electrodes. This mismatch in concentration leads to the reversal of reaction 2.3 and is shown in reaction 2.17.



Due to an increase in the concentration of  $\text{H}_2\text{O}$  near the anode, the reaction shifts backward and hence starts to form  $\text{H}_2$  and  $\text{O}_2$ . Reaction 2.17 is an endothermic reaction, which means that it takes energy from the surroundings in order to move forward. Hence, the energy released by reaction 2.3 to create a potential is being used to form the  $\text{H}_2$  and  $\text{O}_2$ . This leads to a loss of potential which is called the concentration losses or  $V_{conc}$ . Reaction 2.18 shows the equation to calculate the concentration loss and reactions 2.19, 2.20 and 2.21 shows the partial pressure at the anode and cathode for specific species.

$$V_{conc} = \frac{RT}{nF} \ln \frac{P_{\text{H}_2\text{O}tpb} * P_{\text{H}_2}}{P_{\text{H}_2tpb} * P_{\text{H}_2\text{O}}} + \frac{RT}{nF} \ln \frac{P_{\text{O}_2}}{P_{\text{O}_2tpb}} \quad (2.18)$$

where

$$P_{\text{H}_2tpb} = P_{\text{H}_2} - \frac{RT\tau_{an}}{nFD_{an}} i \quad (2.19)$$

$$P_{\text{H}_2\text{O}tpb} = P_{\text{H}_2\text{O}} + \frac{RT\tau_{an}}{nFD_{an}} i \quad (2.20)$$

$$P_{\text{O}_2tpb} = P - (P - P_{\text{H}_2}) * \exp\left(-\frac{RT\tau_{ca}}{2nFD_{ca} * P}\right) i \quad (2.21)$$

Figure 2.4 shows the dominant concentration losses at current densities above  $750 \text{ mA/cm}^2$ . The exponential dip in the voltage is due to the concentration losses which became dominant at higher current densities.

Both temperature and pressure have a significant impact on the concentration losses. The temperature has two effects on concentration losses. First, an increase in temperature increases the diffusion rate which decreases concentration loss. Second, an increase in temperature increases the rate of reaction 2.17 which means that the concentration loss will increase. Hence, an increase in temperature has both positive and negative impacts.

An increase in the operating pressure of fuel cell has a positive impact on concentration loss. An increase in pressure increases the absolute amount of reactants in the fuel and air channel. This leads to higher diffusion rates for both the reactants and hence decreases the concentration loss.

### 2.2.5. OTHER LOSSES

There are other small losses as well which are due to the practical operation of the fuel cell. One of them is the fuel crossover where fuel reaches the cathode and reacts with oxygen to form water via the combustion process which is a loss as this does not contribute to the electrical energy and just produces heat inside the fuel cell.

Another loss is due to the temperature gradients. Fuel cells, especially High-Temperature fuel cells have high-temperature gradients which lead to higher ohmic losses at anode, cathode, and current collectors.

But all these losses are fairly small compared to the three losses mentioned above and are usually negligible and hence are not considered for zero-dimensional and one-dimensional models.

### 2.2.6. FUEL CELL EFFICIENCY

The efficiency of the fuel cell is defined as the ratio of electrical power delivered by the fuel cell and the amount of fuel consumed by the fuel cell. Equation 2.22 shows the fuel cell efficiency and equation 2.23 shows the equation to calculate the total current delivered by the fuel cell. The current delivered is directly proportional to the moles of hydrogen consumed.

$$\eta_{fuelcell} = \frac{V * I}{U_f m_{fc} LHV_f} \quad (2.22)$$

$$I = znF \quad (2.23)$$

where I= current produced by one cell, A

$U_f$ = fuel utilization of cell

$m_{fc}$ = mass of fuel supplied to one cell, kg/s

$LHV_f$ = lower heat value of fuel, j/kg

$z$ = number of moles of hydrogen consumed

### 2.2.7. EFFECT OF PRESSURE AND TEMPERATURE ON FUEL CELL

Sub sections 2.2.2, 2.2.3 and 2.2.4 explain the effects of pressure and temperature on each loss. This section will explain these effects with some examples.

Joshua et al [33] developed a zero-dimensional SOFC model for a NASA research study and compared the result with the experimental data. The fuel cell delivered the power of 186 kW and used methane as the fuel. Figure 2.5 shows the effect of operating pressure on the fuel cell voltage for increasing current density. The figure shows the comparison between experimental data and the results from the zero-dimensional model developed. It can be seen for the reference case of 1 atm that it complements the different losses that have been explained in previous sections. The graph does not show clearly the effect of activation losses as the data for low current density where activation losses are dominant is not shown. But for higher current densities, the voltage decreases because of an increase in ohmic losses, and above the current density of  $0.5 A/cm^2$ , the voltage starts to decrease non-linearly, which is the result of higher concentration losses. But for higher pressures, the voltage increased. First because of the increase in  $V_{oc}$  as shown in equation 2.13. This increase in  $V_{oc}$  shifts the whole curve up and increases

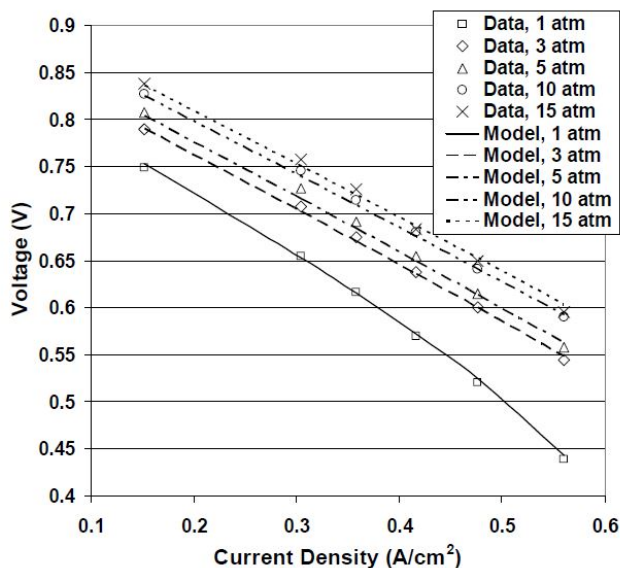


Figure 2.5: Voltage vs Current density for different operating pressures

[33]

the cell voltage for all current densities. As the current density is increased, there is no change in the ohmic losses as pressure has no effect on the resistivity of the charge carriers. The slope of the curves is the same despite different pressures, which proves this point. But at the current densities above  $0.5 \text{ A/cm}^2$ , unlike for the case of 1 atm, at higher pressures, the curve did not become nonlinear, which means the effect of concentration loss did not become dominant. This is because the increase in pressure increases the absolute number of molecules in the channel. As the TPBs are constant and the number of molecules has increased, it is comparatively easy for molecules to find a TPB, hence increasing the diffusion rates as explained in subsection 2.2.4.

Figure 2.6 shows the effect of operating temperature on the fuel cell voltage for increasing current density. The reference temperature is  $650^\circ\text{C}$  and the voltage is decreasing as the current density is increased. With the increase in temperature, first, the activation losses have decreased as explained in section 2.2.2. The slope of the curves is decreasing as the temperature is increased at lower current densities. This decrease in slope is also true as current density is increased (in the ohmic loss dominant region) and this is because of the increase in conductivity of ions in electrolytes as explained in section 2.2.3.

Joshua et al analysis of the 186 kW system found that the fuel cell electrical efficiency of 64.9% at an operating temperature of  $900^\circ\text{C}$  and the pressure of 4.5 bar. The activation, ohmic and concentration losses consist of 4.05%, 81.75%, and 13.4% of the losses, respectively, which proves that the biggest contribution to loss is ohmic loss. Hence, an increase in temperature would be more beneficial. But as mentioned earlier, the losses highly depend upon the properties of the electrode and electrolyte as well. In

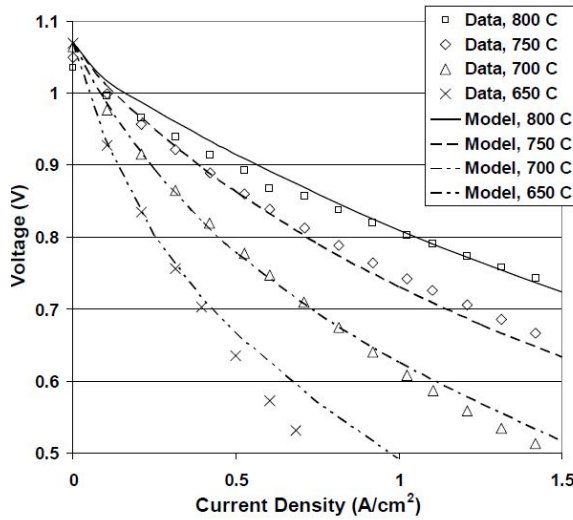


Figure 2.6: Voltage vs Current density for different operating temperatures [33]

some cases, activation losses could be most dominant because of the catalyst used in the fuel cell.

Cadou et al [35] found similar results in which increasing the temperature from 700°C to 800°C improved the system by 27% and increased the pressure from 1 atm to 10 atm improved the system by 30%.

Seidler et al [34] did an experimental analysis of a pressurized SOFC setup at the German Aerospace Center (DLR). The study showed the effect of pressure and temperature on different losses of the fuel cell. Figure 2.7 shows the contribution of different losses in the fuel cell. The losses due to the transportation of ions in the electrolyte are shown in black, the cathode concentration and activation losses are shown in red and green respectively and the activation and concentration losses of the anode are shown in light and dark blue respectively. One thing that should be noted is that the ohmic losses in electrodes are included in the concentration and activation loss of the electrode. Also, it should be noted that the fuel cell is anode supported fuel cell, which means that anode is multiple times thicker than the cathode and hence have higher losses which can be seen in figure 2.7.

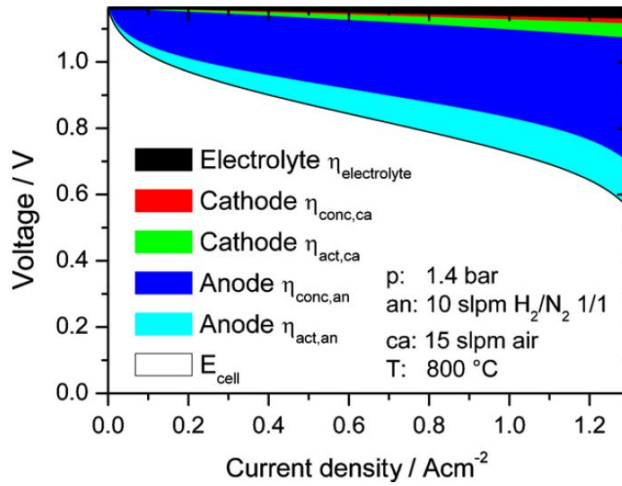


Figure 2.7: Contribution of different losses in the fuel cell operation

[34]

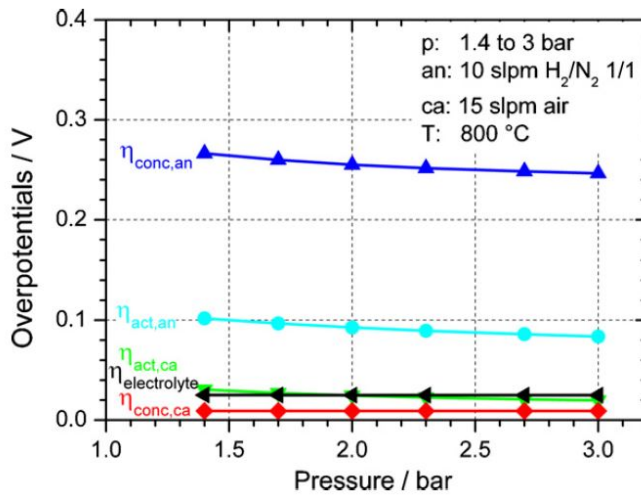


Figure 2.8: Losses vs Pressure

[34]

The figure 2.8 shows the variation of different losses due to changes in pressure. As predicted, both activation and concentration loss decrease with an increase in pressure and it is clear from the anode losses. The same is true for the cathode as well but the change is small because the cathode activation and concentration losses are small due to the smaller size of the cathode. Also, the electrolyte ohmic losses are constant as pressure has no impact on ohmic losses.

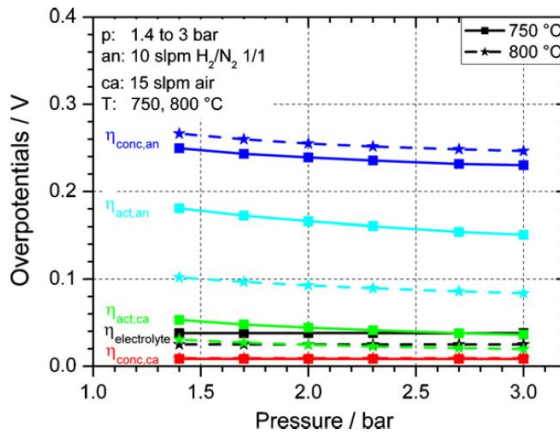


Figure 2.9: Losses vs pressure at different temperature

[34]

Figure 2.9 shows the variation of different losses due to changes in pressure at different temperatures. It can be clearly seen that the activation losses reduce significantly even with a small increase in temperature. Also, the ohmic losses of the electrolyte decrease as well but the concentration losses of both anode and cathode increase. This is because the reaction starts to reverse when maximum diffusion rates have been achieved and energy is being extracted from the environment rather than inserted in the environment. So increase in temperature increase the rate of reverse reaction as it reduces the energy barrier, explained in subsection 2.2.2, for the reverse reaction, hence increasing the losses.

### 2.2.8. EFFECT OF FUEL UTILIZATION

This section talks about the effect of fuel utilization ( $U_f$ ) on fuel cell efficiency. Fuel utilization refers to the ratio of the fuel that has been consumed by the fuel cell and the fuel which has been fed to the fuel cell. The fuel cell does not consume all the fuel that has been fed because it leads to the decrease in Nernst voltage as per equation 2.5. The concentration of the fuel reduces significantly which leads the reaction 2.3 to go in the backward direction.

Another reason is the increase in concentration loss. As concentration is a physical phenomenon and depends on the diffusion of the fuel, reduction in fuel concentration will increase the loss as explained in section 2.2.4 and hence, reduce the cell voltage,  $V$ . Figure 2.10 shows the effect of increasing fuel utilization on the efficiency of the fuel cell. Initially, when the fuel utilization is increased, more current is produced by the fuel cell as more fuel is being consumed. An increase in current increases the power produced and increases the numerator in equation 2.22 and hence, the efficiency.

But if the fuel utilization is increased more than 0.85, then the efficiency starts to decrease and this is because of the reduction in cell voltage. The increase in current is not able to complement the decrease in cell voltage and hence the total efficiency tends to decrease. This means that there is a need to optimize for the best fuel utilization for a

specific fuel cell operating condition.

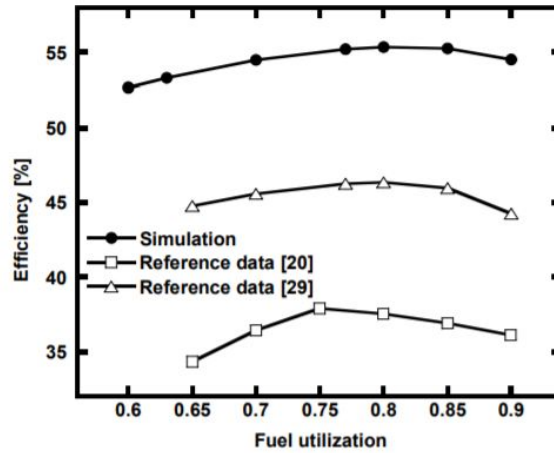


Figure 2.10: Fuel Utilization vs Efficiency

[36]

### 2.3. DIFFERENT TYPES OF FUEL CELL

The working principle of fuel cell is discussed in section 2.1 but there are different types of fuel cells each of which has its own advantages and disadvantages. Tables 2.2, 2.3 and 2.4 gives an extensive insight into different fuel cell technologies and their advantages and disadvantages.

fuel cell	Anode	Cathode	Electrolyte
<b>Proton Exchange Membrane Fuel Cell (PEMFC)</b>	Platinum	Platinum	Nafion
<b>High Temperature Proton Exchange Membrane (HTPEMFC)</b>			Phosphoric Acid
<b>Solid Oxide fuel cell (SOFC)</b>	YSZ doped Ni CeO <sub>2</sub> doped Ni	Lanthanum Strontium Manganite (LSM) or Lanthanum Thynacite (LSCN)	Ytria Stabilized Zirconia (YSZ) or Gadolinium Oxide doped Cerium Oxide
<b>Molten Carbonate fuel cell (MCFC)</b>	Nickel	Nickel Oxide (NiO)	Molten Lithium, Sodium or Potassium Carbonate

Table 2.2: Comparison of different fuel cells (Part A)

[31][37] [38] [39] [18] [40]

<b>fuel cell</b>	<b>Operating Temperature °C</b>	<b>Efficiency %</b>	<b>Specific Power kW/kg</b>
<b>Proton Exchange Membrane Fuel Cell (PEMFC)</b>	70-80	40-60 electrical	1.2 (Stack) 0.7 (System)
<b>High Temperature Proton Exchange Membrane (HTPEMFC)</b>	140-180	38-49 electrical	1
<b>Solid Oxide fuel cell (SOFC)</b>	500-1000	60 electrical 85 Integrated	0.5(Stack) 0.277(System) 2.5(NASA)
<b>Molten Carbonate fuel cell (MCFC)</b>	600-700	50 electrical 75 Integrated	

Table 2.3: Comparison of different fuel cells (Part B)

[31][37] [38] [39] [18] [40]

fuel cell	Advantages	Disadvantages
<b>Proton Exchange Membrane Fuel Cell (PEMFC)</b>	<ol style="list-style-type: none"> <li>1) High Power Density</li> <li>2) High Specific Power</li> <li>3) High TRL</li> <li>4) Faster Start-up</li> </ol>	<ol style="list-style-type: none"> <li>1) High sensitivity to Sulphur and other impurities</li> <li>2) Very low temperature operation range</li> <li>3) Requires robust cooling system</li> <li>4) Requires humid electrolyte.</li> </ol>
<b>High Temperature Proton Exchange Membrane (HTPEMFC)</b>	<ol style="list-style-type: none"> <li>1) High Power Density</li> <li>2) High Specific Power</li> <li>3) Faster Start-up</li> </ol>	<ol style="list-style-type: none"> <li>1) High sensitivity to Sulphur and other impurities</li> <li>2) Low temperature operation range</li> <li>3) Requires robust cooling system</li> <li>4) Low TRL.</li> </ol>
<b>Solid Oxide fuel cell (SOFC)</b>	<ol style="list-style-type: none"> <li>1) High Efficiency especially in integrated system</li> <li>2) Fuel Flexibility</li> <li>3) Suitable for hybrid gas turbine cycles</li> <li>4) High TRL than MCFC</li> <li>5) High resistance to sulphur poisoning</li> </ol>	<ol style="list-style-type: none"> <li>1) Low Specific Power due to auxiliary systems</li> <li>2) High temperature corrosion</li> <li>3) Long Start-up</li> <li>4) Slow Transient Response</li> </ol>
<b>Molten Carbonate fuel cell (MCFC)</b>	<ol style="list-style-type: none"> <li>1) High Efficiency especially in integrated system</li> <li>2) Fuel Flexibility</li> <li>3) Suitable for hybrid gas turbine cycles</li> </ol>	<ol style="list-style-type: none"> <li>1) Low resistance to sulphur poisoning</li> <li>2) Low specific Power</li> <li>3) Long Start-up</li> <li>4) High temperature corrosion</li> <li>5) High Thermal Stresses</li> </ol>

Table 2.4: Comparison of different fuel cells (Part C)

[31][37] [38] [39] [18] [40]

### 2.3.1. LOW TEMPERATURE FUEL CELL(LTFC)

As the name describes, the LTFC operates at low-temperature range of 70° to 200°C. Even though with similar temperature ranges, the fuel cells operate with different materials and different chemical reactions. Different type of LTFC are given below.

### 2.3.2. PROTON EXCHANGE MEMBRANE FUEL CELL (PEM FC)

Proton Exchange Membrane or PEM as the name suggests is a type of fuel cell in which the proton or  $H^+$  ion (if hydrogen is considered as a fuel) travels from anode to cathode and reacts with oxygen at TPB on the cathode side.

The working principle is similar to what has been explained in section 2.1. The  $H_2$

enters the fuel channel and in presence of the catalyst, usually, platinum converts to  $H^+$  ion and gets adsorbed on the catalyst. The electrolyte membrane of the PEM is called Nafion and uses water as the electrolyte medium to transport ions from one side to another. The  $H^+$ , in the presence of TPB, reacts with the water in the Nafion to form  $H_3O^+$  ion or Hydronium as shown in reaction 2.24. This Hydronium ion transport the  $H^+$  ion from anode to cathode where the final reaction 2.3 takes place.



PEM is one of the most researched and applicable fuel cell present in the market. It has applications not only in energy conversion units but also in automobiles. This is because of its high power density, high specific power, high technology readiness level and high efficiency of up to 60% for  $H_2$  and 40% for reformed or hydrocarbon fuel. Another advantage of PEM is its high Gibbs Free Energy. According to equation 2.7, as fuel cell operates near to the standard temperature, the Gibbs Free Energy is high and hence, a high open-circuit voltage 2.5. This means the losses due to entropy are less compared to high-temperature fuel cell.

#### Disadvantages of PEMFC:-

- **Low-Temperature Range:-** As mentioned in table 2.3, PEM works in the range of  $70^\circ\text{-}80^\circ\text{C}$ . This is because it uses water as an electrolyte which gets converted to steam at temperatures above  $100^\circ\text{C}$ . Hence, if the temperature goes near to  $100^\circ\text{C}$ , water in the Nafion will convert to steam which will reduce the conductivity of the electrolyte as explained above. So, an average temperature range of  $70^\circ\text{-}80^\circ\text{C}$  is ideal for PEMFC. This is the reason that PEMFC requires a robust cooling system because even a small deviation in temperature can lead to drastic changes in fuel cell performance. This cooling system also reduces the efficiency of the fuel cell as it is being run by the fuel cell.
- **Constant Humidification:-** Due to the requirement of water for fuel cell operation, there is a need for constant humidification in the cell. Even though the average temperature of the fuel is less than  $100^\circ\text{C}$ , the local temperature of some regions is quite high which leads to the formation of steam and hence, reduction of water in Nafion. Hence, constant humidification is required and water is being provided along with the fuel.
- **Higher Losses:-** As the temperature has a significant impact on the losses of the fuel cell, all the three losses, Activation, Concentration, and Ohmic, will increase as explained in section 2.2. So, even though the open circuit voltage is higher for the PEM, the system efficiency is lower than the High-Temperature fuel cells, especially in the case of reformed fuels.
- **Sulphur and Carbon Poisoning:-** Noble metals are used as electrodes in PEMFC because the activation energy of the reaction is very high at the lower operating temperature, these metals are susceptible to poisoning even if a small amount of

sulfur or carbon or other impurities is present in the fuel, it reacts with the electrode and forms a layer which reduces the amount of TPBs and hence, reduce the activity and affect the Cell Performance.

## 2

### 2.3.3. HIGH TEMPERATURE PROTON EXCHANGE MEMBRANE FUEL CELL (HT-PEM FC)

High-Temperature Proton Exchange Membrane fuel cell is PEM fuel cell that operates at a higher temperatures. Unlike PEM which uses Nafion as an electrolyte and needs constant humidification, HTPEM fuel cell has phosphoric acid and hence can go to higher temperatures of up to 200°C [38]. This fuel cell is still in its preliminary stage of development and the company(HyPoint) which is developing this fuel cell, has claimed that this fuel cell will have significantly higher specific stack power of 2.5 kW/kg [38] because of using a smaller balance of plant due to not so strict cooling requirements. But the cooling requirements are still there and hence, the electrical efficiency is still lower than PEMFC and high-temperature fuel cells.

### 2.3.4. HIGH TEMPERATURE FUEL CELL(HTFC)

High Temperature fuel cells are the fuel cells that operate in the temperature range of 500° to 1000°C. Due to its high temperature, the losses of the fuel cell are significantly low when compared to LTFC. But at the same time, the open-circuit voltage of HTFC is lower due to lower Gibbs Free energy

### 2.3.5. SOLID OXIDE FUEL CELL(SOFC)

SOFC operates in the temperature range of 500° to 1000°C [18]and has a solid electrolyte made of ceramic as the name suggests. The electrolyte is doped with ceramic because ceramic has high temperature sustenance. The porous solid electrolyte is doped with either Ytria Stabilized Zirconia(YSZ) or Gadolinium Oxide doped Cerium Oxide( $GdCeO_2$ ) which conducts the  $O^{2-}$  ions from cathode to anode as explained in section 2.1. SOFC is among one of the highest efficiency fuel cells with 60% electrical and 85% in integrated systems [24] and hence is being researched for big power units among the high temperature fuel cells.

**Advantages of SOFC are given below:-**

- **Fuel Flexibility:-** SOFC has the highest fuel flexibility which means a large variety of fuels can be used in the fuel cell. In LTFC, due to higher activation energy, noble metals are required but it is not the case in the HTFC. Abundant metals like Nickel doped with electrolyte works well and hence HTFC is less prone to Sulphur poisoning and impurities. Because of this, multiple fuels can be used including hydrocarbons and Ammonia.
- **High Exergy Heat:-** One of the big advantages of SOFC or HTFC, in general, is the high exergy heat that they release via byproducts of anode and cathode. Due to the high operating temperature, the heat that comes out of fuel cell is of high exergy which can be further used either for heating the fuel, reforming the process of the hydrocarbon fuel or can be expanded in the turbine to increase the overall

efficiency in an integrated system. This is one of the reasons that SOFC is the first choice for integrated systems and works very well with gas turbines in a hybrid set-up. This is also the reason that HTFC has higher efficiency for reformed fuel.

- **High Temperature Range:-**The SOFC has a wide operating range unlike LTFC because of the ceramic electrolyte as they can sustain higher temperature fluctuations. The temperature fluctuation in the SOFC can go up to 200 K compared to 15-20 K in PEMFC and 40 K in HTPEMFC. This means there is no need for a sophisticated external cooling system like a liquid cooling system. The air which acts as an oxidizer can also act as a coolant for fuel cell, which also increases system efficiency.

#### Disadvantages of SOFC are given below:-

- **Specific Power:-** The specific power of SOFC is significantly lower than the PEMFC and has three reasons. First, the SOFC needs a balance of plant-like reformer, desulfurized, heat exchangers, etc which increases the system weight and volume. Second, as the temperature of the system is high, the stresses inside the fuel cell are high and hence it needs a strong structure that increases system weight. Third, the system has always been researched from the perspective of a stationary system in which system-specific power is not a constraint. But NASA has developed a SOFC specifically for Aerospace applications and has been able to achieve a specific power of 2.5 kW/kg and Volumetric Power Density of 7.5 kW/L, which is 5 times and 8 times higher than the commercial SOFC respectively[27].
- **High Temperature Corrosion:-**Due to high temperature, the materials used inside the fuel cell are more prone to chemical attacks. Hence, regular maintenance is required for the fuel cell.
- **Thermal Stresses:-** The temperature inside the fuel cell along the fuel channel varies significantly. For example, near the entry of the fuel cell, the concentration of fuel is high and hence a bulk reaction is taking place at the beginning of the fuel cell. This leads to a release of a lot of heat and hence high temperatures at the beginning of fuel cell. But as the concentration of fuel reduces along the channel, the number of reactions reduces, and hence the end of fuel channel is at a relatively less temperature. The temperature difference between the start and end of fuel cell could be as high as 200 K. These large temperature gradients lead to more stresses inside the fuel cells.

Another reason for thermal stresses is the difference in Thermal Expansion Coefficients(TEC) of different sub-components like electrodes, interconnectors, electrolytes etc. One of the reasons that electrolyte is doped with the electrode, along with the increase in TPB, is to reduce the TEC difference between electrode and electrolyte.

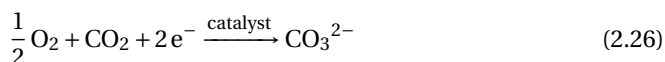
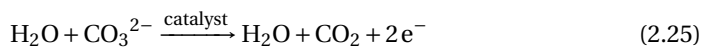
- **Long-Startup Time:-** As SOFC operates at a higher temperature, it takes longer to start a SOFC as the temperature of the fuel cells needs to reach at least 500°C so that the reaction starts inside fuel cell.

- **Transient Response:-** As the electrolyte and electrode in SOFC are made of ceramic so that it can sustain high temperatures, it has a negative impact as well. When the demand for current is rapidly increased, there is a need to increase the current density which can be attained by increasing the operating temperature of fuel cell. Increasing the temperature will increase the diffusion rate and hence the increase in access of TPBs by  $H_2$  and  $O_2$ , which will increase the current density. Also, increasing the temperature will reduce the losses inside fuel cell which will increase the voltage and hence the power delivered. But as ceramic has high resistance to temperature, the increase in temperature is slow as well. Hence, the transient response of SOFC is slow.

### 2.3.6. MOLTEN CARBONATE FUEL CELL(MCFC)

Molten Carbonate fuel cell operates within the temperature range of  $600^\circ$  to  $700^\circ$  [18]. MCFC is similar to SOFC but the electrolyte is either molten Lithium, Sodium, or Potassium carbonate. The reaction for the MCFC Anode and cathode is given in reaction 2.25 and reaction 2.26 respectively.

MCFC has all the advantages that SOFC offers except the lower efficiency it offers as well as the lower resistance to sulfur poisoning and other impurities. This is because MCFC uses molten carbonate which is more susceptible to sulfur poisoning.



The efficiency of MCFC is 50% electrical and up to 75% for integrated systems[18]. This is due to higher losses in the electrolyte and relatively low temperature than SOFC which lead to higher activation energy and higher area specific resistance.

### 2.3.7. SELECTION OF FUEL CELL

The characteristics of multiple fuel cells have been explained in section 2.3.1 and section 2.3.4 but in order to integrate fuel cell with the jet engines, there is a need to understand the advantages and disadvantages of different fuel cell types and how to complement their disadvantages with minimum addition of complexity and weight while maintaining the reliability of the system. Following are the parameters on which the selection of fuel cell is based.

- **Efficiency:-**One of the main reasons to use the fuel cell is the efficiency it offers. When it comes only to electrical efficiency, both PEM and SOFC have similar efficiencies and there is no favorite. But in an integrated, SOFC performs much better because of the reasons given in 2.3.4. Both HT PEM and MCFC have lower efficiencies and hence in terms of efficiency, **SOFC** is a better choice.
- **Specific Power:-**In specific power, LTFC is significantly better than HTFC. Especially the HTPEM which comes under the category of state of the art fuel cell technology. But on the other hand, NASA's Bi-Electrode fuel cell promises 2.5 kW/kg which is five times the current commercially available SOFC. But HTPEM has tested results available and hence **HTPEM** is a clear winner.

- **Balance of Plant:-** All fuel cells need some basic balance of plant-like power converters, batteries, and control systems but other auxiliary systems depend completely on the type of fuel cell. For example, LTFC requires a robust cooling system, desulfurizer and reformer which increases the system weight and decreases the overall efficiency but still has higher specific power than HTFC. HTFC requires auxiliary systems like heat exchangers, insulation, turbine, heat pumps, etc which increases weight but also increases efficiency. Hence, it completely depends on the type of application needed.

But it should also be understood that in an integrated system, some of the balance of plant requirements for SOFC like compressor, heat exchangers, etc are already present in the propulsion system. Hence, the balance of plant requirements for SOFC will reduce compared to PEM. This will also increase efficiency as extra energy is not needed to drive these systems. Hence, SOFC may be better but the calculation has to be done.

- **Sensitivity to Temperature Fluctuation:-** Sensitivity to temperature fluctuation is an issue in a gas turbine integrated fuel cell because the temperature of a gas turbine varies based on the conditions in which it is operating. For example, during take-off, climb, or transient high power conditions, the temperature variations are high in compressors of gas turbines, and in an integrated fuel cell gas turbine hybrid system, it may lead to large and abrupt temperature variations in the inlet of fuel cells as air at the cathode is coming from the compressor of the gas turbine. LTFC has a very high sensitivity to temperature as explained in section 2.3.1 and even after using a robust cooling system, may have a bad impact on fuel cell performance. Also, in the conditions of failure of cooling systems, the fuel cell may need to shut down as well.

On the other hand, HTFC has very less sensitivity to temperatures and can have large variations in temperature hence more suitable for integration with gas turbines.

- **Technology Readiness Level(TRL):-** Technology Readiness Level is important because of the safety and reliability that Aerospace industry standards demands, especially for the propulsion systems which is comparatively very high. The TRL of PEM is the highest because of intense research and testing done in past few years by the automobile industry. TRL for SOFC is also high but not as high as PEM and hence needs robust testing and practical applications for further improvements, especially for the transportation applications. MCFC, even though being in existence for a long time, still has lower TRL because of the lower efficiency compared to SOFC and HTPEM which is promising, but has low TRL as it is still in the development and testing phase. Hence, from the TRL perspective, both PEM and SOFC have an advantage but for the specific application of transportation, **PEM** is the clear winner.
- **System Integration:-**fuel cell System integration into the current aircraft system architecture is one of the most important factors because it is very improbable that a new aircraft will be designed just to integrate the fuel cells into the aircraft.

Hence, fuel cell systems should be safe, compact, and easy to integrate. LTFC are usually more compact because of their high volumetric power density of 3.1kW/L [41] compared to SOFC which has a volumetric power density of less than 1 kW/L. Although multiple startups and research institutions are expecting to significantly increase the volumetric power densities for both PEM and SOFC, the values given above are the current commercial systems. The expected volumetric power density for PEM is more than 5 kW/L [42] and for SOFC is near 7.5 kW/L [27].

But the Volumetric power density given above is for stack only and does not include the balance of plant required by the fuel cell. Hence, the system volumetric power density decreases significantly and depends on the operation for which it is being used. But **PEM** is still more compact than SOFC.

- **Fuel:**-The type of fuel used in fuel cells will also have a big impact on its suitability for the aircraft. LTFC have an excellent performance for hydrogen but for other fuels like hydrocarbons, they need a very efficient fuel reformer, humidifiers, desulfurized, etc which increases the weight as well as decreases the efficiency of the whole system. On the other hand, HTFC can use practically any fuel which is being used in aircraft along with natural gas, ammonia, and sustainable aviation fuels which are more probable in the future. HTFC also need fuel reformer and desulfurized but they have very high resistance to impurities. Hence, HTFC are better suited for current and future aviation fuels.

Based on the comparison given above, both HTPEM and MCFC are not a good fit because of their low TRL and low efficiency. Between PEM and SOFC, there is a need for a more thorough discussion. PEM looks great for aircraft applications as it is more compact, has higher specific power, better transient response, high TRL, and good efficiency. This is the reason that for general aviation which has smaller power requirements, PEM is the first and currently the only choice when it comes to fuel cells. But for a commercial aircraft and especially for a turbofan integrated propulsion system, PEM might not be a good choice because of its low-temperature operation range, lower efficiency, and high dependency on the balance of the plant.

SOFC, on the other hand, does have lower specific power and volumetric power density but has higher efficiency for the integrated systems. A big fraction of the balance of plants for SOFC like compressors, heat exchangers, combustors, etc is already present in a gas turbine. This will lead to lower fuel consumption and the author believes that this may compensate for the weight it adds to the aircraft. Also, the fuel flexibility and low sensitivity to temperature fluctuation are a big advantage in the integrated systems. For the problem of transient response, in the integrated systems, the gas turbines are still the major part of the system and hence can be used for a transient response as done in the current aircraft.

It is clearly understood that compromises have to be made on both, PEM and SOFC but compromises made on SOFC has very little impact on its efficiency and emissions compared to PEM which has an efficiency of nearly 40-45% with the balance of plant which is only a few points higher than a conventional gas turbine and weakens the argument of using it in the first place.

Also, as mentioned in section 2, SOFC has not been explored for the application of transportation and hence the performance from the perspective of specific power and the transient response was not a priority for researchers and industries. But when the option was explored by NASA, the specific power has been improved by 5 times.

Hence by considering all the factors, **Solid Oxide fuel cell** has been chosen as the right choice for fuel cell integrated turbofan propulsion system for commercial aviation.



# 3

## SOLID OXIDE FUEL CELL-GAS TURBINE CONCEPTS

A Solid Oxide fuel cell-Gas Turbine (SOFC-GT) hybrid is not a new concept. There have been multiple studies in the past for both ground and stationary systems. Some studies for Aerospace applications like Auxilliary Power Unit(APU) have also been done. This section is going to explore these studies in order to understand the working principle and the challenges of SOFC-GT concepts in a more detailed manner.

### 3.1. SOFC-GT CONCEPTS FOR GROUND APPLICATIONS

Figure 3.1 shows a detailed system architecture of the SOFC-GT hybrid system. This configuration is one of the most common configurations used for the SOFC-GT hybrid systems. It consists of a compressor, a pre-reformer, a burner, a turbine, a SOFC stack, a booster, and multiple heat exchangers. The working principle of the system is below.

- First, air is compressed in the compressor which increases the pressure and temperature of the air. The compressed air is pre-heated using two heat exchangers. The first one is being heated by exhaust air coming from the turbine and the second one is heated from the byproducts of the cathode.
- Second, fuel, in this case, methane ( $CH_4$ ), is pre-heated in a similar manner as the air by using the heat exchangers. The exhaust gas from the turbine is used to heat the fuel. Then the fuel is fed to the pre-reformer.
- The fuel is then reformed in the pre-reformer. Reformer is a device which converts hydrocarbon fuel into  $CO_2$ ,  $CO$  and  $H_2$ . The reactions of the reformer are given in reaction 3.1 and 3.2. Pre-reformer, just like a reformer, partially converts fuel into  $CO_2$ ,  $CO$  and  $H_2$ . This is done so that when the fuel mixture enters the anode, the reaction starts to take place immediately. The rest of the unreformed fuel is reformed inside the fuel cell.

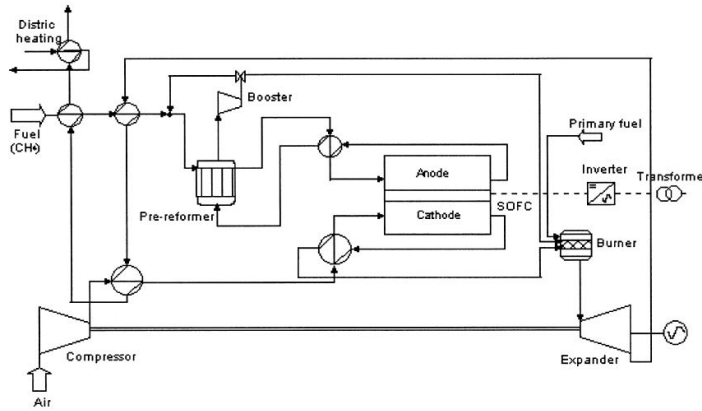
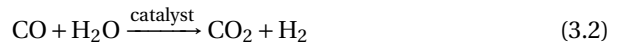
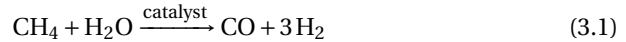


Figure 3.1: SOFC-GT system architecture

[24]

The reforming process requires two things, heat and steam (as can be seen from reaction 3.1 and 3.2). Both are provided by the fuel cell. The byproducts of the anode include high exergy heat and steam, as mentioned in reaction 2.1, are put into the reformer.



- The partially reformed fuel is then put inside the SOFC which reacts with air to form steam and electric power. The byproducts of both anode and cathode, as mentioned before, are used for reforming and heating purposes respectively. These by-products are then fed to the combustor to generate heat.
- The combustor burns the unutilized fuel ( $\text{H}_2$ ) coming from the fuel cell and some extra primary fuel which is being directly fed to the combustor to produce heat and increase the temperature of the combustor outflow. This flow is then used by the turbine to extract the energy it. The turbine (expander in fig 3.1) uses this energy to run the compressor and an external generator which produces more electricity. The energy left in the exhaust gas is then used to increase the temperature of air and fuel using heat exchangers.

The biggest advantage of the SOFC-GT integrated system is that both systems complement each other.

- As explained in section 2.2.7, increasing the pressure and temperature of fuel cell increase the fuel cell efficiency. As a gas turbine works at high temperature and pressure, the working fluid from the gas turbine, or compressor in specific, can be

Reference	Pressure (Bar)	SOFC Temperature(K)	SOFC-GT Power	GT Power Fraction	SOFC Power Fraction	Thermal Efficiency (%)
Massardo[43]	8	1307	-	63%	37%	76
Campanari[44]	3.8	1173	259.5 kW	78.5%	21.5%	64.9
Chan[45]	5	1200	1.3 MW	80%	20%	61.9
Calise[46]	7	1073-1273	1.5 MW	-	-	60
Costamagna[47]	4	1173	250 kW	80%	20%	60
Haseli[48]	4	1273	2.42 MW	-	-	60.55
Whiston[49]	15	1200	545.9 MW	67%	33%	68.1

Table 3.1: Comparison of different SOFC-GT researches

extracted and fed to the fuel cell. Then the byproducts of the fuel cell is fed directly into the combustion chamber. This extraction and injection of air from the fuel and into the fuel cell respectively is very beneficial as the pressure losses in the fuel cell are low, hence the impact of using the air for fuel cell operation on gas turbine efficiency is small but the increase in the efficiency of the system is very high due to no external auxiliary systems to heat and pressurize the inlet air and fuel for SOFC.

- The byproducts of the fuel cell which includes high exergy heat and unutilized fuel can be used directly in the gas turbine. This makes these two technologies highly complementary in nature as the losses of one technology (fuel cell) are fuel (in terms of heat and unutilized fuel) for another technology (gas turbine). This complementary nature makes the system more efficient.

Because of the reasons given above, the efficiency of the SOFC-GT hybrid system has increased significantly when compared to the stand-alone SOFC and GT systems. Palsson et al [24] researched a 500 kW system running on methane and has an external pre-reformer that reforms the 30% of fuel entering the fuel cell (fig 3.1). In the baseline configuration, 30% of fuel is being consumed by the turbine and the system achieved an electrical efficiency of 65% and total system efficiency (electricity +heat) of more than 85% at an operating pressure of 2 bar and operating temperature of 950°C.

Table 3.1 shows the operating pressure, temperature, gas turbine power, SOFC-GT hybrid system power, and the efficiency of multiple studies done in past. It is clear that there is a significant increase in the efficiency of the SOFC-GT hybrid system when compared to a gas turbine alone. For example, Campanari [44] researched a SOFC-micro-gas turbine system of 260 kW and achieved an efficiency of 64.9% compared to a gas turbine efficiency of 29.9%. Similarly, Haseli et al [48] achieved an efficiency of 60.55% which is 27.8% higher than a traditional gas turbine. The power distribution between gas turbine and fuel cell has not been mentioned in the paper. Haseli also researched on the entropy generation in different components and compared it with the conventional gas turbine and the results have been discussed in detail below.

Figure 3.2 shows the entropy generation in different components and it is clear that the combustor and SOFC are the major entropy generators with 31.4% and 27.9% fol-

lowed by the recuperator with 17.4% of total entropy generated. The high entropy generation is because of the high heat transfer rates in these components.

Along with this, the entropy generation increased due to an increase in pressure and temperature. An increase in pressure requires more work output from the compressor and turbine and an increase in temperature requires more fuel to be added which leads to higher heat transfer. Both of these phenomena generate more entropy.

Figure 3.3 compares the entropy generation rate vs the compression ratio for SOFC-GT hybrid and conventional gas turbines. The SOFC-GT produces 154 W/K more power entropy than a conventional engine because of the additional SOFC but the overall efficiency of the SOFC-GT is still 27.8% higher in absolute terms when compared to a conventional gas turbine. This is because the high exergy flow gas coming out of fuel cell is being used in the gas turbine to extract the energy and produce electricity. This provides the mathematical proof for the explanation of the higher efficiency of SOFC-GT given above.

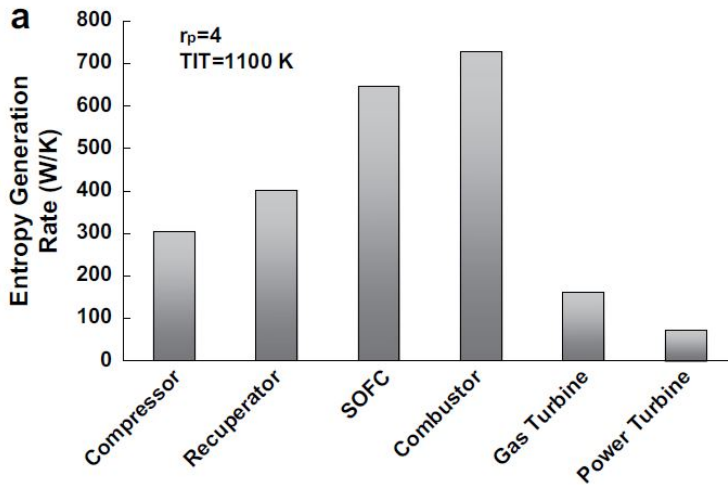


Figure 3.2: Entropy generation in different components of SOFC-GT hybrid system

[48]

All systems explained above-used methane or natural gas as fuel and had similar system architectures as shown in figure 3.1 with the only difference of the reforming process. Unlike [24], which had a pre-reformer to partially reform the fuel, internal reforming has been used in all the studies mentioned in table 3.1.

Compared to other studies, Massardo et al[43] show a comparatively higher efficiency of 76%. Although the system total power is not known which will have an impact on the system efficiency as bigger gas turbines have higher efficiency, the efficiency of 76% is still very high. The reason for this is the high operating pressure and temperature of the system which has been explained in section 2.2.7. Increasing the pressure beyond 8 bar will lead to a decrease in efficiency because the work consumed by the compressor

outweighs the increase in efficiency of SOFC and work output of the gas turbine. This is a similar case [43].

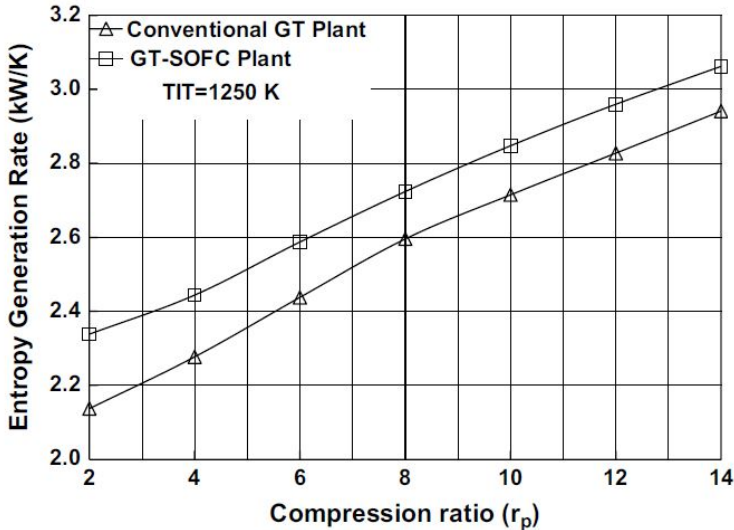


Figure 3.3: Entropy generation vs compression ratio

[48]

### 3.1.1.1. SHORTCOMINGS OF SOFC-GT SYSTEMS FOR GROUND AND STATION-ARY APPLICATIONS

Even though the SOFC-GT hybrid system for ground applications shows the significant improvement in the system efficiency, it should be noted that these significant improvements will not be possible for a SOFC-GT hybrid propulsion system for a commercial aircraft and they are as follows:-

- **Power Fraction:-**One of the biggest reasons for higher efficiency is that the large fraction of power is coming from the SOFC as given in table 3.1. The gas turbine is only used as a bottoming cycle to use the waste fuel and heat. No extra air is being put in the combustor to increase the power output of the gas turbine.

But for aircraft propulsion systems, turbofan will still be the major thrust producer and SOFC will either aid the turbofan shaft or a distributed propulsion system along with the aircraft electricity requirement. This is because the specific power of commercially available SOFC is significantly less than a turbofan.

- **Use of Auxiliary systems:-** Multiple auxiliary systems like heat exchangers, air and fuel pre-heaters, etc. have been used in ground systems which helps in very efficient heat recovery and reduces the losses to the environment. For example,

Palsson[24] system (figure 3.1) used 5 heat exchangers in the system which is not possible in an aircraft propulsion system because of weight constraints.

- **High operating pressure:-** Ground systems mostly work in the pressure range of 3-8 bar which is lower than a turbofan operating pressure. So, it makes sense to think that the SOFC performance will be improved by the higher operating pressure of turbofan 2.2.7. But the rate of improvement in efficiency with pressure at higher pressure is very low (a detailed explanation has been given in section 3.2). Hence, the higher pressure of air especially at take-off and landing will not be of many benefits. But operating the fuel cell at higher pressure will have an impact on the specific power as the fuel cell structure needs to be able to sustain those high pressures during take-off. Hence, the efficiency improvement due to the increase of pressure may have a negative impact on the performance of the overall fuel cell.

### 3.2. SOFC-GT CONCEPTS FOR AEROSPACE APPLICATIONS

Due to multiple advantages offered by the SOFC-GT hybrid concept, the system has been researched for multiple Aerospace applications along with all segments of aircraft as well. Most of the studies were done for smaller systems with low power output and hence, were done either for Auxiliary Power Unit (APU) for large commercial aircraft or for the propulsion system of High Altitude Long Endurance (HALE aircraft).

Steffen et al [50] at NASA researched a SOFC-GT APU with a power output of 440 KW developed for a 300-passenger aircraft. The system architecture is shown in figure 3.4. It is similar to a SOFC-GT system for ground applications with an exception of an additional water process which is used for the steam reforming process. The results of the study concluded that with the current SOFC technology (the year 2005), during the cruise, the SOFC-GT hybrid APU was not able to outperform turbine-driven generators even though the SOFC-GT concept has a system efficiency of 62.6%. The fuel cells used have the stack specific power of 0.265 kW/kg and a system-specific power of 0.315 kW/kg compared to the Honeywell APU turbine which is being currently used in Boeing 777 and has a specific power of 2.92 kW/kg. The system-specific power is higher than SOFC specific power because 34% of power is coming from the turbine.

Waters and Cadou[35] researched an engine integrated SOFC for efficient electric power generation for aircraft. The aircraft considered is a small regional aircraft and a HALE aircraft. The system is shown in figure 3.5. The system working principle is similar to what has been explained before with two exceptions. First, the SOFC has been implemented directly into the engine nacelle and second is the Catalytic Partial Oxidation ( $CPO_x$ ) reforming process. Unlike steam reforming which requires water or steam for the reaction to take place,  $CPO_x$  does not need steam and hence reduces the weight of the system. The study also considered the impact of fuel cell on the overall drag of the aircraft and included it in overall fuel consumption.

The result of the study shows that the fuel burn has been reduced by more than 5% and electric power output potential has increased by more than 500% at a cost of 5-8% specific power. An intriguing thing about the concept is that, unlike other SOFC-GT concepts, there is no separate turbine and compressor for SOFC, which reduced the weight of the system significantly and hence made the system more attractive.

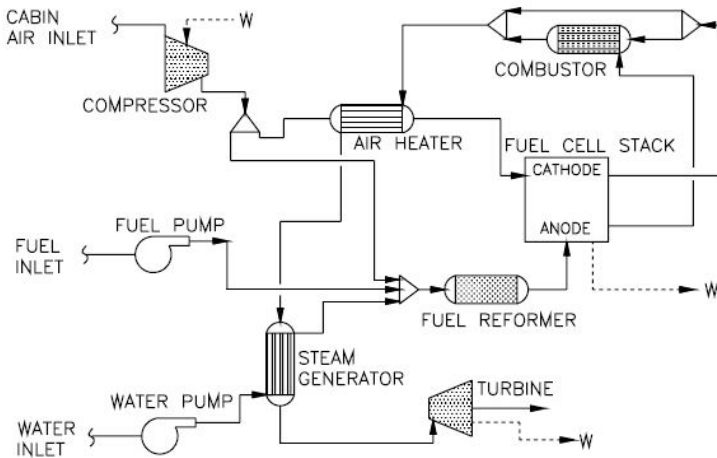


Figure 3.4: The system architecture of SOFC-GT APU

[50]

Three different gas turbines have been used for the research, a turbojet, a low Bypass Ratio (BPR) turbofan, and a high BPR turbofan. The SOFC-GT engine was compared with a conventional engine which has a generator with a specific power of 1 kW/kg, connected to the low-pressure shaft which generates electricity. The results showed that the reduction in fuel burn for a 200 kW power system for a turbojet engine was 14.7%, for a low BPR turbofan is 16.8% and for a high BPR is 11.3%. The different values of the fuel burn for high BPR and low BPR turbofan is because high BPR turbofan is inherently more efficient than a low BPR turbofan. Hence, electricity produced from a high BPR turbofan is more efficient. But the reason for the higher advantage for low BPR turbofan compared to turbojet has not been explained in the paper.

Sensitivity analysis for the system has also been done by changing various operating parameters. From sensitivity analysis, it has been concluded that the gas turbine mass, SOFC exit temperature, fuel cell losses, fuel utilization percentage, and  $CPO_x$  performance has a high impact on overall system performance whereas the impact of  $CPO_x$  mass, turbine, and compressor efficiency and SOFC heat loss does not have much impact on system performance.

The paper also researched the impact of temperature and pressure variation on the fuel cell and  $CPO_x$ . Figure 3.6 shows that the increase in temperature increases the cell voltage as expected. Along with this, the performance of  $CPO_x$  has also improved as an increase in temperature increases the reaction rate.

Figure 3.7 shows the impact of pressure variation on the fuel cell and  $CPO_x$ . The pressure increase improves the fuel cell performance but it should be noted that the increase in pressure to higher values does not have a high impact on the fuel cells. For example, when pressure is increased from 1 atm to 10 atm, at a current density of  $1 A/cm^2$ , the cell voltage increased from approximately 0.6 V to 0.74 V but the improvement from 10 atm to 20 atm is insignificant.

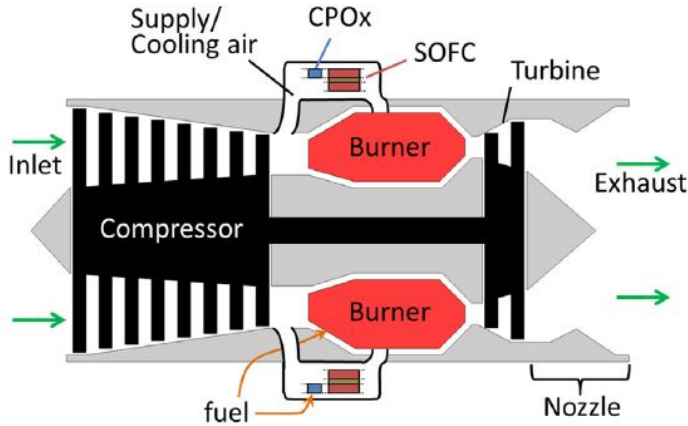


Figure 3.5: System architecture of engine integrated SOFC-GT power system

[35]

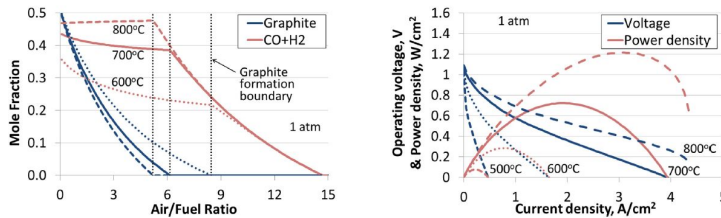


Figure 3.6:  $CPO_x$  and SOFC performance for different temperatures of operation

[35]

Along with this, the increase of pressure has a negative impact on the  $CPO_x$  performance. As pressure is increased, less amount of fuel is being oxidized which will further impact the system performance by increasing the concentration losses and reducing the heat output of fuel cell as fuel needs to be reformed inside the fuel cell which is an endothermic process.

Borer et al [51] compared the different propulsion systems for X-57 distributed propulsion aircraft. Four propulsion systems were compared for a minimum power output of 75 kW, an IC engine, a battery-powered propulsion system, and two different architectures of SOFC-battery hybrid. The SOFC-battery hybrid system architecture is given in figure 3.8. Diesel fuel is being reformed into CO and  $H_2$  and is being delivered to both fuel cell and combustor. The combustor provides heat to the reformer for the reaction and steam coming directly from the fuel cell is fed into the reformer for steam reforming. A turbocharger is also being used to provide pressurized air to the fuel cell and combustors. Electricity produced by the fuel cell is used to charge the battery and to run the propellers.

SOFC Power system 1 has a specific power of 302 W/kg and efficiency of 62 % and

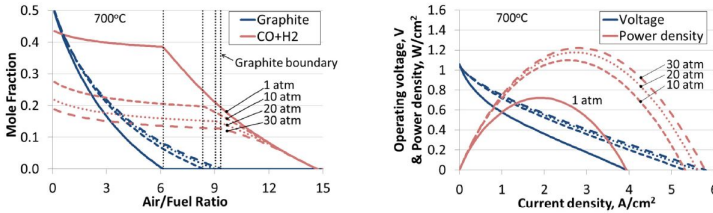


Figure 3.7:  $CPO_x$  and SOFC performance for different pressures of operation [35]

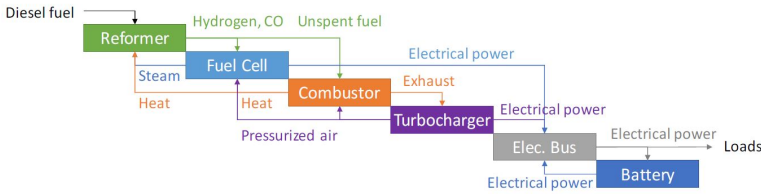


Figure 3.8: System architecture for SOFC-battery hybrid propulsion system [51]

SOFC Power system 2 has a specific power of 281 W/kg and efficiency of 55 %. The specific power includes the mass of all systems including the electrical system, support structures, and battery. The difference between system 1 and system 2 is the use of a hot recycle blower which reduces the weight and increases system efficiency. According to Borer, in order to be competitive with an IC engine and a battery-powered aircraft, the SOFC battery hybrid system must reach the specific power of 300 W/kg and efficiency of 60% with reforming which is significantly higher than the current SOFC-battery hybrid-specific power of less than 100 W/kg and an efficiency of 30-40%. Similar conclusions were provided by Stoia et al[52] as well who researched how to reduce the fuel cost by 50% for a small light aircraft or an APU for a large aircraft. The research[52] also showed that along with high efficiency, the SOFC-battery hybrid system has the potential to reduce  $NO_x$  emissions and carbon emissions significantly on the ground for both APU and propulsion systems. A comparison of different types of fuel reformers was also done and  $CPO_x$  reformer turned out to be a better option in terms of weight, start-up, and volume. The system has the lowest weight, smallest size, and mature technology compared to Steam Reforming and Auto-thermal Reforming and does not need steam to reform the fuel, which is a big requirement. In some past research [50], an external water tank and water process needs to be implemented for the steam reforming process which reduced the specific power of the system. But in order to achieve the efficiency of 60%, steam reforming needs to be used. Both papers provide great insights on a realistic SOFC system for the propulsion system and APU with the required specific powers and efficiencies to be competitive with the status quo.

There are very few studies done on the SOFC-GT hybrid concept for the application in aircraft propulsion systems where SOFC is also providing power to produce thrust

along with the aircraft's electrical power requirement. Most of the studies are focused on APU systems as mentioned earlier when it comes to commercial aircraft. But Okai et al [53] researched the feasibility of a SOFC-GT hybrid-electric propulsion system for a 150-seater regional aircraft. The size of the propulsion system is 15 MW (each engine is 7.5 MW) with an engine pressure ratio of 55. The system architecture is shown in figure 3.9. The concept is quite straightforward, the air is compressed by the compressor, and part of the compressor air is fed to the SOFC. Then the byproducts of the SOFC are mixed with the rest of the air coming from the compressor and are fed to the combustor directly. A small compressor has also been used before the SOFC whose purpose is to increase the temperature of the incoming air as well as to reduce any fluctuations that might occur in the incoming air. Both SOFC and turbofan are producing electricity which is being used to run the fan.

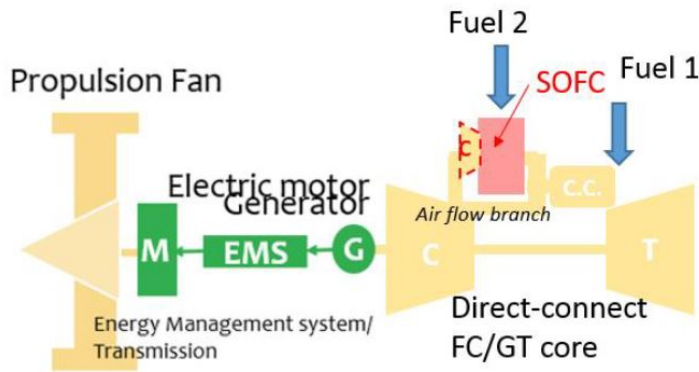


Figure 3.9: System architecture for SOFC-GT hybrid-electric propulsion system [53]

The study did research on two types of fuels, hydrogen, and kerosene. Two cases were researched and in both cases, the fuel cell was run on hydrogen but the gas turbine was run on hydrogen in the first case and kerosene in the second case. The results for the first case are given in the figure 3.10. The X shows the reference point for a conventional engine that is being run on jet fuel. The black line shows the efficiency of the SOFC-GT hybrid engine which is increasing as more power is extracted from the fuel cell. Also, the weight of the engine is increasing as a result of increasing the fraction of power coming from the fuel cell because fuel is getting bigger. Even though the efficiency of the propulsion system is increasing, adding a fuel cell has a negative impact on the range of the aircraft. For this analysis, the weight of the propulsion system and fuel is kept constant, which means if the weight of the propulsion system is increased, as in the case of adding a fuel cell, the weight of fuel needs to be reduced. This is the reason that the range of aircraft is reducing. As the weight of the propulsion system is increased, the aircraft have to carry less fuel and hence less range. This also means that the increase in core efficiency due to the addition of fuel cells has not complemented the increase in weight. One more thing that should be noted is that the gas turbine for the reference case and the SOFC-GT system is different. For example, the core efficiency of a reference

gas turbine is approximately 28% compared to 40% of the SOFC-GT with no fuel cell.

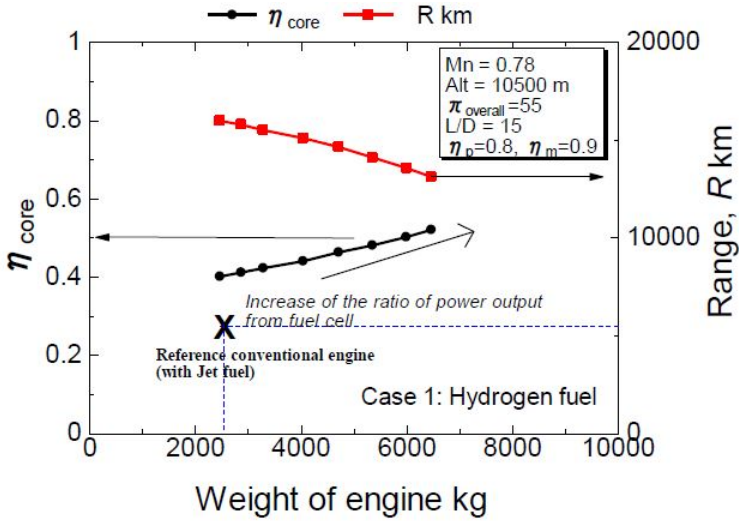


Figure 3.10: Core efficiency vs engine weight vs aircraft range for case 1, hydrogen [53]

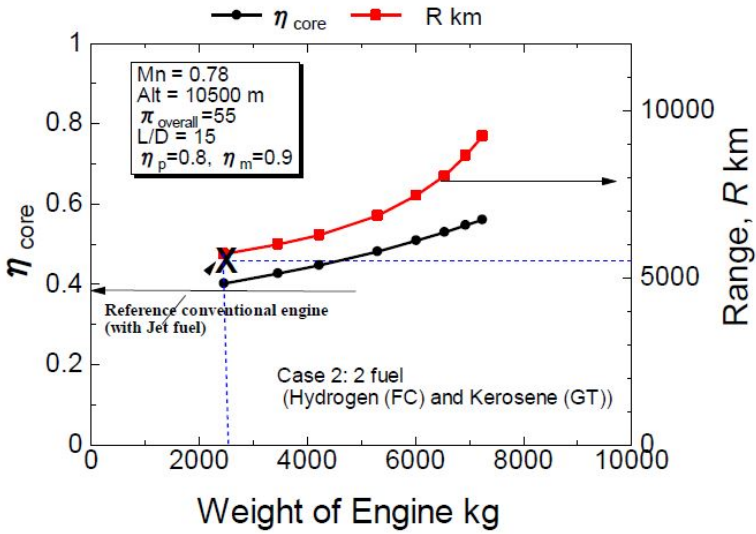


Figure 3.11: Core efficiency vs engine weight vs aircraft range for case 2, hydrogen (SOFC) & kerosene (gas turbine) [53]

Figure 3.11 presents the results of case 2 where a gas turbine is being run on kerosene. In this case, the reference engine which has been considered is highly efficient with a core efficiency of approximately 45%, even higher than the SOFC-GT hybrid system. Similar to case 1, as the size of fuel cell is increased, the core efficiency is increased. Also, the weight of the engine has increased at maximum system efficiency for case 2, which is approximately 7500 kg compared to case 1, which is 6500 kg. The reason for this increase has not been explained. But the range of the aircraft has increased as the fuel cell is added to the system, which is counterintuitive. First, kerosene is 11.5 times denser than hydrogen and 2.6 times less energy-dense which means less amount of total energy is being carried on the aircraft. If the efficiency of the SOFC-GT hybrid core system is similar in case 1 and case 2, the range must decrease because of the higher weight of the kerosene, even though there should be more decrease because of less amount of energy carried on aircraft. Also, the weight of the engine is higher in case 2, than in case 1 for similar efficiency, hence less fuel has to be carried. So, again the range should decrease.

Back-of-the-envelope calculations are done by the author of this report with similar methods (Breguet range equation) mentioned in the paper show that the range of the aircraft should increase in both cases, case 1 and case 2.

Another study done by Seyam et al [54] in recent times shows that integrating the SOFC with a gas turbine does increase the total efficiency of the system. Figure 3.12 shows the architecture of the SOFC-GT hybrid propulsion system analyzed in this study. The architecture is similar to the architecture of Okai [53] but with the integration of fuel reformer. Seyam et al analyzed multiple fuels like methanol, ethanol, etc. blended with a fraction of hydrogen to understand the impact of different fuel types on the system performance and efficiency. The SOFC net power output is 944 kW and the thermal efficiency has increased from 43.4% for baseline engine running on kerosene to 48.1% for SOFC-GT hybrid running on 75% methanol and 25% hydrogen. It should be noted that along with the benefit for fuel cell, changing the fuel will also have an impact on the specific heat capacity of the mixture, hence leading to a change in thrust and efficiency. The direct benefit of adding the fuel cell to turbofan with the same fuel has not been given in the study.

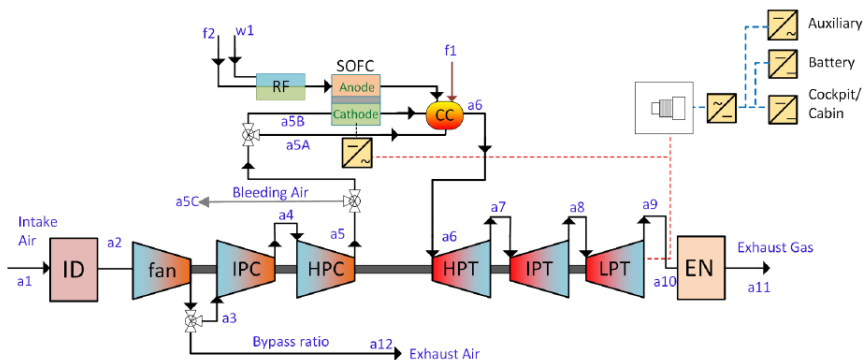


Figure 3.12: SOFC-GT hybrid system architecture

[54]

# 4

## RESEARCH OBJECTIVES, QUESTIONS & METHODOLOGY

This section talks about the research questions and objectives for the research that the author is proposing. But first, a small conclusion of all the sections presented above has been given in order to have a whole picture of why the author is proposing the specific research project and it is as follows:-

Section 1 talks about the current scenario of engine emissions and specific fuel consumption and its trend over the years which proves that the gas turbine technology is maturing. Hence, there is a need for new disruptive innovations in the propulsion sector in order to achieve ACARE 2050 goals. But if the disruptive technologies which are proposed like Boundary Layer Ingestion(BLI), Turbo-electric propulsion, and Distributed Propulsion(DP) were to be implemented in a Boeing 737-800 aircraft, it will reduce the fuel burn by between 7-12% [13], which will not be sufficient for the industry emission reduction targets. Hence, the author believes that along with the technologies which have been proposed, other concepts should also be investigated which could increase efficiency and one of those concepts or technology could be the fuel cell. But fuel cell, due to their low TRL and low specific power could not be used alone for commercial aircraft. Although, there is a possibility of using a hybrid concept called SOFC-GT, which is an integrated system.

Section 3 gives a detailed explanation of multiple concepts researched in the past for ground and aerospace applications which shows that the SOFC-GT hybrid has the capability to reach an electrical efficiency of more than 60% and an integrated system efficiency of 85%. Along with this, the concept does not disregard the gas turbine technology, which has been developed over the decades and achieved an engineering feat when it comes to eliminating inefficiencies. On the contrary, it is complementary to gas turbine technology and provides more scope for improvement. Hence, the author believes that this concept should be explored more and after a thorough analysis of multiple types of research, the author has identified many research gaps and they are as follows.

## 4.1. RESEARCH GAPS

Section 3 gives a thorough explanation of the research done in the past for the SOFC-GT hybrid for both ground and aerospace applications. After doing a thorough analysis, the following research gaps have been identified.

1. **Most research papers that have researched on SOFC-GT hybrid system focus on being the SOFC as the main power source and gas turbine to only use the by-products of SOFC or as a bottoming cycle.** This means that most of the power is contributed by SOFC, which is inherently more efficient than a gas turbine and hence the system efficiency increases significantly to up to 60% for a 1.5 MW system[46].

However, for an aircraft propulsion system, the primary source of power or a significant fraction of power will still be contributed by the gas turbine because of the requirement of peak power, transient responses, and specific power limitations of SOFC. Hence, there is a need to research the benefit of SOFC-GT hybrid for an aerospace propulsion system.

2. **How much the gas turbine should be downsized as a significant fraction of power is being contributed by the fuel cell?** As, a fraction of power is being contributed by the SOFC, the size of the turbofan can be reduced as running a turbofan below its most efficient point will reduce the system efficiency and increase emissions. Also, downsizing the engine will reduce the propulsion system weight as well, which means the contribution of fuel cells can be increased.
3. **Few researches in the domain of SOFC-GT hybrid concept for Aerospace propulsion application.** The researches which have been done in the domain of Aerospace are for either APU or electrical power supply for the aircraft but not specifically for the propulsion system, like the one done by Waters and Cadou [35]. One of the researches done specifically for using SOFC-GT for propulsion systems is done by Okai et al [53] and as explained in section 3, author believes that the research has some discrepancies. The research shows a higher range for the aircraft when fuel cell is added to the turbofan, where the turbofan is running on kerosene and fuel cell on hydrogen, compared to a hybrid system which is running completely on hydrogen even though the efficiency of both the systems is similar. This is counter-intuitive as kerosene has a higher weight and hence, will reduce the range of the aircraft. Another research done by Seyam et al[54] does not present the direct impact of adding the fuel cell to the turbofan. Hence, the idea of using SOFC-GT hybrid as a propulsion and power system for aircraft has not been very well researched.
4. **No research has been found which gives an understanding of the impact of adding a fuel cell to a turbofan on the turbofan engine.** If a fuel cell is added to a Turbofan, then the turbofan is no longer working on its most efficient and optimized

point. This may even lead to a reduction in system efficiency as the fuel cell may be making the turbofan inefficient by shifting it from its higher efficiency points. Hence, the turbofan parameters need to be changed in order to get the maximum efficiency output from SOFC-GT.

5. **No research has been found on the economic analysis of the SOFC-GT hybrid propulsion system for a commercial aircraft.** The author has not found any economic studies which are focusing on the SOFC-GT hybrid-based propulsion system and its impact on the direct operating costs and lifelong economics of the aircraft.

## 4.2. RESEARCH OBJECTIVES & QUESTIONS

After analyzing the research gaps in section 4.1, the following research objective has been developed.

The main research objective of this research is:-

***“To analyze the technical and economic feasibility of the SOFC-GT hybrid propulsion system running on hydrogen for a commercial aircraft by doing a thermodynamic, emission and economic analysis of the system.”***

In order to achieve the research objective, the following research question has been developed.

***“Is it technically and economically feasible to develop a SOFC-GT based hybrid propulsion system running on hydrogen for a commercial aircraft?”***

In order to thoroughly answer this question, many sub-questions need to be answered and they are as follows:-

1. *What is the difference in steady-state performance for the SOFC based hybrid propulsion system compared to a conventional Gas Turbine propulsion system? What is the impact of adding the fuel cell on gas turbine parameters?*
2. *Does the improvement in performance such as reduction in fuel consumption complement the added weight? If not, how much improvement is needed in the specific power of the Fuel Cell?*
3. *What is the reduction in emissions, mainly NO<sub>x</sub> & Water, for the SOFC-GT hybrid when compared to a conventional Gas Turbine propulsion system based upon the correlation method? (0 D emission Analysis)*
4. *Does the improvement in performance complement the increase in fuel cell-related Costs? If not, how much improvement is needed in fuel cell-specific power to achieve*

*feasibility?*

5. *Does an introduction of  $\text{NO}_x$  and Water emission tax make the propulsion system feasible for the current values of fuel cell-specific power? If not, how much improvement is needed in the specific power of the Fuel Cell?*
6. *Can the Gas turbine be downsized while keeping the maximum thrust of the engine similar to the reference case? What is the difference in performance, from both technical and economic perspectives, for the downsized engine when compared to the reference engine integrated with a fuel cell?*
7. *Which parameters of fuel cell and gas turbine have the major impact on the performance and economics of the propulsion system? (Sensitivity Analysis)*

4

### 4.3. RESEARCH METHODOLOGY

This section includes the methodology that will be used in order to answer the research questions and achieve the research objective presented in section 4.2. Figure 4.1 shows the complete methodology of the project. A thorough explanation of each step is given below:-

- First step is to develop and verify the mathematical model of the fuel cell. A detailed explanation of the fuel cell model is given in section 2.2. But in order to develop a model, there is a need for physical data like the properties of anode, cathode, and electrolyte along with specific weight.

There are multiple models which can be used as references for example the Aguiar Model [55], the Campanari model[44], the Chan Model[45], the Haseli model [48] etc. The criteria for choosing the model set by the author is based on the ease of collection of data and the ease of verification of the model and are explained thoroughly in section 5.1.

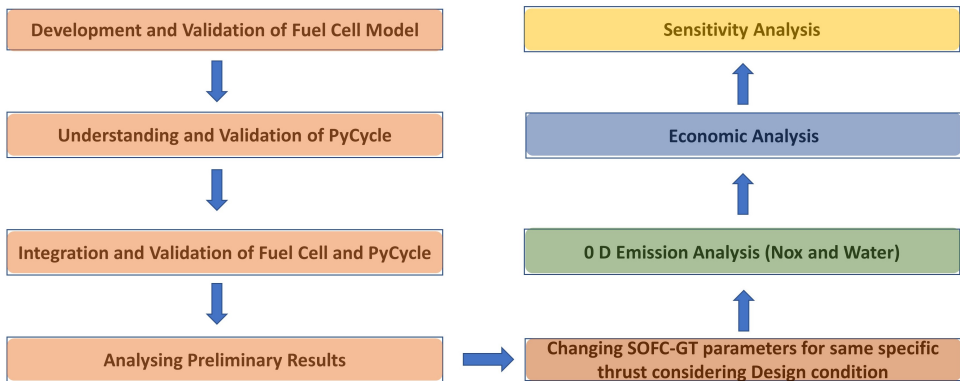


Figure 4.1: Project Methodology

- The second step is the development of the turbofan model and an open-source thermodynamic cycle code, PyCycle, will be used [56]. PyCycle is developed by NASA based on the multidisciplinary design optimization algorithm which is faster than the already available NPSS (Numerical Propulsion System Simulation) which is being used by the industry [57]. A more thorough explanation is given in section 6.1.1.

The next step would be to validate the PyCycle model for multiple conditions like take-off, climb out, and cruise. The validation will be done by taking the ICAO engine database as the reference. [3]

- The third step would be the integration of the fuel cell model with the PyCycle model to build the SOFC-GT hybrid propulsion system. The hybrid model will then be verified by doing the energy balance.

Both, fuel cell and Gas Turbine models will be a zero-dimensional models. The author believes that for system-level analysis, the zero-dimensional model is the best choice. This has been explained in section 5.1.

- The fourth step would be to analyze the preliminary results such as TSFC, efficiencies, mass flow rate, etc. for the SOFC-GT hybrid propulsion system.
- The fifth step would be changing the engine parameters to get the same specific thrust as the reference engine. This has been done in order to fairly compare the SOFC-GT hybrid with the reference engine and is explained in section 8.1.2.
- The sixth step is to develop a 0D emission model which will calculate the  $NO_x$  and water emissions. As the fuel used in this study is hydrogen, there would be no direct carbon emissions. The model will calculate the emissions based on the multiple correlations available in the literature.
- The seventh step would be to do an economic analysis based upon the results of the SOFC-GT hybrid model and emission model. Multiple scenarios for emission tax and SOFC-GT would be analyzed.
- At the end, sensitivity analysis for technical and economic parameters will be done in order to understand the impact of these parameters on the engine performance and economics, respectively.



# 5

## FUEL CELL MODEL

This chapter discusses the complete fuel cell model and its verification. Figure 5.1 shows the architecture of the whole model. The main components of the fuel cell are the heat exchanger and a SOFC.

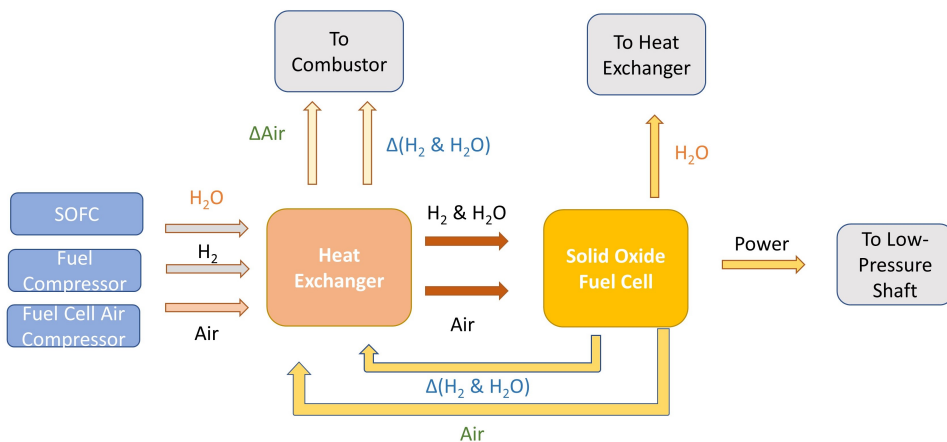


Figure 5.1: Fuel Cell Architecture

The explanation of the model is given below:

- First, the air, hydrogen, and steam go into the heat exchanger from the fuel cell air compressor, fuel compressor, and fuel cell respectively. The reason for using a heat exchanger is to heat the inlets of SOFC to the required inlet temperature of the SOFC. The inlets are heated with the thermal energy of the by-products of the SOFC.

- The heated inlets go into the SOFC and the fuel cell reaction takes place in the SOFC and heat and electric power are produced. The byproducts of the fuel cell, mainly unutilized hydrogen, produced steam and left out air goes into the heat exchanger and acts as a hot fluid that is used to heat the inlets of SOFC. The power produced by the SOFC is then put in the LP shaft using the motor.
- After the heat exchanger, the byproducts are added to the combustor. It should be noted that a part of the steam from SOFC goes into the heat exchanger. The reason for re-circulation is given in equation 2.9. The reaction shows that the equation fails if the concentration of water/steam reaches close to zero. Hence, in the anode inlets of SOFC, a small concentration of water/steam is required and this has been done by using a re-circulation loop.

## 5.1. REFERENCE MODEL

The SOFC mathematical model developed for this study is a Zero-Dimensional (0D) model. The model cannot compute the properties such as temperature, concentration, voltage, etc. along the fuel channel but only at one point. The reason for choosing a 0D model are as follows:

1. **Purpose of the study:** The purpose of the study has a big influence on the type of model that needs to be used. For this study, there is only a need for system-level analysis for the fuel cell and hence, a 0D model is sufficient for the analysis.
2. **Computation Time:** The computation time of a 0D model is multiple times less than a 1D or a higher dimensional model. This reduction in time is very beneficial for a range of analyses that can be done in the same limited time and is required for a feasibility analysis.
3. **Development Time:** Similar to computation time, the development as well as the debugging time for a higher dimensional model is substantially higher, which may lead to a reduction in the scope of the study.

The SOFC model which has been built in this study is based on the Aguiar One Dimensional model [55]. There are multiple models available like Chan model [58] and Kang model [59]. But the reasons for choosing the Aguiar model as a reference are as follows:

1. **Well Renowned Model:** The Aguiar model is a well-renowned model all over the world with more than 808 citations as of the writing of this report. It has been used as a reference model for many studies on SOFC and SOFC-GT hybrid.
2. **Availability of Data:** The data needed to build the model is given in the paper of Aguiar, which is very helpful while building the mathematical model. The component material and properties, which are the inputs of the SOFC mathematical model, are presented in the paper.
3. **Simplicity of the Model:** The model is simple and hence can be used as a reference for a 0D model. The equations used for different losses are simplified, which also leads to a reduction in computation time.

## 5.2. SOLID OXIDE FUEL CELL MODEL

This section explains the architecture of the SOFC model and the assumptions that have been taken to build the model. The model architecture is shown in figure 5.2. The error in the model is defined in equation 5.3.

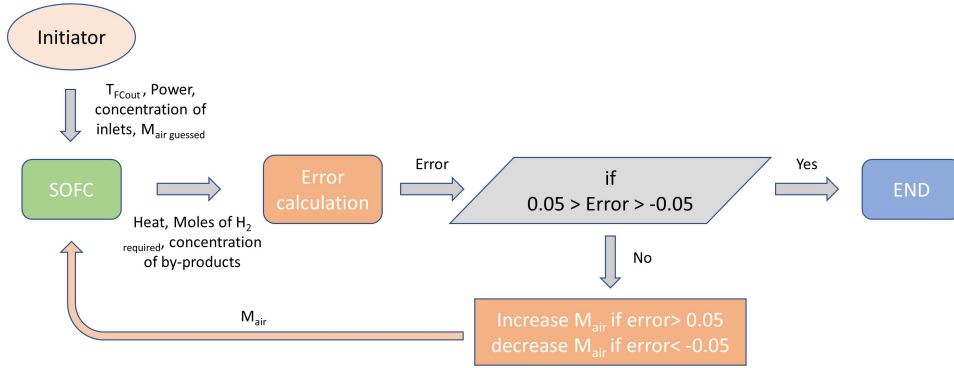


Figure 5.2: SOFC Model Architecture

The explanation of the SOFC model architecture is given below:

- First, the initiator provides the SOFC model with the outlet temperature of SOFC ( $T_{FCout}$ ), the power required from the fuel cell, guessed mass of air and concentration along with the other inputs like operating pressure and fuel utilization. Some inputs, which are constant, have not been shown in figure 5.2 in order to improve readability.
- The SOFC model calculates the cell output voltage ( $V_{fc}$ ) given the temperature, concentration, and pressure of the fuel cell. The equations are given in section 2. The number of moles of hydrogen required ( $H_{2required}$ ) will be calculated using the  $V_{fc}$  as shown in equation 5.1. The  $V_{fc}$  is the output of the SOFC model and  $I$  and  $U_f$  are constant. It should be noted that SOFC does not use all the hydrogen because of the concentration losses as explained in section 2. Hence, utilization factor or  $U_f$  has been used in order to calculate the total amount of hydrogen required that needed to go into the fuel cell.

$$H_{2required} = \frac{P_{fc}}{V_{fc} * I * U_f} \quad (5.1)$$

where

$P_{fc}$  = Power output of fuel cell, W

$U_f$  = Utilization factor

$I$  = Current produced when one mole of hydrogen is converted to water/steam, A

The SOFC model also calculates the amount of by-products, mainly the steam produced and hydrogen and oxygen consumed, and the heat produced. The heat produced is given in equation 5.2.

$$\text{Heat} = (H_{2\text{consumed}} * \Delta h) - P_{fc} \quad (5.2)$$

where

$$H_{2\text{consumed}} = H_{2\text{required}} * U_f$$

$\Delta h$  = Total heat released by the reaction, J

- Once the amount of by-products and heat produced is calculated, the mass of air can be calculated in the SOFC model. The heat produced by the SOFC is extracted by the air which is entering the SOFC. The SOFC has a maximum temperature constraint,  $T_{FCout}$ , which is an input to the SOFC model, and the mass of air is increased or decreased until the  $T_{FCout}$  is achieved. The error shown in figure 5.2 is given in equation 5.3. If the error is less than 0.05 K, the model is stopped and provides the output,  $M_{air}$  along with the  $H_{2\text{consumed}}$  and the concentration of byproducts.

$$\text{Error} = T_{fcout} - T_{fcout\text{required}} \quad (5.3)$$

where

$$T_{fcout} = \text{Temperature of the byproducts coming out of SOFC model, K}$$

$$T_{fcout\text{required}} = \text{Required or maximum temperature constraint of SOFC model, K}$$

The SOFC model is based upon some **assumptions** and they are given below:

- The model is assumed to be adiabatic, hence no loss or gain of heat from the surrounding.
- The calculations for  $V_{fc}$  have been done in the middle of the SOFC. This means that the temperature and the concentration at which the  $V_{fc}$  is calculated is the average of the inlet and outlet of the SOFC.
- The rate of reaction is assumed to be constant inside the SOFC. This means that the consumption of hydrogen along the fuel cell is constant.
- The pressure losses inside the SOFC are assumed to be 5%. This value can differ but an average is assumed based on the data given in [60].

- The inlet and outlet temperatures of the SOFC model have been calculated using the constraints from the Aguiar model. The maximum temperature limit or constraint is 1200 K and hence, the  $T_{FC}$  of the outlet by-products must not exceed 1200 K. Along with this the maximum temperature gradient is 154 K.

Considering the maximum temperature gradient constraint, the minimum inlet temperature of the SOFC cannot be less than 1046 K. Hence, the  $T_{FCin}$  must be greater than 1046 K. The maximum temperature gradient constraint is applied because of the thermal expansion of the electrodes and electrolyte. As the reactions start to take place in the SOFC, the temperature of electrodes and electrolytes increases and they start to expand. Beyond a temperature difference of 154K, the thermal expansions at the inlet and outlet may increase to such levels that the SOFC structure may crack. Hence, a temperature gradient limit is established. Hence, values for  $T_{FCout}$  and  $T_{FCin}$  are assumed to be 1200K and 1050K respectively for the SOFC model.

### 5.2.1. VERIFICATION OF SOFC MODEL

This section consists of the verification of the SOFC model. The verification has been done against the Aguiar model [55]. The Aguiar model uses a hydrocarbon fuel and uses an internal steam reforming process to convert hydrocarbon fuel into hydrogen and Carbon dioxide. A thorough explanation of the steam reforming process is given in section 3.1 and equations 3.1 and 3.2. This means that in addition to the SOFC model, there is a need for a 1D steam reforming model as well.

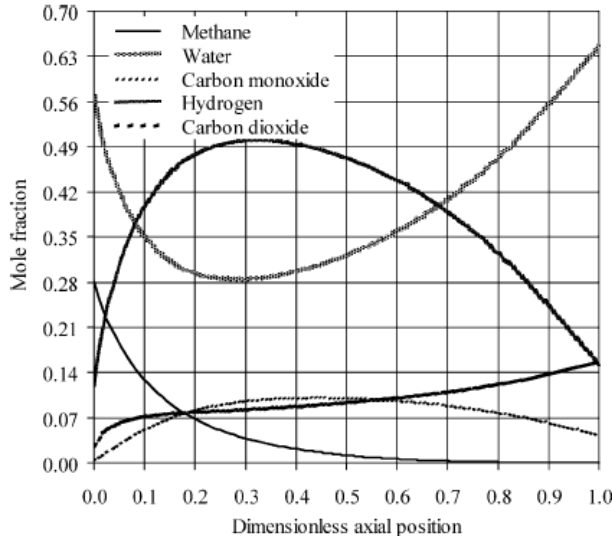


Figure 5.3: Concentrations of species along the fuel channel

[55]

Along with this, the Aguiar model is a 1D model and hence, the model can evaluate

the rate of reactions based upon the local temperature, current density, and concentration, along with the fuel and air channel, and hence the fuel cell voltage. However, the 1D model for SOFC and reformer, as mentioned in section 5.1, is out of the scope of this study.

Hence, in order to do the verification for a 0D model, the input data like the concentrations, temperature, and current densities at different points along with the SOFC fuel and air channel have been taken from the paper of Aguiar itself.

Figure 5.3 shows the concentration change of species along the SOFC. It can be seen that the methane is getting converted to hydrogen until it reaches near zero concentration. Figure 5.4 shows the variation of temperature and it is clear from the figure that there is a dip in temperature initially and then it increases till the end of SOFC. This is because of the reforming process. As reforming is taking place at the beginning of the SOFC and it is an endothermic process, the temperature of SOFC decreases. It should be noted that in figure 5.4, temperatures of multiple components have been shown. For the verification purpose, the temperature of PEN(Positive-electrode/ Electrolyte/Negative-electrode) the structure has been used as the reactions are taking place on the PEN structure.

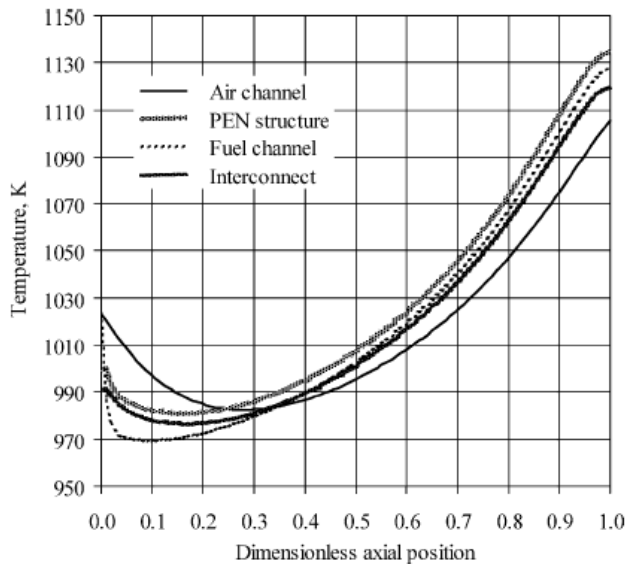


Figure 5.4: Temperatures of different SOFC components along the fuel and air channels [55]

Figure 5.5 shows the corresponding cell voltages (shown as operating voltage in the figure 5.5), losses and current density along the fuel channel. Figure 5.6 shows the comparison between the cell voltages and losses along the fuel channel for the Aguiar model and the SOFC model developed for this study. It is very clear from the figure that the SOFC model is co-relating very well with the Aguiar model. The blue solid and dashed lines are the open circuit voltages, which is the maximum achievable voltage by the SOFC

at a specific temperature and pressure. The biggest loss, as can be seen from the figure is the activation loss and it includes both, anode activation loss and cathode activation loss. After the activation loss, the second-biggest loss is the ohmic loss. It is clear from the figure that for a big part of the fuel channel, the ohmic loss is almost constant even though the temperature of the PEN structure is increasing. The reason is the increase in the current density along the fuel channel as shown in figure 5.5.

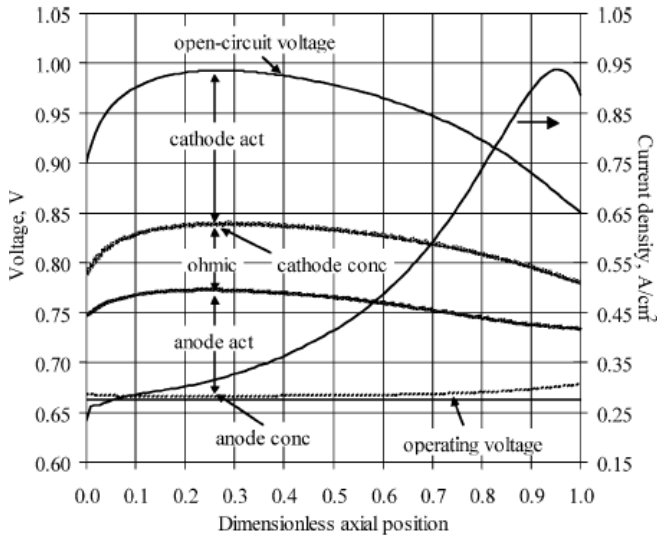


Figure 5.5: The SOFC output voltage, losses, and current density along the fuel channel [55]

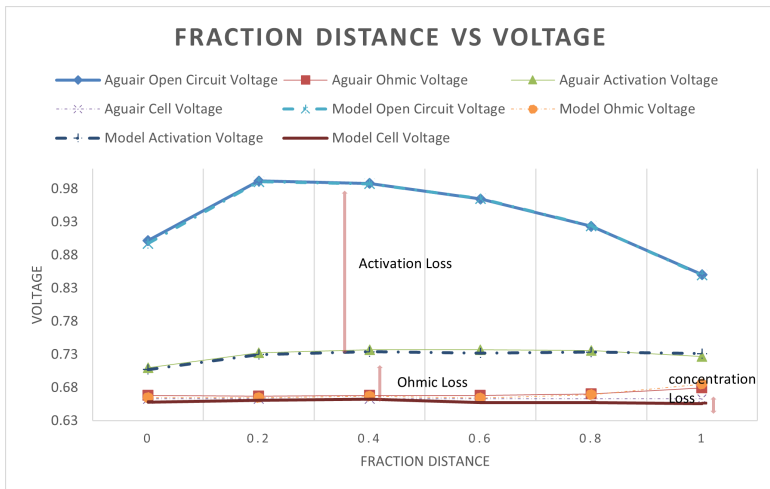


Figure 5.6: Comparison between SOFC model and Aguir model

The smallest loss in the SOFC is the concentration loss. The concentration loss is initially higher and the reason is the lower concentration of hydrogen at the inlet. The steam reforming process is taking place in the first 20-30% of the fuel channel and hence the concentration loss is higher. But then as the hydrocarbon is converted into hydrogen, the concentration losses reduce until it increases again near the outlet as the hydrogen concentration is at a minimum near the outlet.

The lowest and maximum error encountered among the six points taken along the fuel channel for analysis is 0.12% and 1.07% for the SOFC 0D model compared to the Aguiar 1D model. The error has been found to be very low and hence, the impact of this error on the whole system-level analysis would be below as well. Given the advantages in terms of computation and development time and simplicity of the model, it can be concluded that the SOFC model is verified.

### 5.2.2. SENSITIVITY ANALYSIS OF SOFC MODEL

This section shows the sensitivity analysis of the SOFC model in which pressure and temperature are changed respectively while keeping all the other parameters constant and their impact on the SOFC cell voltage and losses has been analyzed.

The impact of change in temperature and pressure on OCV, losses, and cell voltage has been thoroughly discussed in section 2. A summary has been given in table 5.1. It should be noted that the trend of concentration losses in figure 5.7 is not very visible because of the lower absolute value but the concentration losses are increasing with temperature.

Voltage or Loss	Temperature Increase	Pressure Increase
Open Circuit Voltage	Decrease	Increase
Activation Loss	Decrease	No Impact
Ohmic Loss	Decrease	No impact
Concentration Loss	Increase	Decrease
SOFC Cell Voltage	Increase	Increase

Table 5.1: Pressure and temperature impact on SOFC OCV, losses and Cell Voltage

Figure 5.7 shows the changes in OCV, losses, and cell voltage as temperature increases. The OCV is decreasing as expected due to a decrease in the Gibbs Free Energy as the operating temperature is increased. Both ohmic and activation losses are decreasing as an increase in temperature decreases resistivity in the electrolyte, hence reducing the ohmic loss. Increasing temperature also increases the energy available to the reactants for crossing the energy barriers, leading to a reduction in activation energy and hence the loss. Concentration losses are increasing as more backward reactions are possible due to higher temperature as the higher temperature will act as a catalyst to move reaction backward, as explained in section 2.2.4. But the change in concentration loss is insignificant because the concentration loss is the smallest contributor of all losses. Hence, overall, the cell voltage increases significantly and it can be seen clearly from figure 5.7. An increase of operating temperature from 900 K to 1100 K or 22.23%, increases

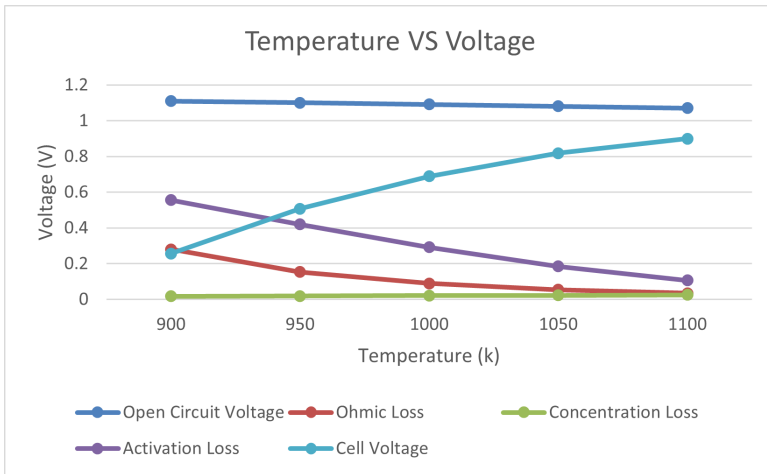


Figure 5.7: Temperature vs SOFC cell Voltage and losses

the cell voltage from 0.25 V to 0.9 V, an increase of 260% in cell voltage.

Figure 5.8 shows the changes in OCV, losses, and cell voltage as pressure increases. Unlike temperature increases, the OCV increases due to an increase in pressure. The activation and ohmic losses are not affected by changes in pressure and hence they are constant as pressure increases. The concentration losses decreased significantly because an increase in pressure increases the number of molecules of the species in the fuel and air channel, hence decreasing the concentration loss. An increase of operating pressure from 50 kPa to 3 MPa or 5900%, increases the cell voltage from 0.658 V to 0.7822 V, an increase of 18.89% in cell voltage. It is clear from both the figures that cell voltage is more sensitive to temperature to pressure, which was also mentioned in section 2.2.7.

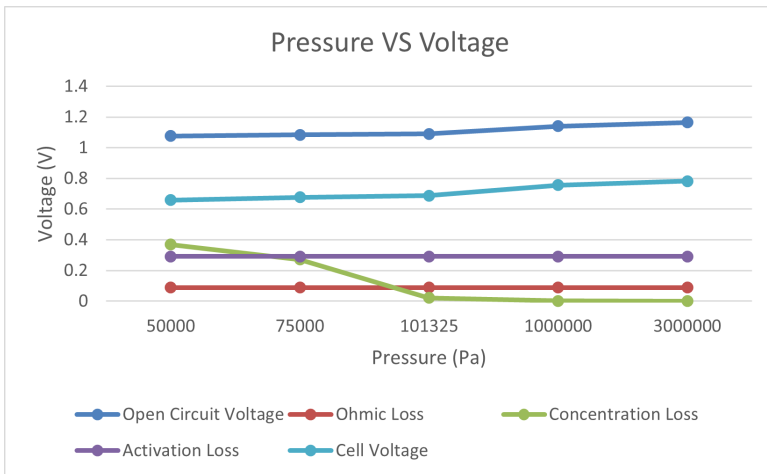


Figure 5.8: Pressure vs SOFC cell Voltage and losses

Hence, from the qualitative analysis, the SOFC model is reacting to the change in temperature and pressure as expected and is concluded to be verified.

### 5.3. HEAT EXCHANGER

As explained in section 5.2, the inlets of SOFC need to be above 1046 K because of the maximum temperature difference constraint of the SOFC. However, the temperature of air coming from the fuel cell air compressor is around 860 K for **Sea Level Static condition (Design)** and 770 K for **Cruise condition (Off-Design)** because of the difference in absolute pressures at the exit of the high-pressure compressor at these conditions. Hence, the temperature of the air is too low to enter into the SOFC. Similar to air, the fuel temperature is also low, 298 K and hence, a high-temperature heat exchanger is required to increase the temperature of air and fuel to the inlet temperature.

Figure 5.9 and 5.10 shows the complete architecture of the two heat exchangers used to heat the anode and cathode inlets respectively. The process for heat exchanger anode is explained below:

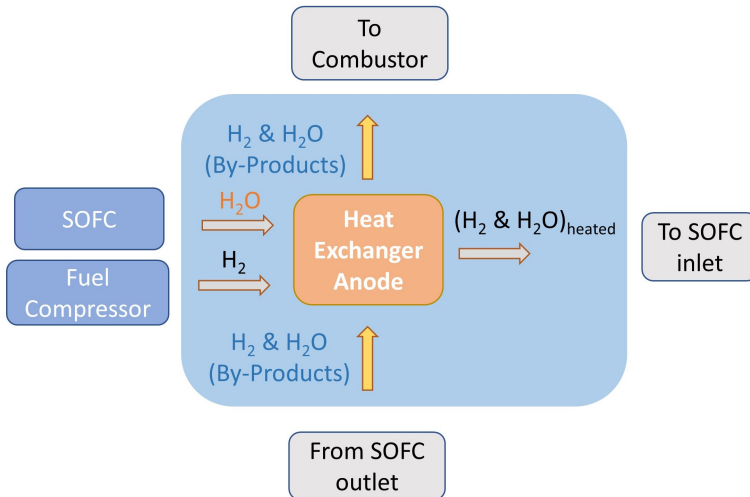


Figure 5.9: Heat Exchanger Architecture Anode

- First, the  $H_2$  and  $H_2O$  from the fuel compressor and SOFC respectively, enter the heat exchanger as explained at the beginning of the chapter.
- The  $H_2$  and  $H_2O$  enter as cold fluid and get heated to the inlet temperature,  $T_{FCin}$  which is 1050 K, from the thermal energy of the outlets of the anode of SOFC, which is the hot fluid. The outlet of the anode constitutes left out  $H_2O$  and  $H_2O$  produced in the SOFC at a temperature of  $T_{FC}$  which is 1200 K.
- Then the SOFC anode outlets goes into the combustor after providing the required thermal energy to the inlets of the anode. The heated anode inlets then go into the SOFC as shown in figure 5.9.

- Similar process is followed by the heat exchanger for the cathode side as shown in figure 5.10.

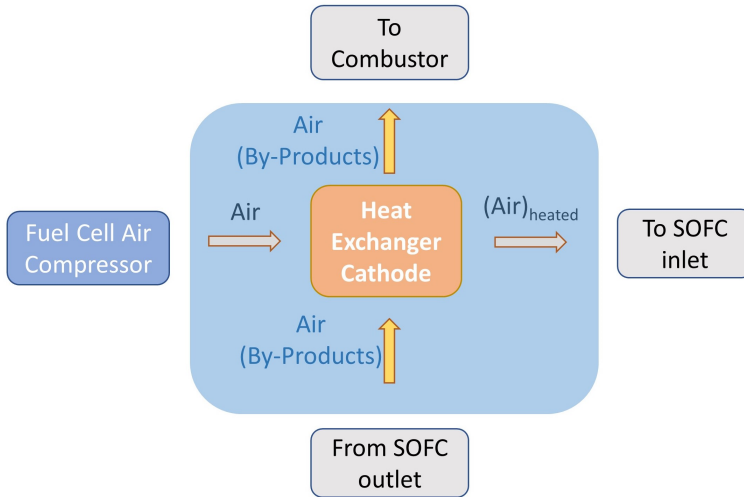


Figure 5.10: Heat Exchanger Architecture Cathode

**Assumptions** for the heat exchanger model are given below:

- The heat exchanger model is a 0D model.
- The heat exchanger is assumed to be adiabatic, hence no loss or gain of heat from the surrounding.

The heat exchanger model used in this study is based on a simple energy balance. It has been assumed that a heat exchanger would be able to provide the heat required to increase the temperature of inlets to 1050 K. A preliminary analysis done by the author for a heat exchanger model based on the eps-NTU method [61] suggests that the variation of the outlet temperature of cold fluid for Design and Off-Design condition is low and hence a simple energy balance analysis would not lead to a major change in the final results. Also, the heat exchanger needs to be designed for the Off-Design condition because the mass flow rate is higher, especially for the cathode. If the heat exchanger is designed for Design condition (Sea Level Static), then the temperature of the air entering the cathode of the fuel cell would be lower than 1050 K, leading to an efficiency drop of the fuel cell.

The temperature of the inlet and outlet of the cold fluid (fuel cell inlets) is known along with the temperature of the inlet of the hot fluid (outlet of fuel cell). Hence, the temperature of the outlet of hot fluid from the heat exchanger can be calculated from the enthalpy of the fluid as given in equation 5.4.

$$H_{h_{out}} = H_{h_{in}} - [H_{c_{out}} - H_{c_{in}}] \quad (5.4)$$

where

$H_{h_{out}}$  = Enthalpy of hot fluid coming out of heat exchanger, J

$H_{h_{in}}$  = Enthalpy of hot fluid going in the heat exchanger, J

$H_{c_{out}}$  = Enthalpy of cold fluid coming out of heat exchanger, J

$H_{c_{in}}$  = Enthalpy of cold fluid going in the heat exchanger, J

## 5.4. FUEL CELL MODEL VERIFICATION

This sections consists of the verification of the complete fuel cell model. The model architecture is shown in the figure 5.1 and the explanation of architecture is given at the beginning of the chapter.

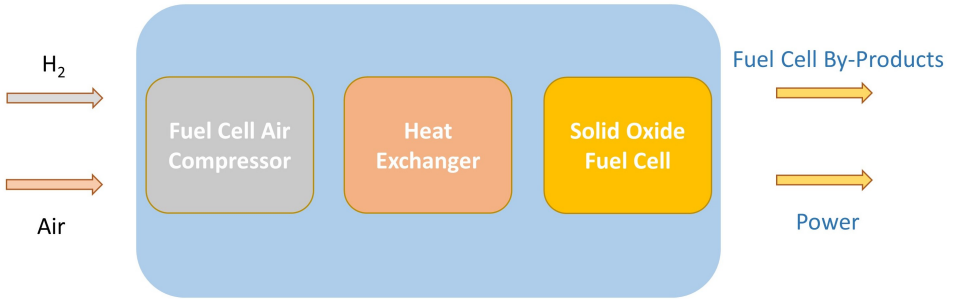


Figure 5.11: Total energy in and out of Fuel Cell

The verification of the complete fuel cell model is done by doing the energy balance across the fuel cell. The total energy going in and coming out of the fuel cell is shown in figure 5.11. The total energy going in the fuel cell is the  $H_2$  coming from the fuel compressor and air coming from the fuel cell air compressor. The energy coming out of the fuel cell is the fuel cell by-products and the power generated by the SOFC.

Figure 5.12 shows the error in the complete fuel cell energy balance as the power output of the fuel cell is increasing for Design condition. The error is defined in equation 5.5. It can be observed from the figure that the error in the energy balance is below 0.08%, almost negligible and for all the cases of fuel cell power output is changing. The reason of the error is because of the error margins used to calculate the amount of air required in the fuel cell given in figure 5.2 and equation 5.3. The margins can be reduced further but it leads to an exponential increase in the computation time. For example, reducing the error margin from 5000 J to 500 J led to a computation time increase from 4.7 minutes to more than 37 minutes. Hence, the author believes that keeping the error margin of 1000 J is a fair compromise in terms of computation time and error. Therefore, it can be concluded that the complete fuel cell model is verified.

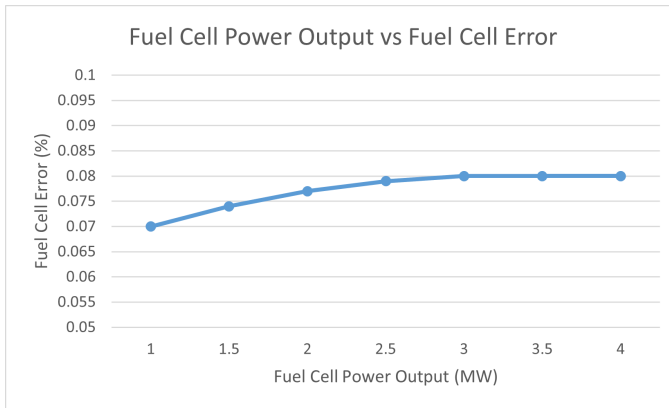


Figure 5.12: Error in Energy Balance of fuel cell for different fuel cell Power Output for Design Condition

$$Error = \frac{(Energy\ In - Energy\ Out) * 100}{Energy\ In} \quad (5.5)$$

5

where

Energy In= Summation of the enthalpy of  $H_2$  and air going in the fuel cell, J/s

Energy Out= Summation of the enthalpy of fuel cell by-products and Power coming out of the fuel cell, J/s



# 6

## GAS TURBINE MODEL

This chapter discusses the Gas Turbine model which has been used to analyze the turbofan and the validation of the gas turbine model.

### 6.1. GAS TURBINE TOOL

In order to analyze the SOFC-GT hybrid propulsion system, a robust gas turbine model needs to be developed which can accurately calculate the Design (Sea Level Static) and Off-Design (Cruise) properties of the turbofan engine. The requirements for gas turbine tool are given below:

- A robust tool that can analyze the 0D Design and Off-Design conditions with the component level analysis capability. The component-level analysis capability is because of the changes which will be done on the components when the fuel cell model will be integrated with the gas turbine.
- The tool should be easy to integrate with fuel cell model. The tool should provide the manipulation capability to the developer so that the developed model can fit the developer's requirements.
- The tool should require low computation power and have low computational time. As this study is a feasibility study, a wide range of results on the system-level needs to be analyzed. Hence, the tool must have low computational time.

Based on the requirements presented above, there are multiple options available like GSP [62], PyCycle [56], and many more. The author has experience with both tools, GSP and PyCycle, and based on the experience, the author has chosen the PyCycle as the gas turbine tool. The major reason for choosing PyCycle is its ease of use.

Even though both GSP and PyCycle are modular, the user interface and extraction of results from GSP are not up to the mark. The user interface of GSP, as per the author's experience, is not intuitive, especially for the engine model development. On the other hand, PyCycle has no user interface. It consists of multiple Python modules and hence,

is very easy to navigate. Along with this, it is also comparatively easier to manipulate the source code and change it according to the requirements of the author. More explanation on the working of PyCycle is given in section 6.1.1.

### 6.1.1. PYCYCLE

PyCycle, developed by NASA, is a gradient-based optimization tool for propulsion systems and has been developed with a perspective to be used as a next-generation propulsion system analysis tool [56]. Some of the key characteristics of PyCycle are given below.

- PyCycle is a modular and flexible tool that can be used for unique architectures like Boundary Layer Ingestion, Turbo-electric hybrid propulsion, Battery-electric hybrid propulsion, and many more. Hence, it is perfect for the study of SOFC-GT hybrid, which is in itself a unique architecture.
- PyCycle uses analytical derivatives for exploring the design space while using gradient-based optimization. Because of this, the computation time is 3 orders of magnitude less than its predecessor, Numerical Propulsion System Simulation (NPSS), which is an industry-standard tool for gas turbine analysis [57].
- PyCycle accuracy is very high and is within the accuracy of 0.03% when compared to Numerical Propulsion System Simulation (NPSS) [56].

## 6

### 6.2. REFERENCE TURBOFAN MODEL- CFM-56-5B1

This section talks about the turbofan model which has been developed in the PyCycle. The model which has been used as a reference engine is the CFM-56-5B1 which has been used on the Airbus A321 and Boeing 737 [63]. The reason for using the CFM-56 as the reference engine is the availability of data for different parameters required to build the engine model. CFM-56 is one of the most successful and researched engines and has been used as a reference for many studies because of the availability of the data. The side view of the turbofan model with the station numbers and component nomenclature is given in figure 6.1. The block diagram of the reference engine model developed in PyCycle is given in figure 6.2

The block diagram shows all the components and modules which has been connected together to build the reference engine. The black arrows show the flow connection and hence the flow path from one module to another. For example, the air is flowing from Fan to Splitter where it gets separated into Bypass Bleed and Duct 21, eventually flowing into Bypass Nozzle and LPC respectively. The cooling air required to cool the turbines is also shown in the diagram. The red arrows show the shaft connections in which the LP shaft is connected to Fan, LPC, and LPT, and the HP shaft is connected to HPC and HPT. The green line shows the connection for data that is required to make calculations in the particular module. For example, nozzles are connected to the Ambient module because nozzles need data like ambient pressure to compute thrust. The Performance module shown in figure 6.2 is the module that calculates all the performance parameters like Thrust-Specific Fuel Consumption (TSFC), Power-Specific Fuel Consumption (PSFC), Gross Thrust, Net Thrust, etc.

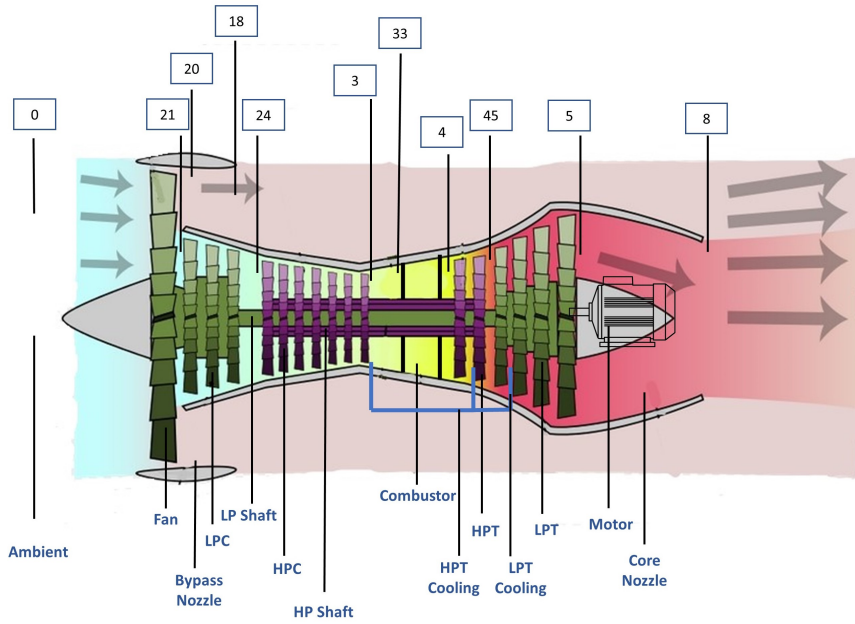


Figure 6.1: Turbofan Nomenclature and station numbers (Adapted from [64])

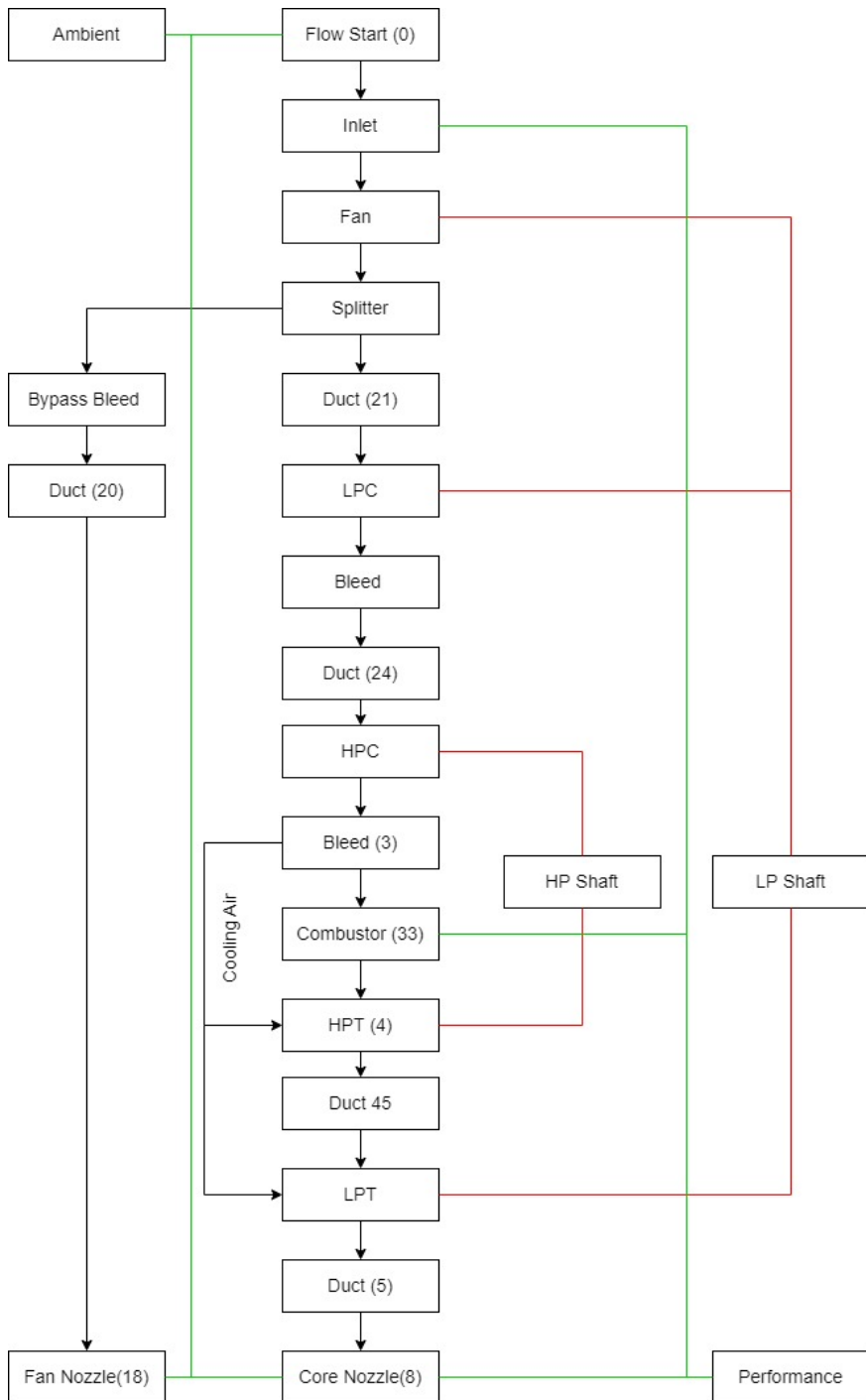


Figure 6.2: Block Diagram of CFM-56-5B1 Reference Engine (Adapted from [56])

Sr. No.	Parameter	Units	Value
1	By-Pass Ratio	-	5.7
2	Fan Pressure Ratio	-	1.7
3	Low Pressure Compressor Pressure Ratio	-	2.22
4	High Pressure Compressor Pressure Ratio	-	8
5	Overall Pressure Compressor Pressure Ratio	-	30.2
6	Isentropic Efficiency of Fan	%	87
7	Isentropic Efficiency of Low Pressure Compressor	%	87
8	Isentropic Efficiency of High Pressure Compressor	%	83
9	Combustor Efficiency	%	100
10	Isentropic Efficiency of High Pressure Turbine	%	87
11	Isentropic Efficiency of Low Pressure Turbine	%	89
12	Core Nozzle Efficiency	%	99.33
13	By-pass Nozzle Efficiency	%	99.39
14	Maximum Turbine Inlet Temperature	K	1722
15	Maximum Turbine Blade Temperature	K	1222
16	Turbine Blade Temperature Safety Factor	K	150

Table 6.1: Parameter Values for the Reference Engine

Sr. No.	Parameter	Units	Value
1	Duct 4 Pressure Loss	%	0.48
2	Duct 6 Pressure Loss	%	1
3	Duct 11 Pressure Loss	%	0.5
4	Duct 13 Pressure Loss	%	0.1
5	Duct 15 Pressure Loss	%	0.15
6	Duct 17 Pressure Loss	%	0.15
7	Combustor Pressure Loss	%	5.4

Table 6.2: Default Parameter Values for the Reference Engine taken from PyCycle example

Table 6.1 reports the reference values for the CFM-56-5B1 engine for Design condition, which is Sea Level Static. The values have been taken from [65]. However, the data for the combustor, ducts, and bleed air Pressure losses have not been found on the public database. Hence, the default values given in PyCycle example cycle for the CFM-56 engine have been taken for the reference case. The values are given in table 6.2.

Table 6.3 shows the parameter values for the Design and Off-Design condition. The Design condition is the Sea-Level Static and the Off-Design condition is the cruise. These values have been taken from [65].

Sr. No.	Parameter	Units	Design Condition (Sea Level Static)	Off-Design Condition (Cruise)
1	Mach Number	-	0.001	0.8
2	Altitude	m	305	11280
3	Thrust	kN	133.6	22.87
4	Fuel	-	Hydrogen	Hydrogen

Table 6.3: Parameters for Design (Sea Level Static) and Off-Design (Cruise) Condition

### 6.2.1. TURBINE COOLING

Turbine cooling flow is very crucial, especially for the HPT because of the high TIT during gas turbine operation. But the turbine cooling is a big penalty to the engine efficiency as the HPC air required for cooling is bypassing the core and not participating in the combustion reaction. Hence, the required amount of cooling air to keep the turbine blades under the maximum permissible limit is dependent on the TIT. *This research assumes that the turbofan has active cooling* and hence, the TIT is different for different operating conditions hence Turbine Cooling module, already available in PyCycle, has been implemented. The module calculates the cooling flow based on the TIT and the maximum permissible blade temperature and safety limit. For example, in the case of the reference engine in Design condition, the cooling air requirement is 15.8% of the core mass flow rate and for Off-Design condition, the cooling air requirement is 4.86% of the core mass flow rate. The cooling flow has not been assumed constant for different conditions and is dependent on the parameters mentioned above.

### 6.3. VALIDATION OF THE REFERENCE ENGINE MODEL

This section consists of the validation of the reference engine model which has been discussed in section 6.2.

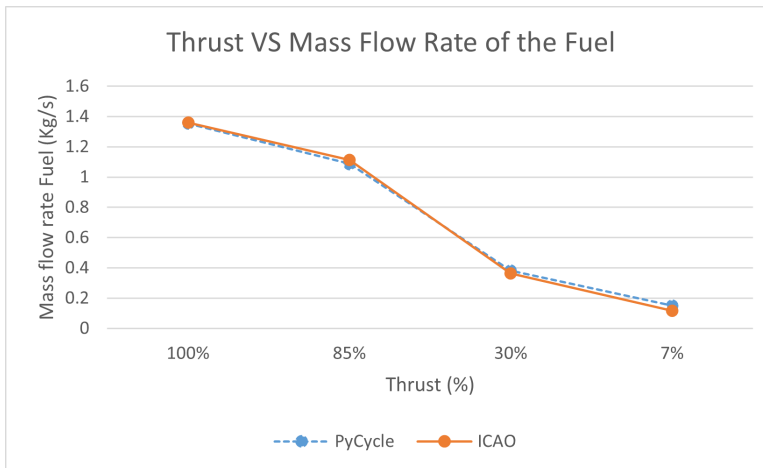


Figure 6.3: Reference Engine Validation

The validation has been done against the ICAO engine data which is publicly available on the ICAO engine emissions databank [66]. Figure 6.3 shows mass flow rate of fuel flow for different thrust percentages at Sea Level Static Condition. The maximum thrust is 133.6 kN and the fuel is Jet-A. It is clear from the figure that the reference engine model built-in PyCycle for the CFM-56-5B1 engine is related very well to the ICAO engine data, especially for the 100% and 85% thrust. Even after using the generic turbine and compressor maps of the CFM-56 engine from PyCycle, default values for pressure losses, and using the turbine cooling module for cooling air, the reference engine model has small errors, and hence, it can be concluded that the reference engine model is validated.



# 7

## SOLID OXIDE FUEL CELL - GAS TURBINE HYBRID

This section talks about the complete architecture and verification of SOFC-GT hybrid propulsion system.

### 7.1. SOFC-GT HYBRID ARCHITECTURE

Figure 7.1 shows the side view of the SOFC-GT hybrid and figure 7.2 shows the block diagram of the complete SOFC-GT hybrid system model which has been built in PyCycle along with the in-house developed fuel cell model. Two new stations have been added, station 31 and station 32, which are the inlets and outlets of the fuel cell. The model developed in PyCycle is similar to the reference model shown in figure 6.2 but with some extra modules for the fuel cell. As explained in section 6.1.1, the black arrows show the flow connection, the green arrows show the data connection and the red line shows the shaft connection. Along with this, the blue arrows show the flow connection for the fuel cell. The yellow arrow shows the electric power connection and the dark red line shows the shaft connection between the motor and LP shaft.

The air required for the fuel cell is taken from the Bleed 3 which is between the HPC and the combustor. The air goes into the Fuel Cell Compressor (FCC), station 31, from Bleed 3 where the pressure of air is increased by 10%. Then the air goes into the fuel cell, station 32, where it generates power and the by-products from the fuel cell go into the Combustor (station 33). The unutilized  $H_2$  burns in the combustor and the other byproducts like air and  $H_2O$  mix with the air which is coming from HPC. The power generated by the fuel cell goes into the motor where it converts electrical power into mechanical power which is added to the shaft as shown in figure 7.1 and 7.2. The data for all the stations for the reference engine and SOFC-GT hybrid is given in appendix A.

The reason for using an FCC is to complement the pressure losses in the Heat Exchanger and SOFC. The pressure loss of 5% has been estimated for SOFC and heat exchanger each. Pressure losses in SOFC vary and depend upon the type of electrodes,

electrolyte, and architecture. However, as this study is a system-level analysis, a detailed SOFC model has not been developed, and hence empirical data for pressure losses presented in the paper [25] has been used. Similarly, the heat exchanger pressure loss value has been taken from [67]. It should also be noted that this pressure loss value includes the losses of duct and piping as well. Hence, the complete fuel cell pressure loss has been estimated to be approximately 10% and the pressure increase in the FCC is also 10% so that when by-products enter the combustor, they are of similar pressure as HPC air.

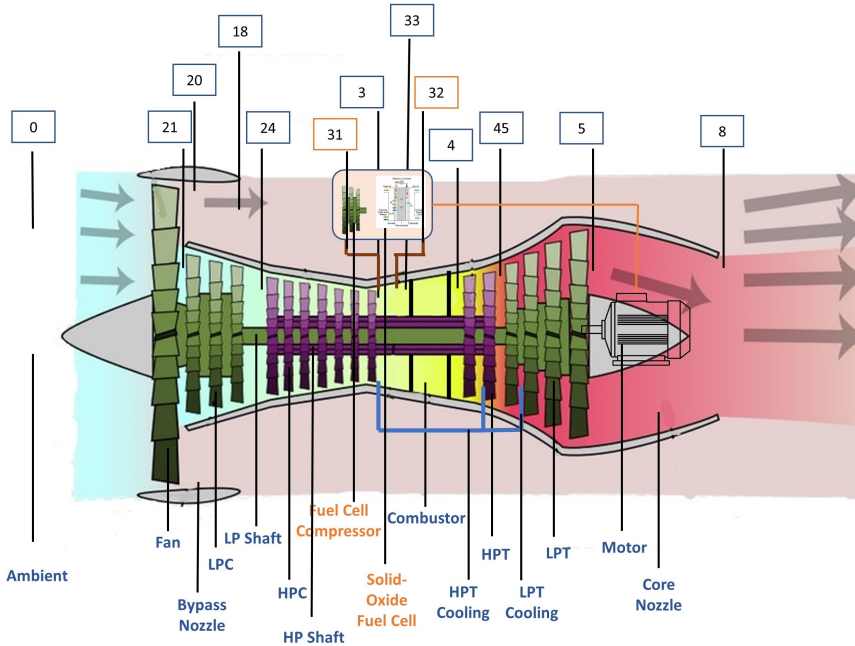


Figure 7.1: SOFC-GT Hybrid Nomenclature and station numbers (Adapted from [64])

It should also be noted that the mechanical power from the motor is added to the LP Shaft. The main reason for this is the loss reduction in transmission. The motor is more efficient than the turbine and hence, the transmission loss is reduced. More explanation is given in section 8.1.3. As the LP Shaft transfer higher power than the HP Shaft, this means the loss in transmission is higher for LP Shaft even after including the higher efficiency of Fan, LPC, and LPT. Also, the power transfer through LP shaft is increasing as fuel cell is added to the turbofan. More explanation is given in section 8.1.2. Hence, it is beneficial to add the fuel cell power to LP Shaft and reduce the losses by a higher amount. The second reason is the physical space needed to add the motor in the engine. If the motor needs to be connected to HP Shaft, it needs to be added at the end of the HPT but there is no space to add the motor because of LPT at the end of HPT as can be seen from figure 7.1. But in the case of the LP Shaft, the motor can be connected just after the LPT. Along with this, if the motor is to be added after the HPT, the high temperature of flow would increase the cooling requirements in the motor.

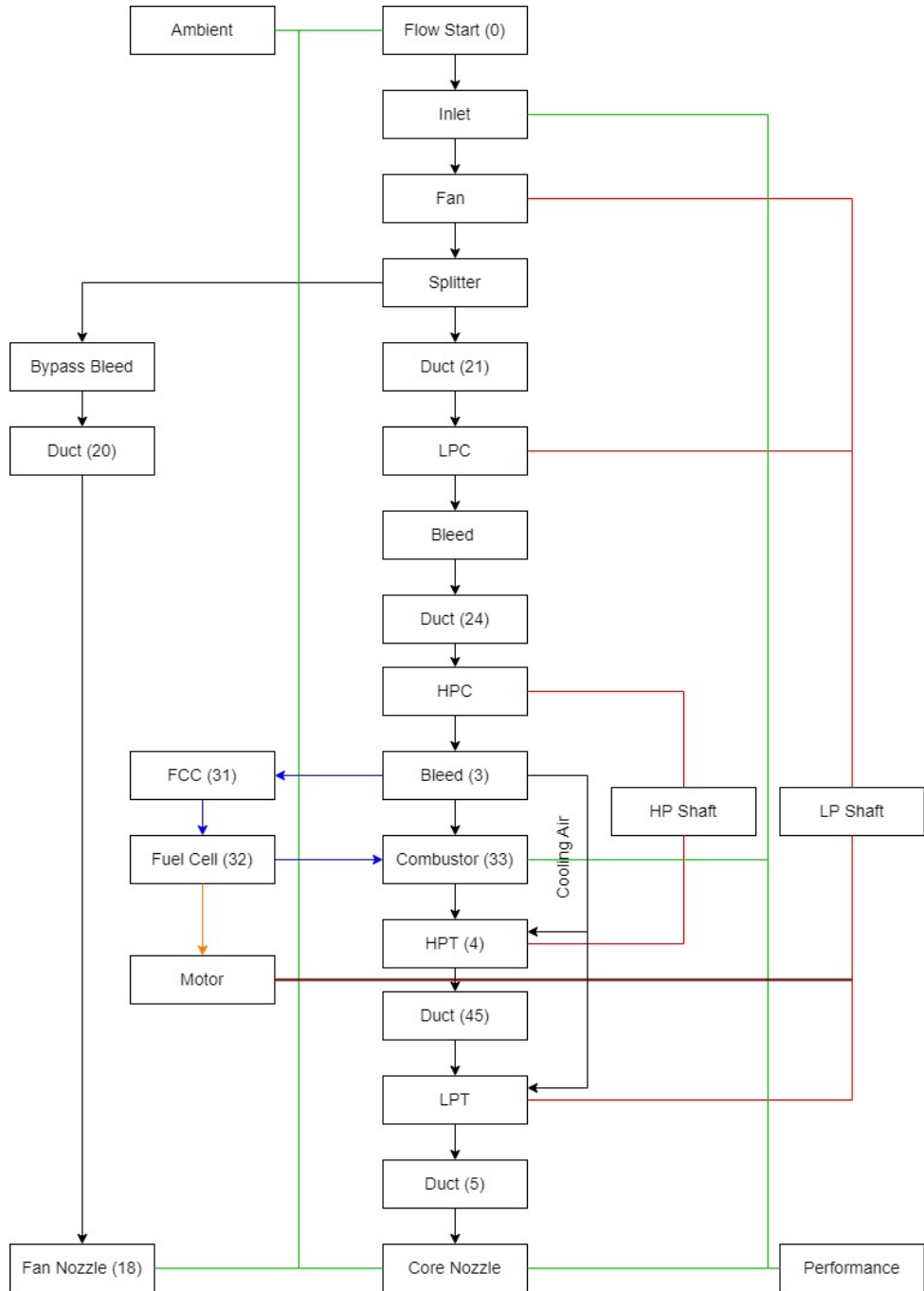


Figure 7.2: Block Diagram of SOFC-GT Hybrid Propulsion System

Equation 7.1 shows the net fuel cell power added to the LP Shaft. The power required for FCC is coming directly from the fuel cell itself and hence, it has been subtracted from the total power output of the fuel cell. Similarly, the motor efficiency has also been accounted for the power which is added to the LP Shaft. Figure 7.3 shows the net power added to the LP shaft compared to the power output from the fuel cell and it is lower because of the reasons mentioned above.

$$P_{fc_{LP}} = (P_{fc} - P_{fc_c}) * \eta_m \quad (7.1)$$

where

$P_{fc_{LP}}$  = Net Fuel Cell Power added to the LP Shaft, W  
 $P_{fc}$  = Fuel Cell Power Output, W  
 $P_{fc_c}$  = Fuel Cell Compressor Power Input, W  
 $\eta_m$  = Motor Efficiency, %

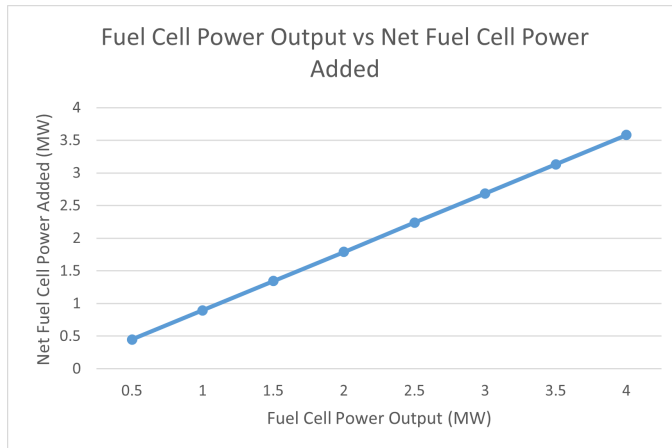


Figure 7.3: Net Fuel Cell Power added to the Low Pressure Shaft

The **assumptions** for the integration of SOFC-GT Hybrid system are given below.

- The mixing of byproducts coming from the fuel cell and the high pressure compressor is assumed to be adiabatic.
- No gearbox has been added to transfer the mechanical power from the motor to the Shaft. It has been assumed that both motor and LP Shaft have the same RPM.
- No cooling for the motor has been assumed.
- The motor efficiency has been assumed to be 96% [68]. There are multiple sources which are estimating the motor efficiency close to 99% [11]. However, a conservative value of 96% is presented in the paper [68].
- Fuel Cell Compressor efficiency is assumed to be 87% [65].

## 7.2. VERIFICATION OF SOFC-GT HYBRID PROPULSION SYSTEM

This section consists of the verification of the SOFC-GT hybrid propulsion system. Figure 7.4 shows the error, as per equation 5.5, for the different fuel cell power output. The secondary axis shows the fuel cell power fraction and is defined in equation 7.2. It should be noted here that this fuel cell power fraction is the ratio of total fuel cell power output and the total power added in the form of fuel to the propulsion system. It is not the ratio of net power added to the LP shaft and the total power input as discussed in the last section.

It is clear from the figure that the maximum error for the Design condition is 0.062% and for Off-Design condition is 0.033%, which is very low and can be considered negligible. In order to understand the scale of error, for 2 MW Power output, the total enthalpy of the flow leaving the combustion chamber is around 24.5 MJ while the error is around 15000 J.

$$f_{fc} = \frac{P_{fc_{LP}} * 100}{P_{in}} \tag{7.2}$$

$$P_{in} = \dot{m}_f * LHV_{Hydrogen} \tag{7.3}$$

where

$f_{fc}$ = Fuel Cell Power Fraction

$P_{fc}$ = Fuel Cell Power Output, W

$P_{in}$ = Total Power input, W

$\dot{m}_f$ = Total fuel input in fuel cell, kg/s

$LHV_{Hydrogen}$ = Lower Heating Value of hydrogen i.e.  $120 * 10^6$ , J/kg

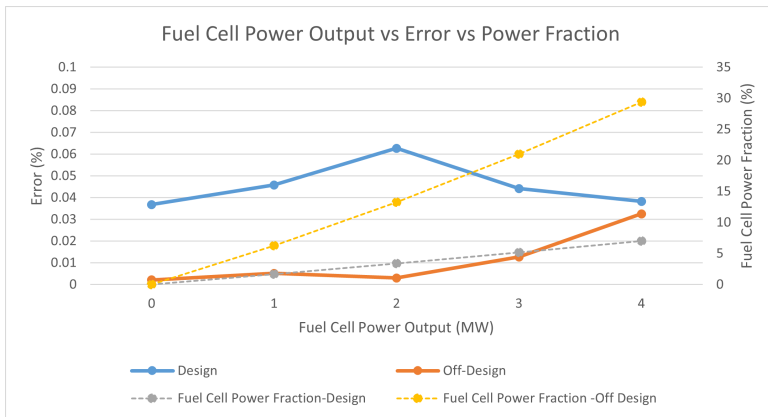


Figure 7.4: Error in Enthalpy Balance of SOFC-GT Hybrid for different Fuel Cell Power Output

### 7.3. TEMPERATURE-ENTROPY (T-S) DIAGRAM

This section reports the Temperature-Entropy or T-s diagram for the Brayton cycle and the impact on the cycle after the addition of the fuel cell. Figure 7.5 shows the ideal T-s diagram for reference engine (left) and SOFC-GT hybrid engine (right).

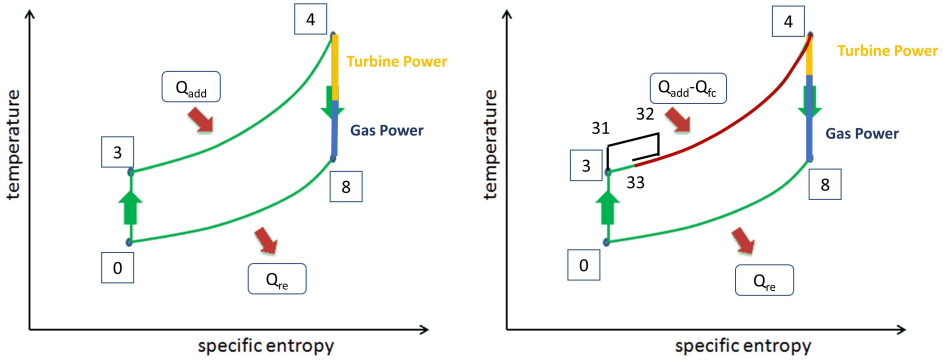


Figure 7.5: T-s diagram for reference engine(Left) and T-s diagram for SOFC-GT hybrid engine(Right) (Adapted from [69])

First, let's discuss the T-s diagram for the reference engine, and the explanation of the diagram is given below.

- **Process 0-3:** Process 0-3 is the compression process that increases the pressure of the flow.
- **Process 3-4:** Process 3-4 is the heat addition process in which the fuel is combusted inside the combustion chamber is converted to heat and the flow temperature is increased from 3 to 4. The pressure is constant when heat is added as the process is ideal.
- **Process 4-8:** Process 4-8 is the expansion process in which the power is extracted from the flow and used in two ways given below.
  - *Turbine Power:* A fraction of power extracted from the flow is used to run the compressor via turbine in processes 1-2. It should be noted that the losses in transmission and the turbine have been included in the compressor power.
  - *Gas Power:* Gas power is the remaining power in the flow after the turbine has extracted the required power. This gas power is used to produce thrust and is shown in figure 7.5.
- **Process 8-0:** This process is the heat release that is left in the flow until it reaches the ambient temperature. The pressure at 8 is actually ambient but the temperature is higher and hence the extra heat needed to be extracted.

Now, let's understand how the T-s diagram will change when the fuel cell is added and the explanation is given below.

- **Process 0-3:** Process 0-3 is the compression process and is similar to the reference engine.
- **Process 3-31:** Process 3-31 is the fuel cell compressor, as explained in section 7.1, is used to increase the pressure of the air going into the fuel cell.
- **Process 31-32:** Process 31-32 is the heat addition in the flow inside the fuel cell as explained in section 5.2.
- **Process 32-33:** Process 32-33 is the pressure loss and adiabatic mixing. There are pressure losses inside the fuel cell and heat exchanger and is explained thoroughly in section 7.1. Hence, the byproducts coming out of the fuel cell have the same pressure as HPC air.

Then the flow is mixed with the HPC air adiabatically which leads to the increase in the temperature of the mixture from 3 to 33. As a result, the heat required to increase the temperature of the flow to 4 has reduced as a fraction of heat is added by the fuel cell ( $Q_{fc}$ ) which is shown by the red curve in the figure 7.5.

- **Process 4-8:** Process 4-8 is the expansion process similar to the reference engine where a fraction of power is provided to the compressor via turbine and the rest of the work is the gas power. The gas power for the SOFC-GT hybrid is presented in equation 7.4. As explained in section 7.1, the fuel cell power is added to the shaft and hence it is reducing the total turbine power extracted from the flow which is clearly shown in figure 7.5. The total turbine power has reduced and as a result, the gas power available has increased. It should also be noted that the losses in the motor and the fuel cell compressor power has been extracted from the fuel cell power directly.

$$\text{Gas Power}_{SOFC-GT} = \left( \frac{(\text{Total Power Output} + \text{FC Power}) - (\text{Turbine Power} - \text{FC Compressor Power})}{\text{Total Power Output} + \text{FC Power}} \right) \quad (7.4)$$

Hence, the addition of fuel cell to gas turbine eventually increased the gas power and reduce the amount of fuel added into the combustor for the same TIT. This will lead to an increase in thermodynamic efficiency which is explained in section 8.



# 8

## TECHNICAL ANALYSIS RESULTS

This section talks about the results which have been evaluated from the model discussed in the last section in order to answer the research questions mentioned in section 4. Three different types of analysis have been done and they are given as follows:

- **No Constant Specific Thrust and No Optimum point analysis:-** The first analysis done includes the integration of fuel cell with turbofan with no change in turbofan parameters. The analysis presents the results when engine parameters are kept constant.

It has been observed that the thermodynamic efficiency of the whole system increased while the mass flow rate entering the engine reduced when the fuel cell is added. As a consequence, the propulsive efficiency dropped and hence the total efficiency of the system dropped in the Design (Sea-Level Static) condition.

- **Constant Specific Thrust and Optimum point analysis:-** As the efficiency of the engine dropped because of a decrease in mass flow rate, an analysis has been done by keeping the specific thrust of the engine constant. This means that the mass flow rate entering the engine and thrust output is similar to the reference engine. This has been done in order to have a fair comparison between the SOFC-GT hybrid and the reference engine as mass flow rate has a direct impact on the thrust and efficiency of the propulsion system. Along with this, the engines have been compared at their most optimum points to understand the maximum benefit that can be achieved from the SOFC-GT hybrid.

The results show that TSFC for both the conditions, Design and Off-Design (Cruise), has reduced along with the reduction in core size or core mass flow rate and the cooling mass flow rate requirement.

- **Downsized Turbofan:-** The third technical analysis is done in the project is to answer the sub-research question number 6. This analysis presents the result of the impact of downsizing the turbofan while having a similar amount of thrust output

as the reference engine. The analysis is done for constant specific thrust and most optimum point.

The results show that the engine can be downsized but the required fuel cell power is very high.

In the end, sensitivity analysis for a SOFC-GT hybrid for constant specific thrust and at the most optimum point has been done which shows that the gas turbine parameters have the most impact on thermodynamic efficiency but the impact is reducing as fuel cell contribution is increased. More details are given in the coming sections.

## 8.1. NO CONSTANT SPECIFIC THRUST AND NO OPTIMUM POINT ANALYSIS

This section presents the result of the analysis done by adding the fuel cell to the turbofan without any change in the engine parameter. The results are given in the following subsections.

### 8.1.1. RESULT 1

#### *Adding fuel cell to reference engine increases TSFC for Design(Sea Level Static) Condition*

Adding the Fuel Cell in the reference engine increases the TSFC and it can be seen from figure 8.1 on the secondary axis. The TSFC has increased by 1.3% when fuel cell power output is 4 MW even though the Thermodynamic and Thermal efficiency is increasing, as shown in figure 8.3.

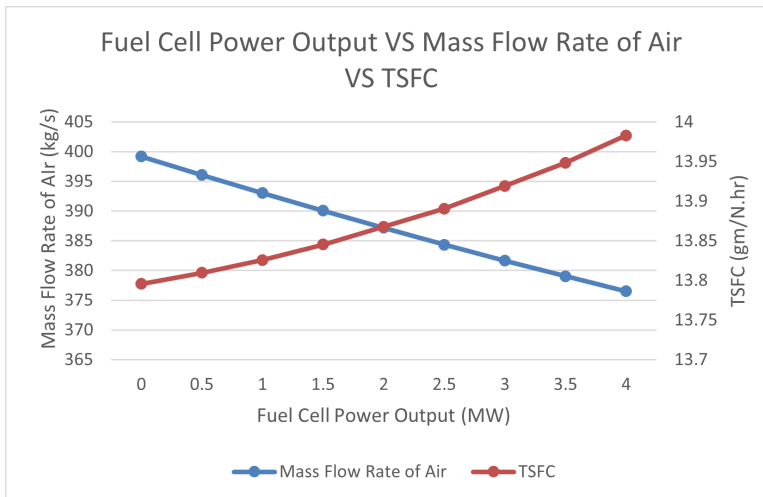


Figure 8.1: Change in Mass Flow Rate of Air and TSFC for an increase in Fuel Cell Power Output for Design Condition

The reason for this is given below.

- As mentioned in section 7.1, the power from the fuel cell is added to the LP shaft. Complementing the shaft means that the turbine has to extract less power from the core flow because a fraction of power is coming from the fuel cell. As TIT and OPR are constant, this will lead to more energy in the core flow after LPT compared to the reference engine.
- The increase in the core flow energy will eventually lead to an increase in the core thrust. As the total thrust requirement is constant, this will eventually lead to a reduction in by-pass thrust. This can be clearly seen in figure 8.2.
- The bypass thrust can be reduced either by reducing Mass Flow Rate ( $\dot{m}$ ) or by reducing the Fan Pressure Ratio (FPR). As all the engine parameters have been kept constant, the FPR cannot be changed.  $\dot{m}$  is a variable and hence, it has been reduced in order to reduce the bypass thrust. This has been shown in figure 8.1. As the fuel cell power output is increased,  $\dot{m}$  is decreasing leading to the decrease in bypass thrust as shown in figure 8.2.

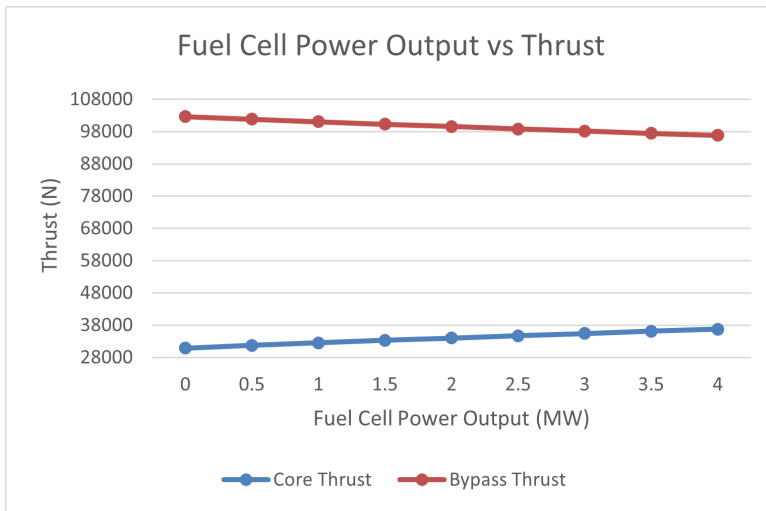


Figure 8.2: Change in Thrust for an increase in Fuel Cell Power Output for Design Condition

- The reduction in mass flow rate and bypass thrust leads to a reduction in propulsive efficiency, even though the thermodynamic and thermal efficiency is increasing as shown in figure 8.3. The Thermodynamic efficiency has increased by 7.6% when the fuel cell with fuel cell power output of 4 MW is integrated but the TSFC still increased by 1.3%. This means that the increase in thermodynamic efficiency did not counteract the reduction in propulsive efficiency, hence, leading to a total reduction in engine efficiency and an increase in TSFC. These results are different from the results of Okai [36] and the integrated system discussed in section 3 as

Okai kept the propulsive efficiency of the engine constant, which is not possible without changing any engine design parameter.

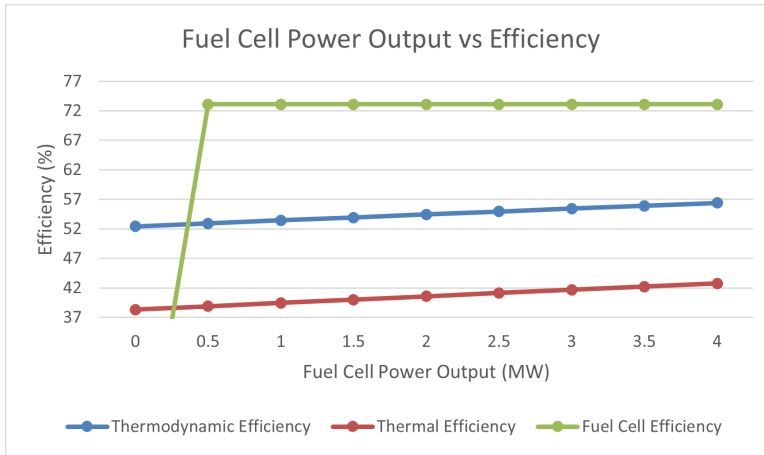


Figure 8.3: Change in Efficiency for an increase in Fuel Cell Power Output for Design Condition

### 8.1.2. RESULT 2

**The TSFC reduction for a 1 MW Power output (6.2 % of power input), is 6.4% in relative terms for Off-Design (Cruise) Condition.**

Contrary to the Design condition where adding the fuel cell to the reference engine increased the TSFC, in Off-Design or cruise condition, the TSFC is reducing and it can be seen from figure 8.4 on the secondary axis.

8

The reason for the reduction in TSFC is given below.

- In PyCycle, the Design condition takes the user inputs and calculates the engine output parameters based upon the given inputs. For example, Turbine Inlet Temperature (TIT), Overall Pressure Ratio (OPR), Bypass Ratio (BPR), and other parameters are user inputs. The engine varies the Fuel to Air ratio (FAR) and  $\dot{m}$  in order to achieve the specified thrust.
- On the other hand, in the Off-Design condition, the  $\dot{m}$  is dependent on the Design condition, mainly the nozzle areas, and the parameters like OPR, BPR, and FPR are dependent on the corrected mass flow rates and speeds. TIT is variable and is changed by changing the amount of fuel flow in order to achieve the required thrust. It should be noted that the stall margins for all the compressors including fan are higher than 9% for all the values of fuel cell power output.
- Hence, as the fuel cell power is added to the LP Shaft during Off-Design condition, TIT reduces as extra power is coming from the fuel cell as shown in figure 8.5. In the

design condition, TIT was fixed and hence, the gas power, as defined in equation 7.4, was increasing when fuel cell power is added but in the Off-Design condition, gas turbine's gas power will reduce by reducing the fuel flow and hence the TIT. This is one of the major factors for the improvement of TSFC.

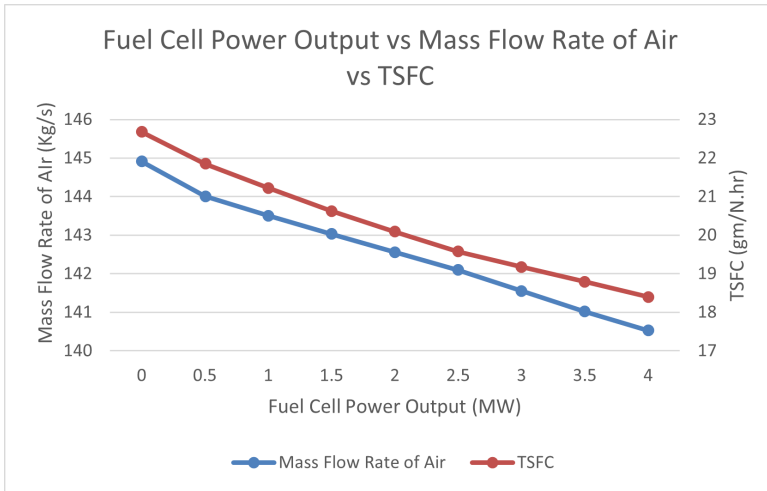


Figure 8.4: Change in Mass Flow Rate of Air and TSFC for an increase in Fuel Cell Power Output for Off-Design Condition

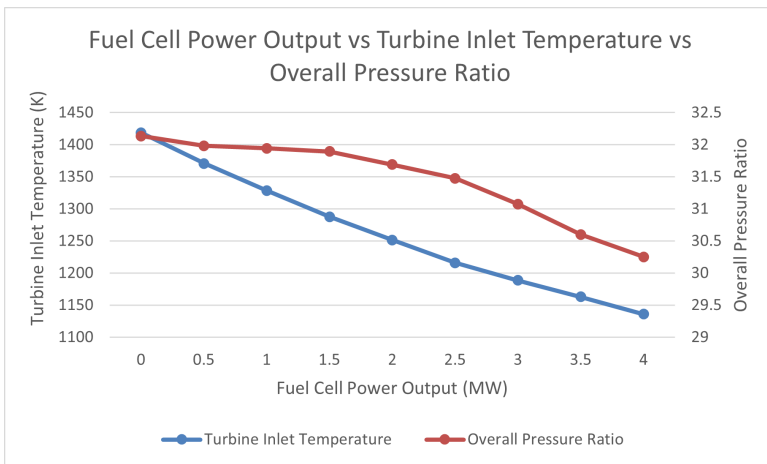


Figure 8.5: Change in TIT and OPR for an increase in Fuel Cell Power Output for Off-Design Condition

- This is precisely the reason that, unlike the Design condition where the core thrust is increasing because of the increase in gas power leading to a total efficiency reduction, in the Off-Design condition it is reducing which eventually leads to an

increase in bypass thrust and hence the Propulsive efficiency. Figure 8.6 shows the change in thrust and figure 8.7 shows the slight increase in propulsive efficiency as fuel cell power output is increased.

- Both Propulsive and Thermodynamic efficiency are increasing and this is the reason that in Off-Design condition, the TSFC is reducing.

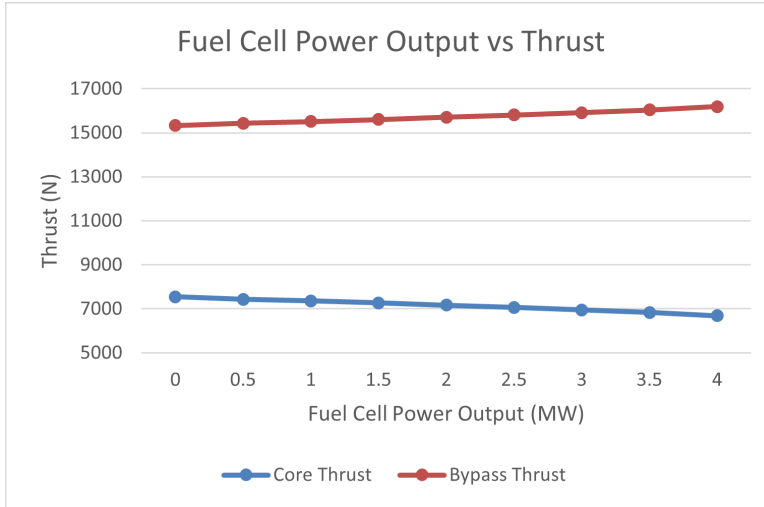


Figure 8.6: Change in Core and Bypass thrust for an increase in Fuel Cell Power Output for Off-Design Condition

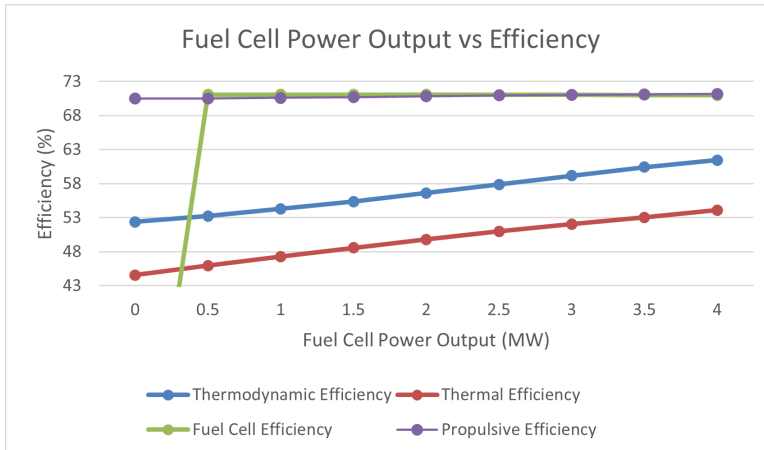


Figure 8.7: Change in Efficiency for an increase in Fuel Cell Power Output for Off-Design Condition

The change in the OPR in the Off-Design condition is also the reason for the decrease

in the temperature entering the combustor. As the OPR is decreased, the temperature of the air coming from HPC also decreases as shown in figure 8.8.

Figure 8.7 also shows the change in fuel cell efficiency against fuel cell power output. The efficiency is almost constant even though the OPR is decreasing. The reason for this is the less sensitivity of SOFC on pressure. As explained in section 5.2.2, SOFC is more sensitive to temperature than pressure and temperature is constant for all the fuel cell power output. However, the fuel cell Efficiency for Off-Design condition does vary from the Design Condition as presented in figure 8.3. The fuel cell efficiency is 73% for the Design conditions and 71.1% for the Off-Design conditions. This improvement in fuel cell efficiency is due to the substantial increase in absolute pressure at Design condition but the improvement is still small because of the reasons given above.

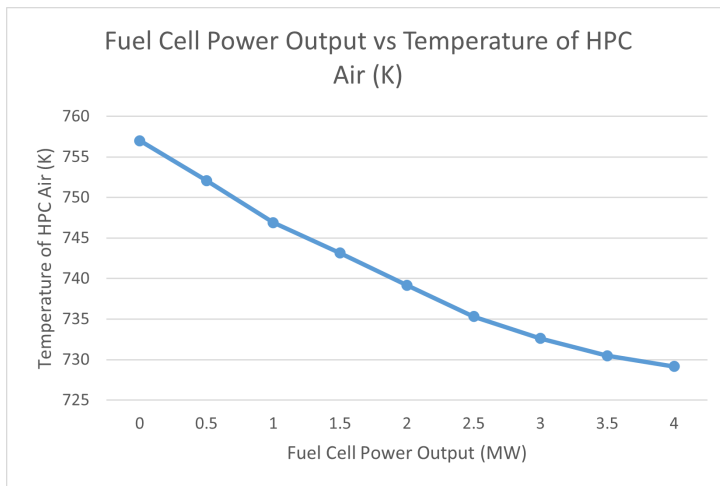


Figure 8.8: Change in Temperature of HPC Air for an increase in Fuel Cell Power Output for Off-Design Condition

### 8.1.3. REASONS FOR A REDUCTION IN TSFC

As shown in section 8.1.2, the TSFC is reducing for Off-Design condition and this section talks about the reasons for the improvement in TSFC due to the addition of SOFC to the reference engine and they are given below.

- Higher efficiency of fuel cell:** The SOFC efficiency, when compared to Gas Turbine, is relatively high because of the lower losses inside the SOFC. The total efficiency of SOFC is 71.12 % and the efficiency of the complete fuel cell , including the fuel cell compressor and motor, is 63.68% after including motor efficiency and fuel cell compressor during Off-Design Condition. When compared to the thermodynamic efficiency of 52.38% for a gas turbine, the total efficiency of fuel cell is 21.57% higher than the gas turbine in relative terms, which eventually leads to higher system efficiency. First, the question arises, if, in the case of the fuel cell, the total efficiency of the system has been used for comparison then why only thermodynamic efficiency has been used for the Gas Turbines? The reason for this is the

fair comparison. The gas turbine's thermodynamic efficiency provides the value of the useful work that the gas turbine delivers for a particular operating condition. Using this useful work to create thrust will inherent more losses and will eventually decrease the efficiency of the turbofan.

Similarly, in the case of the fuel cell, the power delivered after removing the FCC and including the motor efficiency, will eventually then be used to create thrust, just like in a gas turbine. Hence, the thermodynamic efficiency of the Gas Turbine and the total efficiency of the fuel cell must be compared for a fair comparison.

- Heat addition into the combustor:** One of the biggest advantages of an integrated system is that the thermal energy of the fuel cell byproducts can be used to produce the thrust in the gas turbine. In this case, the waste heat of SOFC has been added to the combustor and has been used as the fuel for the gas turbine. For example, in the case of 1 MW, fuel cell power output, 2.377 kg of air is entering the fuel cell at a temperature of 747 K and the fuel cell by-products are entering the combustor at a temperature around 900 K. This additional thermal energy helps in reducing the fuel flow in the combustor, eventually leading to an increase in thermodynamic efficiency as shown in the figure 8.7 and hence reducing TSFC. A more thorough explanation is given in section 7.3.
- Loss reduction in transmission:** Figure 8.9 shows the transmission of power from core flow to bypass flow and the related efficiencies of each component. First, energy from the core flow gets converted into mechanical power via turbine with an efficiency of 87%. Then the power is transmitted to the fan via a shaft at the efficiency of 99.5% and the fan adds the mechanical power to bypass flow again at an efficiency of 87%. This leads to a total transmission loss of 24.69%.

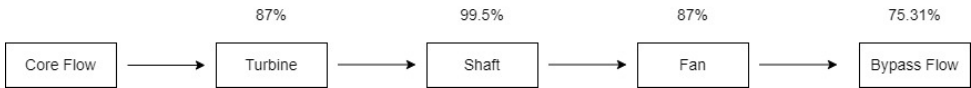


Figure 8.9: Transmission of energy from Core flow to By-Pass flow in gas turbine

On the other hand, figure 8.10 shows the transmission power from the fuel cell to the fan and the respective efficiencies. The total transmission loss is 16.9%, which is 31.55% lower in relative terms when compared to gas turbine transmission. The reason for this improvement is the more efficient motors compared to the turbine. The subsequent components are the same in both cases. This reduction in transmission loss also led to a reduction in TSFC.

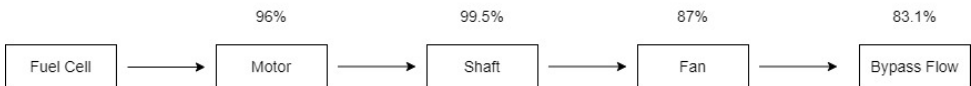


Figure 8.10: Transmission of energy from Fuel Cell to By-Pass flow in SOFC-GT hybrid

It should also be noted that in figure 8.4, even though the TSFC is decreasing, the  $\dot{m}$  for off-design condition is still decreasing, as it depends on the Design condition. This means that the propulsive efficiency shown in figure 8.7 is not the most optimum and hence the SOFC-GT hybrid has not achieved its maximum efficiency as it could have been achieved if the  $\dot{m}$  would be similar to the reference engine.

This means that the comparison is done with the reference engine by just adding the fuel cell to the gas turbine without any change in the reference engine, **is not a fair comparison**.  $\dot{m}$  is directly proportional to the thrust produced and has a big impact on the whole engine efficiency and TSFC. Reduction in  $\dot{m}$  even while the TSFC is reducing in Off-Design condition, does not represent the true potential of adding the fuel cell.

## 8.2. CONSTANT SPECIFIC THRUST AND OPTIMUM POINT ANALYSIS

This section presents the results of the analysis where the Specific thrust of the engine is kept constant in order to do a fair comparison. In order to keep the specific thrust constant, the mass flow rate of the engine needs to keep constant as thrust output is already the same as reference engine. A methodology has been developed to keep the specific thrust constant and is explained in section 8.2.1

### 8.2.1. CONSTANT SPECIFIC THRUST AND OPTIMUM POINT METHODOLOGY

This section explains the constant specific thrust and the optimum point methodology developed in order to fairly compare the SOFC-GT hybrid with the reference engine. The methodology has been explained in figure 8.11. A thorough explanation of the methodology has been given below.

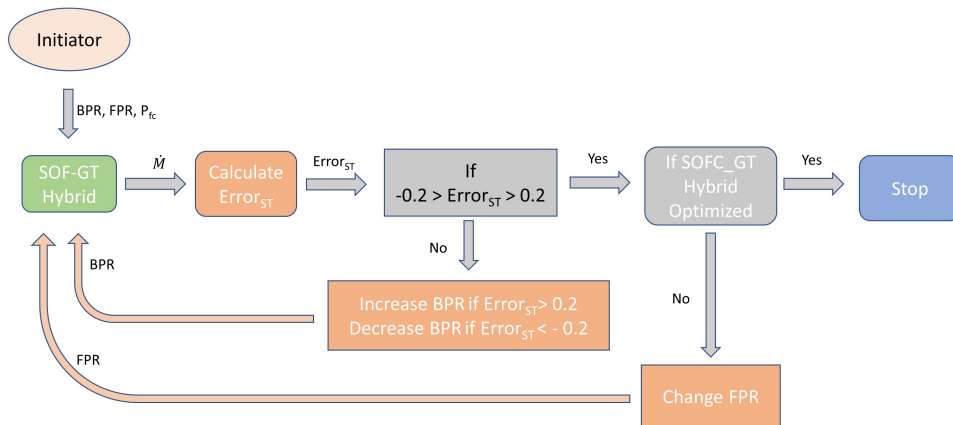


Figure 8.11: Methodology for constant specific thrust and optimum point

- **Step 1: Achieving the constant Specific Thrust**

The first step is to achieve a constant specific thrust as defined in equation 8.1 and shown in figure 8.11. The  $Error_{st}$  is defined in equation 8.2. The aim is to maintain the constant  $\dot{m}$  entering the engine given the same thrust output for the reference engine and SOFC-GT hybrid. Increasing the  $\dot{m}$  will decrease the specific thrust and increase the propulsive efficiency as more thrust is being generated from mass than the increase in velocity, hence increasing the total efficiency and vice versa. This is desired for any engine and the Aerospace Industry is moving towards lower specific thrust.

$$\text{Specific Thrust} = \frac{\text{Thrust}}{\dot{m}} \quad (8.1)$$

$$Error_{st} = \frac{\text{Design Thrust}}{\dot{m}_{SOFC-GT}} - \frac{\text{Design Thrust}}{\dot{m}_{reference}} \quad (8.2)$$

where

$\dot{m}_{SOFC-GT}$  = Mass flow rate of air for SOFC-GT hybrid, kg/s

$\dot{m}_{reference}$  = Mass flow rate of air for reference engine, kg/s

Second, a change in mass flow rate will also change the fan diameter as it depends directly upon the mass flow rate and hence increases the nacelle drag, which is not desired at all. This is the reason that the first step is to keep the mass flow rate constant and eventually the specific thrust.

#### • Methodology to keep the Specific Thrust constant

The specific thrust has been kept constant by varying the BPR as shown in figure 8.11. If the absolute  $Error_{st}$  is higher than 0.2, it means that the lower  $\dot{m}$  compared to the reference engine is flowing into the SOFC-GT hybrid as the thrust output of both engines is constant. Hence, the BPR is changed to reduce the error and it has been explained below.

- When BPR is increased for an engine, less  $\dot{m}$  will go into the core of the engine and as all other engine parameters like OPR and TIT are constant, the gas power ( $P_{gg}$ ) will decrease. This decrease in  $P_{gg}$  will lead to a decrease in core thrust.
- In order to compensate for the reduction in core thrust, bypass thrust needs to increase.
- Bypass thrust can be increased either by increasing the  $\dot{m}$  or the FPR. If FPR is increased, then engine propulsive efficiency will go down as the bypass nozzle would be producing the thrust by increasing the velocity of the flow, rather than the  $\dot{m}$ . This increase in velocity will increase the power loss as power loss is directly proportional to the square of velocity as shown in equation 8.3. However, if  $\dot{m}$  is increased in order to get a higher thrust from bypass,

the power loss will only increase linearly with  $\dot{m}$ . That's why the FPR is kept constant and  $\dot{m}$  is increased to increase the required bypass thrust.

$$\text{Power Loss} = \frac{1}{2} * \dot{m} * (V_j - V)^2 \tag{8.3}$$

where

$V_j$ = Jet velocity, m/s

$V$ = Aircraft velocity, m/s

- The BPR will be increased until the  $\dot{m}$  is similar to the reference engine  $\dot{m}$ , which will lead to a similar Specific Thrust as the thrust output of SOFC-GT hybrid and reference engine is same.

*It should be noted that by increasing the BPR and keeping the  $\dot{m}$  same as the reference engine, the size of the fan of the SOFC-GT hybrid is similar to the reference engine. However, the core of the engine is getting smaller as a result of increasing BPR.*

**• Step 2: Finding the Most Optimum point**

As mentioned in step 1, increasing the BPR will increase the mass flow rate entering the engine given that the other parameters like FPR are constant. However, if the BPR is increased and FPR is kept constant, there is a possibility that the engine is shifted from its most optimum point because of the increase in the bypass power loss and transmission loss. In order to find the engine's most optimum FPR, a new methodology has been developed by the author and is explained below.

The main reason for using a bypass nozzle is to reduce the losses inside the core exhaust, mainly the core power loss which is defined in equation 8.4. It can be understood from the equation that the power loss is directly proportional to  $\dot{m}$  and to the square of jet velocity. As the core mass flow rate and  $V_{jc}$  increases, the core power loss increases exponentially. This is precisely the reason that the air is bypassed around the core in order to reduce the jet velocity and increase the  $\dot{m}_b$ . But bypass thrust generation also has bypass power loss as shown in equation 8.5. Even though  $\dot{m}_b$  is multiple times more than the core mass flow rate, the power loss per unit generation of thrust is lower because of significantly lower  $V_{jb}$ . Along with this, there is a transmission loss as well which has been explained in section 8.1.3 and is a consequence of transmitting the power from the core to the bypass and is given in equation 8.6.

$$\text{Core Power Loss} = \frac{1}{2} * \dot{m}_c * (V_{jc} - V)^2 \tag{8.4}$$

$$\text{Bypass Power Loss} = \frac{1}{2} * \dot{m}_b * (V_{jb} - V)^2 \tag{8.5}$$

$$\text{Transmission Loss} = \frac{W_{fan} * (1 - (\eta_{fan} * \eta_{lpt} * \eta_{shaft}))}{(\eta_{fan} * \eta_{lpt} * \eta_{shaft})} \tag{8.6}$$

where

$\dot{m}_c$  = Core mass flow rate, kg/s

$\dot{m}_b$  = Bypass mass flow rate, kg/s

$V_{jc}$  = Effective core jet velocity, m/s

$V_{jb}$  = Effective Bypass jet velocity, m/s

$V$  = Aircraft Velocity, m/s

$W_{fan}$  = Power required by fan to accelerate the flow, W

$\eta_{fan}$  = Fan Efficiency, %

$\eta_{lpt}$  = LPT Efficiency, %

$\eta_{shaft}$  = Shaft Efficiency, %

Hence, as more thrust is generated from the bypass, the bypass power loss and transmission loss will increase but the core power loss will reduce. But the total power loss, given in equation 8.7 is reducing and shown in figure 8.12. As FPR is increased, the bypass thrust will increase, and hence the core power loss will reduce, leading to a total reduction in power loss.

However, there will be a point when the summation of bypass core power loss and transmission power loss is equal to core power loss. This is a point that is the most optimum point for the gas turbine as the power loss is at its lowest as shown in the figure 8.12. It can also be seen that the TSFC is also lowest at this point for the same reason presented above. **In this case, the most optimum point for the engine is at the FPR of 1.8** and will be used as a reference to compare with the SOFC-GT hybrid from this point onwards.

$$\text{Total Power Loss} = \text{Core Power Loss} + \text{Bypass Power Loss} + \text{Transmission Loss} \quad (8.7)$$

8

*Beyond this FPR, bypassing the air will be less efficient than using it in the core to generate thrust.* This is precisely the reason that when BPR is increased and FPR is kept the same in the SOFC-GT hybrid, there might be a possibility that the engine is not as efficient due to higher loss in bypass and transmission. Hence, the methodology of finding the most optimal point for the engine has been implemented.

However, a common methodology is generally used to find the most optimum FPR using the *Optimum Velocity Ratio Method*. This method basically provides the most optimum point for turbofan based upon the bypass and core jet velocity, LPT efficiency, and Fan Efficiency. The equation 8.8 shows the calculation for optimum velocity Ratio and is explained thoroughly by Guha [70].

$$\left(\frac{V_{jb}}{V_{jc}}\right)_{opt} = \eta_{LPT} * \eta_{Fan} \quad (8.8)$$

where

$V_{jb}$  = Fully expanded bypass jet velocity, m/s

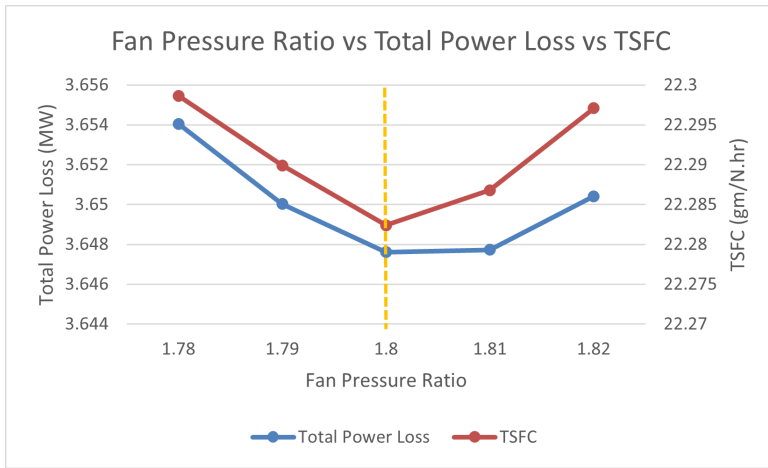


Figure 8.12: Changes in power loss and TSFC as FPR is changed

$V_{je}$ = Fully expanded core jet velocity, m/s  
 $\eta_{LPT}$ = Isentropic Efficiency of LPT  
 $\eta_{LPT}$ = Isentropic Efficiency of Fan

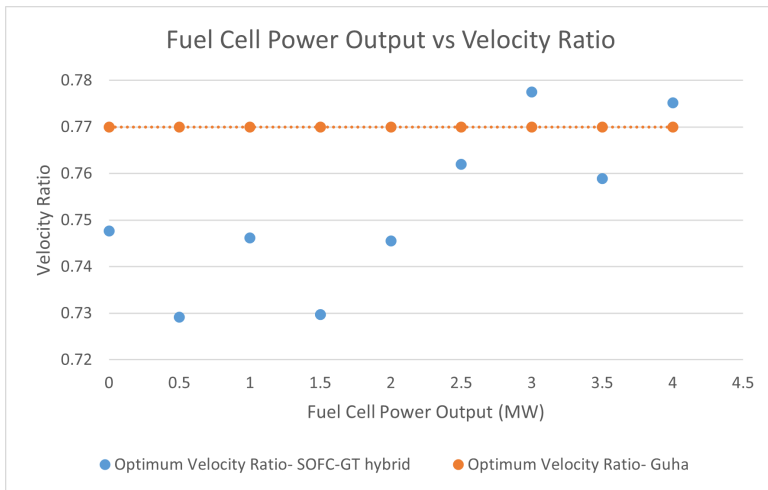


Figure 8.13: Difference in the optimum velocity ratio developed for SOFC-GT hybrid and the method given by Guha

Nevertheless, this methodology **cannot** be used for this study. Figure 8.13 shows the velocity ratios for different fuel cell power output calculated by two methods. The orange line shows the method given by Guha [70] and given in equation 8.8. The blue points shows the optimum velocity points calculated using the method

developed by the author for the SOFC-GT hybrid. It is clear that the optimum velocity ratios for SOFC-GT hybrid is different from the method Guha.

The reason for the difference in the results between the two methods is changing thermal efficiency. Equation 8.8 assumed that the thermal efficiency of the engine remains constant when the engine parameters are changed and the equation fails if thermal efficiency is changed. However, when fuel cell is added to the engine and other parameters like BPR is changed, the kinetic energy of the flow, for bypass and core, changes and hence the thermal efficiency.

*In a nutshell, both, reference and SOFC-GT are compared for the same specific thrust and at their most optimal points.*

### 8.2.2. RESULT 3

***The TSFC reduction for a 1 MW Power output (1.67 % of total power input), is 1.8% in relative terms for the Design (Sea Level Static) condition. The TSFC reduction for a 1 MW Power output (6.26 % of power input), is 6.03% in relative terms for Off-Design (Cruise) condition***

This section talks about the reduction in TSFC for optimum performance and constant Specific Thrust. Figure 8.14 shows the change in TSFC for different fuel cell power output for constant Specific Thrust and optimum point for Design and Off-Design condition. The Specific Thrust is constant only for Design condition. However, the figure shows Off-Design condition with Constant Specific Thrust in order to make a distinction with the reference case. It should be noted that other conditions like OPR and TIT are the same as the reference engine for Design conditions. The figure also shows the TSFC for the reference engine, which is also at its optimum point as mentioned in section 8.2.1.

It is clear from the figure that even though the same amount of fuel cell power is added to the engine, the constant Specific Thrust SOFC-GT hybrid has lower TSFC compared to the reference engine for both Design and Off-Design conditions. The difference is higher for the Design condition because of the increase in mass flow rate, leading to higher efficiency compared to a non-constant Specific thrust engine.

The fig 8.15 shows the reduction in TSFC in percentage for different fuel cell power output compared to the reference case. The TSFC has reduced by 1.8% and 6.03% for 1 MW fuel cell power output for Design and Off-Design conditions. While in the case of 4 MW fuel cell power output, the TSFC reduction is 6.78% and 19.89% for Design and Off-Design condition, respectively.

Along with this, ***addition of fuel cell decreased core size***. As mentioned in above, the BPR has been increased in order to keep the specific thrust of the SOFC-GT constant which is shown in figure 8.16. The BPR is increasing as the fuel cell power output is increasing and as a result, the core mass flow rate is decreasing. It means that the core size is getting smaller. As shown in figure 8.16, the core mass flow rate has been reduced by 3.55% for a 1 MW fuel cell power output and 13.8% for a 4 MW fuel cell power output for the Design condition. It should be noted that the efficiency of compressors and turbines

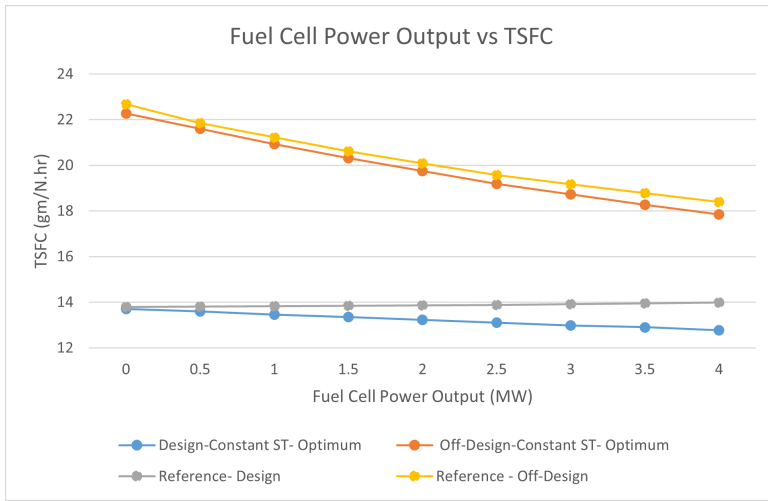


Figure 8.14: Changes in TSFC for different Fuel Cell Power Output for constant Specific Thrust(ST) and constant BPR for Design and Off-Design condition

are assumed to be the same as the reference case, even if the mass flow rate is decreasing. A reduction in core size will lead to an increase in propulsive efficiency.

As more air is bypassing the core increases the propulsive efficiency of the SOFC-GT compared to the reference engine. This increase in propulsive efficiency is the direct result of the addition of fuel cells. The BPR of the standalone gas turbine cannot be increased because of the increase in Bypass power loss and transmission loss.

### 8.2.3. RESULT 4

#### *Adding fuel cell reduced Cooling air requirement*

The TIT is same for the Design condition for both reference and SOFC-GT hybrid but the parameter is changing for Off-Design condition and are shown in figure 8.17. The TIT has been reduced from 1404 K for the reference engine to 1155 K for 4 MW fuel cell power output in Off-Design condition. Along with this, due to a decrease in the size of the core, the absolute amount of air entering the engine is also decreasing in both conditions. As a result, the cooling air requirements will decrease for the engine. Figure 8.17 shows that the cooling air has decreased by 13.56 % for the 4 MW power output in the Design condition, which is due to a decrease in the absolute amount of mass flow entering the combustor. On the other hand, for Off-Design condition, the cooling air requirement has decreased by a staggering 85.4% for Off-Design condition because of a decrease in core mass flow as well as the TIT. *It should be noted that active cooling has been assumed* and the cooling flow rates have been evaluated by the PyCycle based upon the blade temperature limit, safety limit, and TIT which are explained in section 6.2.1.

Reduction in cooling bleed air will increase the fraction of core mass flow rate which

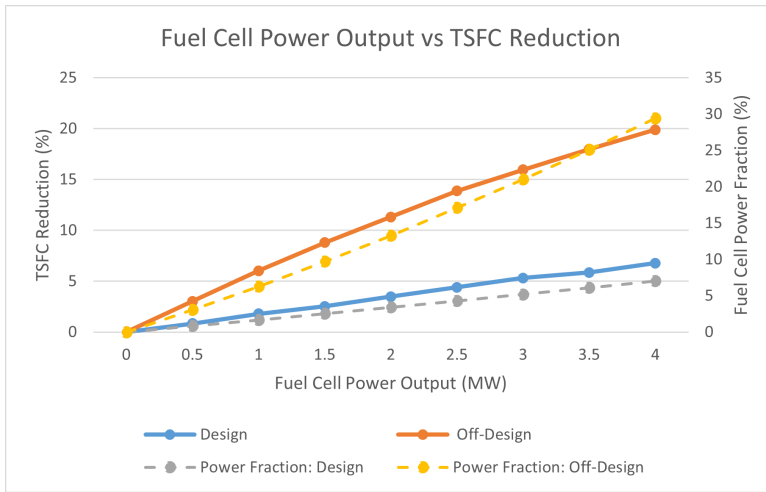


Figure 8.15: Reduction in TSFC for different Fuel Cell Power Output for constant Specific Thrust(ST) for Design and Off-Design condition

is going into the combustor and contributing in providing the gas power rather than bypassing the combustor. This will lead to a further decrease in the requirement of core mass flow rate and hence increase the propulsive efficiency and reduce TSFC. Furthermore, the core size will reduce even more as a result of a decrease in core mass flow rate.

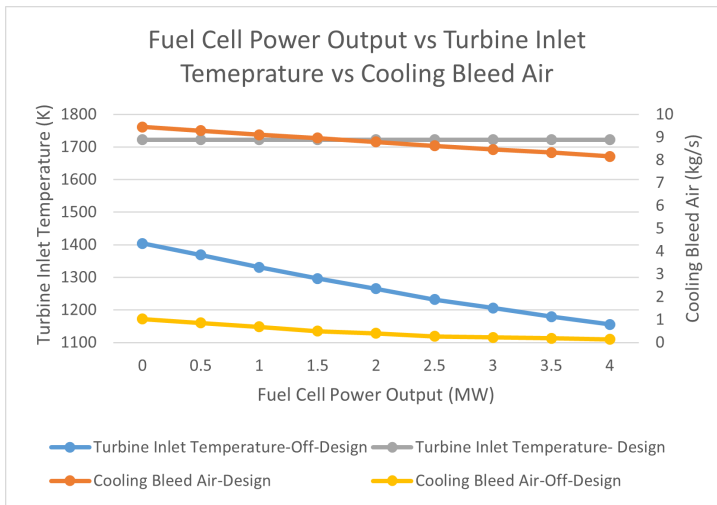


Figure 8.17: Change in TIT and the subsequent cooling air percentage for different Fuel Cell Power Output for Off-Design condition

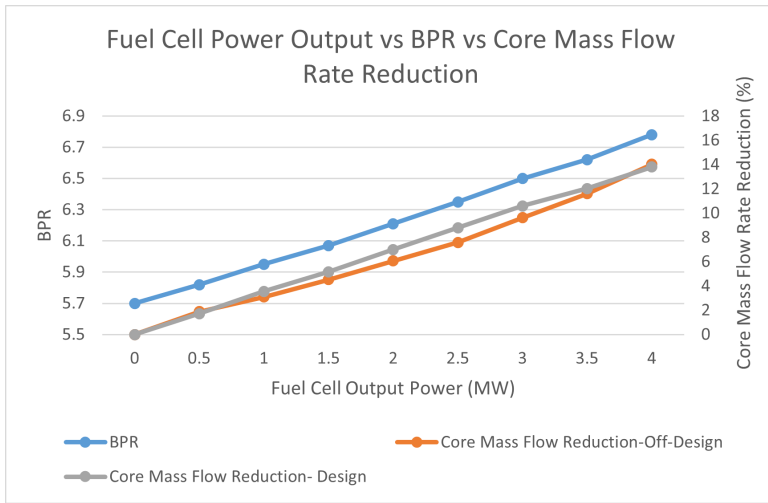


Figure 8.16: Change in the BPR and reduction in mass flow rate as fuel cell power output is increased

### 8.3. DOWNSIZED ENGINE

This section presents the result of downsized turbofan engine integrated with SOFC to generate the similar amount of thrust as reference engine. It should be noted that the analysis has been done for constant specific thrust and optimum point which has been explained in section 8.2. The result is as follows.

#### 8.3.1. RESULT 5

***Addition of fuel cell can help in increasing the total thrust of the engine, hence increasing the range of thrust provided by an engine class for the same core***

CFM-56 provides thrust varying from 90 kN to 151 kN [66] and in order to provide such a high range of thrusts, the engine core is usually changed by increasing the pressure ratio and TIT along with the increase in other parameters like mass flow and BPR. This means adding stages to the compressor and turbine along with the increase in TIT and hence, the cooling bleed air. This brings a higher level of complexity to the engine development process as in order to adhere to the constraints, boundaries need to be pushed for the components which leads to the exponential increase in the research and development costs. But adding a fuel cell can provide an increase in thrust in a more efficient manner with minimal changes to the core, hence reducing development time and cost along with a more efficient propulsion system with lower emissions.

The results which have been presented in section 8.2.2 and 8.2.3 are for the analysis of fixed thrust, which means that when the fuel cell is added to the turbofan, the output thrust needs to be the same as the reference engine. For this purpose, the turbofan core size has been reduced as a fraction of power is complemented by the fuel cell as explained thoroughly in section 8.1.2. However, if the core size of the engine is kept con-

stant, meaning the mass flow rate entering the core stays the same, then more thrust can be extracted from the same engine without any change in the engine's OPR, TIT, and mass flow when the fuel cell is added. Hence, an analysis has been done in which the CFM-56-5A3 turbofan engine, which belongs to the CFM-56 engine family but has lower maximum thrust output, has been integrated with the fuel cell and thrust has been increased to similar levels of CFM-56-5B1, which is the reference engine for this study. A comparison for both the engines without the fuel cell has been presented in table 8.1.

Sr. No.	Parameter	Unit	CFM-56-5B1	CFM-56-5A3
1	Overall Pressure Ratio	-	30.2	27.9
2	Bypass Ratio	-	5.7	6
3	Turbine Inlet Temperature	K	1722	1577
4	Maximum Sea-Level Thrust (Design Condition)	kN	133.58	118
5	Cruise Thrust (Off-Design Condition)	kN	22.8	22.08
6	Mass Flow Rate	kg/s	396.8	390.5

Table 8.1: Comparison between CFM-56-5B1 (reference engine) and CFM-56-5A3 [65]

As can be seen from the table 8.1, the output thrust is lower for the CFM-56-5A3 compared to CFM-56-5B1 and hence, the lower mass flow rate, OPR, and TIT as well. Some other points need to be noted and they are given below:

- The efficiencies for fans, compressors, turbines, and other components are kept the same for both engines because of lack of data.
- The specific thrust for both engines is kept constant. This means that the CFM-56-5A1 integrated with fuel cell will provide the same amount of thrust as the reference engine for the same mass flow rate as the reference engine.
- The mass flow rate of the core or the size of the core of CFM-56-5A3 has been kept constant. This means that the same core is used to get the higher thrust by adding the fuel cell. The bypass ratio of the engine will increase because the total mass flow rate has increased to the same value as the reference engine.

Table 8.2 shows the comparison between the reference engine and CFM-56-5A3 integrated with the fuel cell for a similar specific thrust at their most optimum point. It can be seen that the fuel cell power output required to achieve the thrust for CFM-56-5B1 is 5.5 MW. The value has been achieved by changing the FPR of the engine for the most optimum point along with the constraints of constant specific thrust and constant core mass flow as the reference CFM-56-5A3 engine given in table 8.1. Following conclusions can be drawn from the results:

- **Improvement in TSFC:** The TSFC has been reduced by 7.29% and 23.25% when compared to the reference engine for Design and Off-Design conditions respectively. The decrease in TSFC is significant, especially for the Off-Design condition.

Sr. No.	Parameter	Unit	CFM-56-5B1 (Reference)		CFM-56-5A3 integrated with Fuel Cell	
			Design	Off-Design	Design	Off-Design
1	Thrust	kN	133.58		133.40	
2	Fan Pressure Ratio	-	1.80		1.70	
3	Bypass Ratio	-	5.70		6.10	
4	Specific Thrust	N/kg	336.69		336.23	
5	Fuel Cell Power Output	MW	0		5.5	
-	<b>Operating Condition</b>	-	<b>Design</b>	<b>Off-Design</b>	<b>Design</b>	<b>Off-Design</b>
6	Thermodynamic Efficiency	%	51.97	51.74	53.9	64.83
7	Thermal Efficiency	%	37.40	43.1	42.14	55.32
8	TSFC	gm/N.hr	13.71	22.28	12.71	17.1
9	Mass Flow	kg/s	396.80	144.03	396.8	150.08
10	Mass Flow (Core)	kg/s	59.73	21.53	56.3	19.29
11	Cooling Bleed Air	kg/s	9.44	1.03	5.63	0

Table 8.2: Results of the analysis of CFM-56-5A3 integrated with a fuel cell to achieve thrust comparable to CFM-56-5B1

However, the reduction is lower than when compared to the reference engine. Using the polynomial extrapolation method to calculate the TSFC reduction for reference engine for same amount of fuel cell power, the TSFC reduction of 9.08% and 24.25% is expected for the reference engine integrated with a fuel cell with a power output of 5.5 MW as shown in figure 8.18. However the reduction is lower. The reason for the lower reduction is the lower TIT and OPR of CFM-56-5A3. The thermodynamic efficiency is highly sensitive to TIT and hence a lower TIT will have a major impact on the thermodynamic efficiency.

Lower TIT also contributes to the higher fuel cell power required in order to get the thrust of 133.6 kN in Design Conditions.

- **Reduction in Cooling Air:** As TIT and mass flow of core is lower, the required amount of cooling air decreased by 40.32% when compared with the reference engine for Design condition. Along with this, for Off-Design condition, no cooling air is required as temperature of TIT has dropped below the safety temperature of the metal.
- **Increase in the Bypass Ratio:** The bypass ratio of the engine has been increased from 6 (CFM-56-5A3 without fuel cell) to 6.1 compared to the BPR of 5.7 for the reference engine. The reason for the increase in bypass is basically to keep the specific thrust of the engine similar to the reference engine while keeping the core

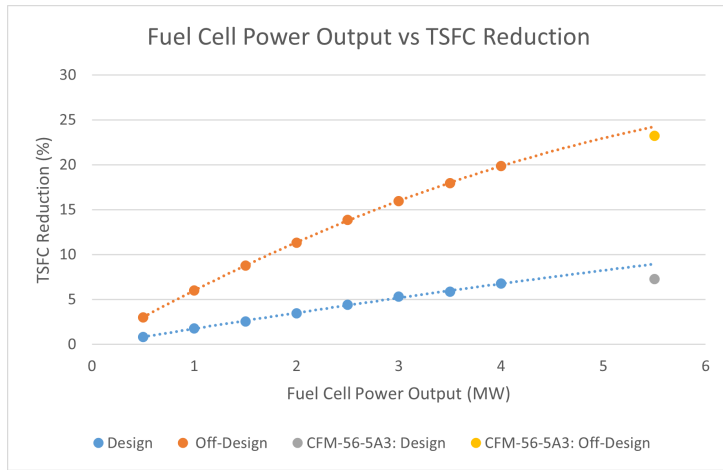


Figure 8.18: Reduction in TSFC for different Fuel Cell Power Output extrapolated to 5.5 MW power output

size constant.

*Based upon the results given above, it can be concluded that not only the thrust can be increased with the addition of a fuel cells, but the engine can become more efficient and sustainable as well, along with the reduction in complexity and development cost. However, the fuel cell power required is too high and that is because of the high power requirement during the maximum power takeoff condition.*

## 8.4. TECHNICAL SENSITIVITY ANALYSIS

This section talks about the technical sensitivity analysis that has been done in order to understand the impact of different parameters on the Thermodynamic Efficiency for 1 MW and 4 MW fuel cell power output for Off-Design conditions. The analysis has been done for SOFC-GT hybrid at its most optimum point and has a constant specific thrust as a reference engine. The results are shown in figure 8.19. The sensitivity coefficient mentioned in the figure is given in equation 8.9.

$$\text{Sensitivity Coefficient}_{technical} = \left( \frac{\eta_{thermonew} - \eta_{thermoref}}{\eta_{thermoref}} \right) * 100 \quad (8.9)$$

where

$\eta_{thermonew}$  = Thermodynamic Efficiency when the given parameter is increased by 1%, %

$\eta_{thermoref}$  = Thermodynamic Efficiency for the reference case, %

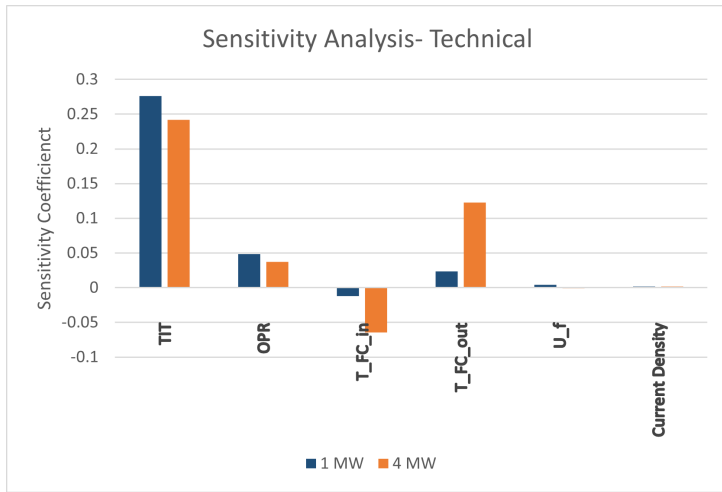


Figure 8.19: Sensitivity Analysis of Thermodynamic Efficiency for a 1 MW and 4 MW fuel cell power output for Off-Design condition

where

TIT= Turbine Inlet Temperature, K

OPR= Overall Pressure Ratio

$T_{FCin}$ = Temperature of fuel cell inlet products, K

$T_{FCout}$ = Temperature of fuel cell outlet byproducts, K

$U_f$ = Fuel Utilization,%

The sensitivity Coefficient shows the % change in the thermodynamic efficiency when the given parameter is increased by 1%. For example, when the parameter 'TIT' is increased by 1% from the reference case, the thermodynamic efficiency for 1 MW and 4 MW fuel cell power output increased by 0.275% and 0.242%, respectively. The conclusions are given below.

- The increase in thermodynamic efficiency with OPR and TIT is expected and the reason is given in section 7.3.
- The thermodynamic efficiency is less sensitive to TIT and OPR at higher fuel cell power output. This is because high TIT and OPR have little to no impact on fuel cell performance. The TIT has no impact on fuel cell performance and at higher OPR, the sensitivity to pressure also reduces significantly as explained in section 2.2.7.

However, as the fuel cell power is increased, the contribution of fuel cell to the overall gas power and fuel consumption will also increase. Hence, when TIT and OPR is increased, it will only have an impact on gas power produced by turbofan and not on the gas power produced by the fuel cell. Hence, the overall thermodynamic efficiency increase would be lower.

- The thermodynamic efficiency is decreasing with the increase of  $T_{FCin}$ . This is a contradictory result as increasing the  $T_{FCin}$  will increase the total efficiency of the fuel cell, explained in section 2.2.7 and hence, should increase the total thermodynamic efficiency of the propulsion system. However, this is not the case. It is true that the increase in  $T_{FCin}$  by 1% has led to an increase in the total efficiency of the fuel cell by 0.56% but it has also increased the mass flow rate of air required to keep the maximum temperature of fuel cell within the prescribed limits.

Increasing the  $T_{FCin}$  will lead to a decrease in  $\Delta T$  across the fuel cell. It means that the same amount of air will now extract less heat from the fuel cell compared to the reference case. The losses in the fuel cell have decreased a bit but not enough to compensate for the effect of reduction of  $\Delta T$ . Because of this, more air is needed to keep the fuel cell temperature constraint and hence the compressor power will increase as well. This will lead to a total reduction in gas power and hence the thermodynamic efficiency. The reduction in efficiency is quite low as for 4 MW power output, the efficiency decrease is 0.064% for a 1% increase in  $T_{FCin}$ .

- On the other hand, an increase in  $T_{FCout}$  will increase the thermodynamic efficiency and is more sensitive compared to  $T_{FCin}$ . There are two reasons for this. The first reason is the increase in  $\Delta T$  when the  $T_{FCout}$  is increased. This increase will lead to a decrease in mass flow entering the fuel cell as more heat can be extracted from the fuel cell by the same mass flow and hence the required mass flow rate will decrease. This will lead to a decrease in fuel cell compressor power and hence the increase in gas power and thermodynamic efficiency. It is the exact opposite of what was happening when  $T_{FCin}$  is increased. The fuel cell efficiency will increase in both cases but other factors influence the thermodynamic efficiency

The second reason is the increase in thermal energy coming from the fuel cell. Increasing the temperature will increase the thermal energy in the byproducts and as the inlet flow temperature of the fuel cell is same, more thermal energy will go into the combustion chamber. More explanation is given in section 7.3.

- Fuel utilization and current density, both have negligible influence on the overall thermodynamic efficiency. This is because the impact of these parameters on fuel cell efficiency is low, hence the impact on overall system thermodynamic efficiency is negligible.

# 9

## EMISSION ANALYSIS

This chapter talks about the emission analysis that has been done in order to understand the impact of fuel cells on the overall emissions of the propulsion system. The fuel used as a reference in this study is hydrogen which mainly has two types of emissions,  $NO_x$ , and  $H_2O$ . There are no carbon emissions but both  $NO_x$  and  $H_2O$  are greenhouse gases and hence result in Global Warming. Global Warming Potential or GWP is a metric that calculates the heat absorbed by the gas as the multiple of heat absorbed by the 1 kg of  $CO_2$ .

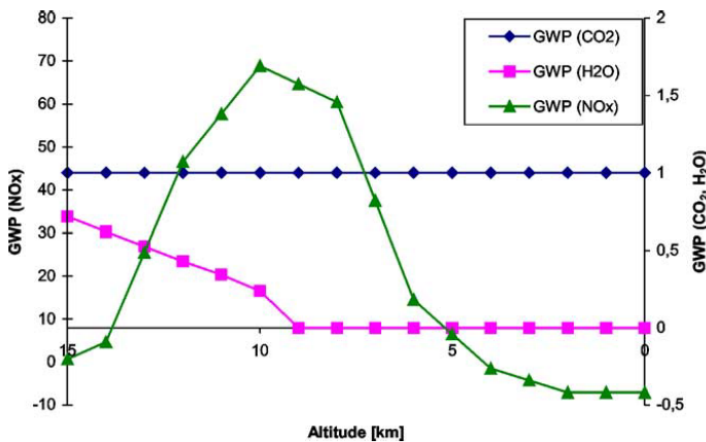


Figure 9.1: GWP of  $NO_x$  and  $H_2O$  per kilogram of GWP of  $CO_2$  as altitude is increased [71]

Figure 9.1 shows the GWP of  $NO_x$  and  $H_2O$  compared to GWP of one kilogram of  $CO_2$  as altitude is changed. It can be seen from the figure that as the altitude is increased, both  $NO_x$  and  $H_2O$  GWP is increasing. For example, at 10 km altitude, 1 kg of  $H_2O$  absorbs

as much heat as 0.2 kg of  $CO_2$  but 1 kg of  $NO_x$  absorbs as much as 70 kg of  $CO_2$  will absorb, which is quite significant. Because of this increase in GWP at higher altitudes, both,  $NO_x$  and  $H_2O$ , should be taken into consideration when emissions are compared for SOFC-GT hybrid and reference engine.

## 9.1. $H_2O$ EMISSIONS

$H_2O$  is the biggest by-product of combustion as well as the electrochemical reactions as given in equation 2.3. 1 kg of hydrogen combustion approximately produces 9 kg of  $H_2O$  which is higher than hydrocarbon fuel and hence reducing the consumption of hydrogen will directly reduce the  $H_2O$  emission.

As shown in section 8.2.2, adding the fuel cell reduces the consumption of hydrogen and hence will directly reduce the  $H_2O$  production as shown in figure 9.2. The  $H_2O$  production decreased by 19.91% when fuel cell power output is increased to 4 MW compared to the reference engine. This means that adding the fuel cell will help to significantly reduce the  $H_2O$  emissions, which is one of the big concerns for using hydrogen as fuel, especially for the purpose of reducing carbon emissions.

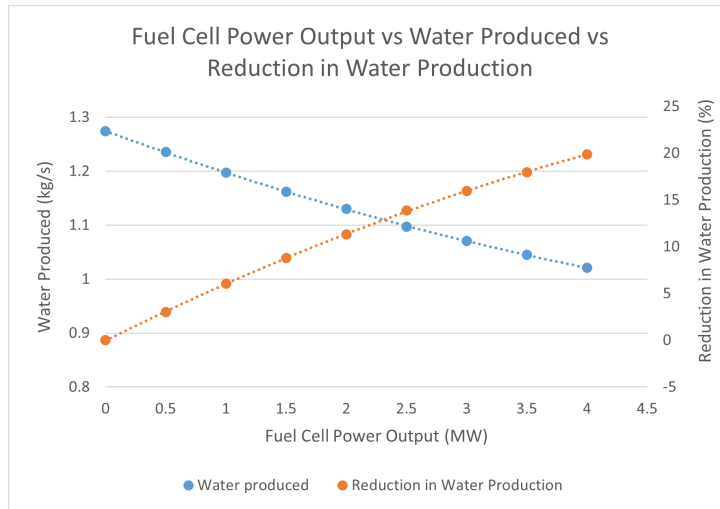
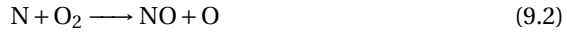
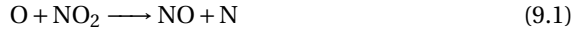


Figure 9.2: Impact on  $H_2O$  production as fuel cell power output is increased

## 9.2. NITROGEN OXIDE EMISSIONS

As  $H_2O$  is the biggest emission in the case of hydrogen fuel,  $NO_x$  is the second major emission when it comes to combustion. There is mainly two phenomena of  $NO_x$  production and they are given as follows:

- **Thermal  $NO_x$ :** Thermal  $NO_x$  is the most prominent and major source of  $NO_x$  production. The  $N_2$  in the air oxidizes along with fuel and converts to  $NO$  at a temperature higher than 1700 K as shown in equations 9.1, 9.2 and 9.3.



Thermal  $\text{NO}_x$  is dependent on 6 factors and they are given below.

- *Temperature:* Temperature is one of the major factors of  $\text{NO}_x$  production. The dissociation of  $\text{O}_2$  shown in equation 9.2 takes place at a temperature higher than 1700 K and it increases as the temperature increases. It should be noted that even if the TIT is lower than 1700 K, for example in the case of Off-Design condition, the temperature in localized regions, especially the flame zone and primary region inside the combustor, can be as high as 2300 K or more, which produces a higher amount of  $\text{NO}_x$ .

*This is the reason that the fuel cell does not produce any  $\text{NO}_x$  because the maximum temperature in the fuel cell does not go above 1200K and hence, no dissociation of  $\text{O}_2$  takes place and no  $\text{NO}_x$  is formed.*

- *Equivalence Ratio:* Increase in the equivalence ratio increases the amount of fuel or hydrogen in the combustion chamber which increases the temperature of localized regions and hence the  $\text{NO}_x$  emissions.
  - *Pressure:* Pressure increases the absolute amount of  $\text{O}_2$  in the combustion chamber and hence the O radical in the combustion chamber. The higher concentration of O radical leads to a more forward reaction and hence increases the  $\text{NO}_x$  production as given in equation 9.2.
  - *Atomization & Mixing:* Atomization means the breaking down of fuel into smaller droplets which reduce the heat generated in localized regions and hence the  $\text{NO}_x$  production. Mixing also has a similar impact as a well-mixed fuel leading to a reduction in high-temperature regions inside the combustion chamber.
  - *Residence Time:* Increase in residence time increases the  $\text{NO}_x$  because it gives more time for the reactions to take place and hence leads to the completion of reactions, eventually leading to  $\text{NO}_x$ .
  - *Type of Fuel:* If the fuel is impure and already contains some amount of nitrogen, then the  $\text{NO}_x$  production increases, and when the fuel burns and a higher temperature is reached, the  $\text{NO}_x$  starts to produce.
- **Prompt  $\text{NO}_x$ :** Another phenomenon of  $\text{NO}_x$  production is the prompt  $\text{NO}_x$  which is produced when  $\text{N}_2$  in air combines with the fuel radicals and form  $\text{NO}_x$ . Prompt  $\text{NO}_x$  is a very small fraction when compared to thermal  $\text{NO}_x$ .

### 9.2.1. $NO_x$ EMISSION ANALYSIS METHODOLOGY

This section talks about the  $NO_x$  emission analysis methodology. In order to calculate the  $NO_x$ , a correlation-based method is used by substituting the operating conditions into the correlation. In this study, the correlation developed by NASA Glenn Research Center has been used and is given in equation 9.4 and 9.5 [72]. NASA has done experiments on multiple types of injectors to understand the impact of injector shape on the  $NO_x$  emissions and compared it with the lean direct injection combustor fuelled by kerosene. The hydrogen injector and combustor chosen for this study is C4, explained in [72] and the reason is that it is the most sustainable option out of all the injectors which have been tested by NASA as it produces the least amount of  $NO_x$ .

$$\text{ppm}_{NO_x} = A * (P_3)^a * (\phi_{H_2})^b * (\tau)^c * \exp\left(\frac{T_3}{d}\right) * \left(\frac{\Delta P}{P}\right)^e \quad (9.4)$$

$$EINO_x = \frac{\text{ppm}_{NO_x} * (1 + f/a)}{630 * f/a} \quad (9.5)$$

Where

A= 9.355

$P_3$ = Flow pressure at the inlet of combustor, pa

a= 0.275

$\phi_{H_2}$ = Equivalence Ratio

b= 4.12

$\tau$ = Residence time= 2 , ms

c= 0.455

$T_3$ = Flow temperature at the inlet of combustor, k

d= 211

$\frac{\Delta P}{P}$ = Pressure loss in the combustor

e= -0.288

$EINO_x$ = Nitrogen Oxide Emission Index, gm  $NO_x$ /1000 gm fuel

f/a= Mass of fuel/ Mass of air

The values required in the correlation like pressure loss, the mass flow rate of fuel, and the mass flow rate of air are taken directly from the SOFC-GT and then used to calculate the  $NO_x$  emissions. It should be noted here that the flow temperature at the inlet of the combustor in the case of a SOFC-GT hybrid would not be the same as the outlet temperature of the High-Pressure Compressor(HPC). This is because the temperature of byproducts coming from the fuel cell has a higher temperature and after adiabatic mixing, the temperature of the whole mixture will increase as explained thoroughly in section 7.3. The fig 9.3 shows the change in temperature of the HPC exit flow and the mixture (fuel cell by-products and HPC exit flow) for different fuel cell power outputs. It can be seen from the figure that the temperature of the mixture is increasing as the fuel cell power output is increasing and the reason for this is the increase in the number of high-temperature by-products coming from the fuel cell. As power required from the fuel cell increases, more air is passed through the fuel cell to maintain its temperature, and hence, the total mixture temperature entering the combustor increases for higher

fuel cell power.

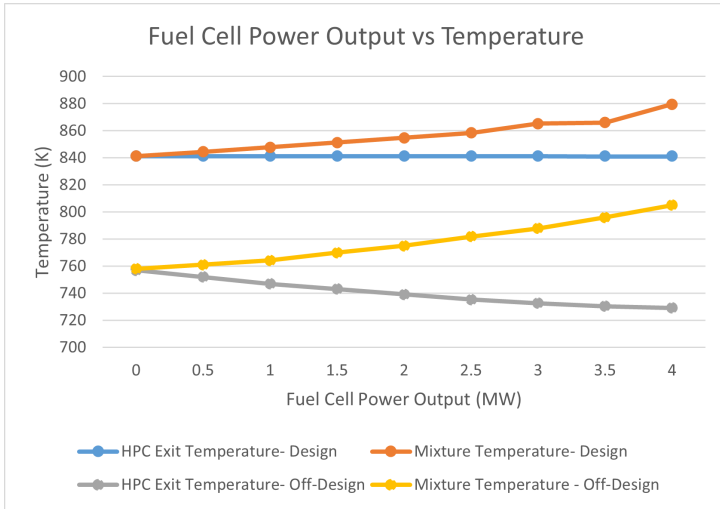


Figure 9.3: Temperature of flow at the exit of HPC and the mixture at different fuel cell output power

It should also be noted that the change in temperature is higher for Off-Design condition than the Design condition and the reason for that is the lower mass flow rate in the core during the Off-Design condition. The mass of by-products from the fuel cell is almost the same for Design and Off-Design conditions but the core mass flow varies significantly and hence the temperature of the mixture. This increase in temperature will increase the  $NO_x$  emissions as increasing the inlet flow temperature will increase the energy available for reaction 9.1, 9.2 and 9.3 to take place and hence increases the formation of thermal  $NO_x$ .

### 9.3. VERIFICATION OF $NO_x$ EMISSION MODEL

This section consists of the verification of the  $NO_x$  emission model used in this study. The model is based on the correlation developed by NASA Glenn Research Center and hence, the model has been verified by the data given in [72]. The operating conditions are given in table 9.1.

Sr. No.	Parameter	Unit	Value
1	Pressure	pa	689476
2	Combustor in flow temperature	k	700
3	Residence time	ms	2
4	Combustor pressure loss	%	4
5	Fuel	-	Hydrogen

Table 9.1: Operating condition used for the verification of  $NO_x$  emission model

The results for the verification are shown in figure 9.4. It can be seen that the  $NO_x$  emissions in Parts Per Million (PPM) is increasing as the combustor out flow temperature increases, which is the result of more fuel added (increasing equivalence ratio) to the combustor. The  $NO_x$  emission model output is also matching very well with the reference model output [72]. Hence, it can be concluded that the  $NO_x$  emission model is verified.

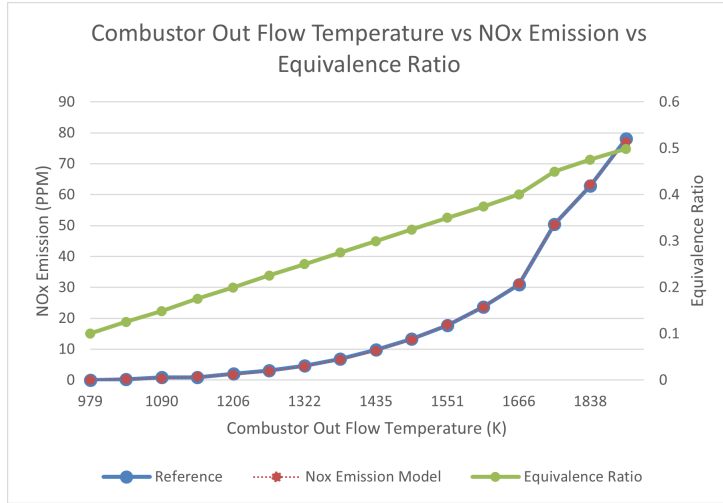


Figure 9.4: Change in  $NO_x$  emissions as equivalence ratio and combustor outflow temperature is changed

## 9.4. LIMITATIONS OF THE MODEL

The emission model developed for this study has some limitations and they have been explained below:

- **0D Model:** The 0D model used in this analysis only considers four parameters; Inlet flow pressure and temperature, equivalence ratio, and pressure loss. However,  $NO_x$  formation is a complex phenomenon and is also dependent on the concentrations of nitrogen and oxygen radicals in localized regions and the mixing of the fuel with the air along with the parameters mentioned above. Hence, the 0D model cannot accurately predict the  $NO_x$  emissions when the fuel cell is added and the reasons are given below:
  - **Reduction in  $O_2$  Concentration:** The concentration of oxygen in the mixture entering the combustor will reduce because some oxygen has already been consumed by the fuel cell. This means that a lower concentration of oxygen will lead to its lower availability of O radical in the primary region of flame. Hence, the production of thermal  $NO_x$ , the most dominated type of  $NO_x$ , will reduce as both  $H_2$  and  $N_2$  radicals will fight for the oxygen in this region [73].

- **Addition of Steam:** The addition of steam coming from the fuel cell has quite a lot of impact on  $NO_x$  emission in multiple ways. First, the addition of steam reduces the high temperature in the localized regions because of its higher specific heat compared to hydrogen and nitrogen. Hence, a lot of heat is absorbed by the steam to raise its temperature. This leads to less local temperature in localized regions and hence less thermal  $NO_x$  [73].

Second, steam displaces oxygen in the combustor and hence suppresses the  $NO_x$  formation [73]. In order to understand these phenomena, more sophisticated models which include chemical kinetics or computational fluid dynamics need to be used. However, the development of such sophisticated models is out of the scope of this study.

- **Limitation of the Correlation:** The correlation used in this study has a limitation on the operating conditions for which the correlation will give acceptable  $NO_x$  values. The correlation works for the range of 588 k to 811 k for combustor inflow temperature and an in-flow pressure of 0.41 MPa to 1.38 MPa along with the maximum equivalence ratio of 0.48. The reason for that is the experiments are done for only this range and hence, the correlation cannot be used for other operating conditions. The impact of this on our study is that the correlation can only be for the  $NO_x$  emission calculation for Off-Design condition and not for the Design condition due to higher pressure and inflow temperature.

## 9.5. RESULTS OF $NO_x$ EMISSION ANALYSIS

This section discusses the results of the  $NO_x$  emission analysis for the SOFC-GT hybrid. Figure 9.5 shows the change in  $EINO_x$  and  $NO_x$  emissions in PPM as fuel cell power output is increased for the Off-Design condition. The  $NO_x$  emissions are reducing as the power output is increased and the reason for that is the decrease in fuel consumption. Even though the inlet temperature of the mixture has increased, for example in the case of 4 MW power output, the combustor inflow temperature has increased from 730 k to 800 k as shown in figure 9.3, but the  $EINO_x$  has reduced to 0.09gm/1000gm of  $H_2$  compared the reference engine of 4.5gm/1000gm. This is a substantial decrease in  $NO_x$  emissions even if the model only captures the impact of fuel reduction and not the reduction in  $O_2$  concentration and addition of steam. In the future study, building a sophisticated model which captures the phenomena discussed in 9.4 may estimate an even further decrease in emissions.

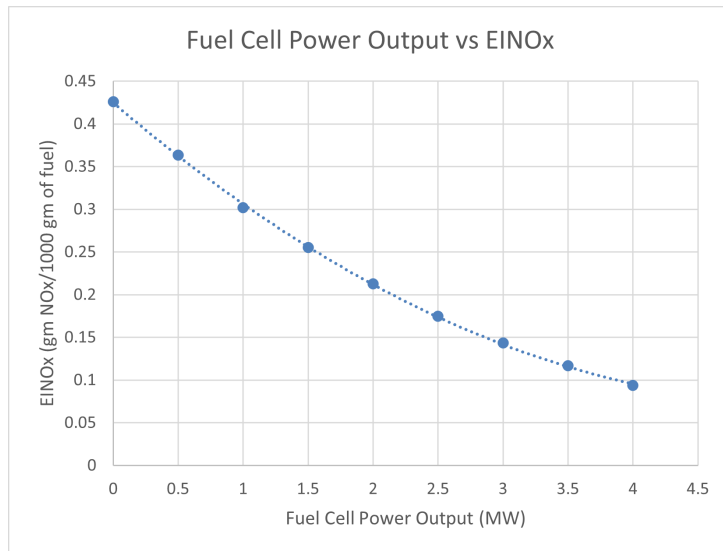


Figure 9.5: Impact of increasing the fuel cell power output on  $NO_x$  Emissions for Off-Design or cruise condition

# 10

## ECONOMIC ANALYSIS

The economic feasibility analysis is the second part of this research project which will answer research questions 5,6 and 7. This section talks about the methodology and results for an economic study done in this thesis. But before going into the methodology, it needs to be understood the impact of adding the fuel cell to a gas turbine and how this change will affect the economics of the whole aircraft. Table 10.1 shows the impact of adding the fuel cell on the reference engine parameters. Section 8 and 9 thoroughly explains the impact on fuel consumption and emissions respectively. Both emissions and fuel consumption decrease due to improvements in efficiency. However, adding the fuel cell would lead to an increase in the weight of the propulsion system due to lower specific power as shown in table 2.3. In addition to this, the initial investment in the propulsion system will also increase because of the addition of multiple systems like SOFC, motors, fuel cell compressor, heat exchanger, and electronics. The next section will explain the complete overview of the Economic Analysis Methodology.

Sr. No.	Parameter	Reference Engine	SOFC-GT Hybrid
1	Fuel Consumption	Reference	Decrease
2	Emissions	Reference	Decrease
3	Propulsion System Weight	Reference	Increase
4	Initial Cost	Reference	Increase

Table 10.1: Impact of SOFC-GT on the Reference Engine

### 10.1. ECONOMIC ANALYSIS METHODOLOGY

Figure 10.1 shows the complete overview of the economic model developed for the Economic Feasibility Analysis. Each step is explained in detail below:

- First the Initiator provides all the required inputs like engine weight, engine cost, fuel cell power, fuel consumption, etc. calculated by the SOFC-GT hybrid model

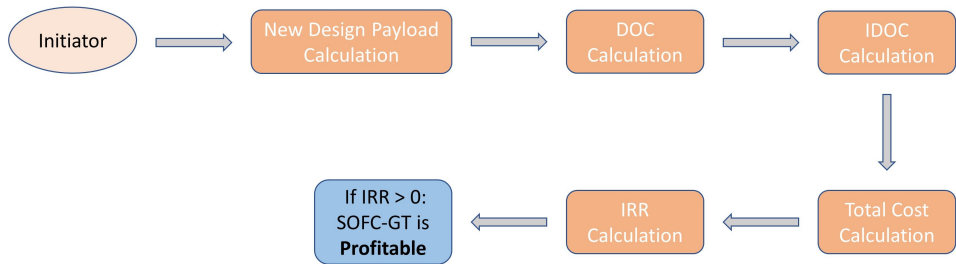


Figure 10.1: Complete Overview of the Economic Model Methodology.

to different functions like *New Design Payload Calculation* and *Direct Operating Cost(DOC) Calculation*.

- Second, the New Design Payload is calculated. The weight of the propulsion system will increase because of the addition of the fuel cell system as mentioned in section 10. This means that this added weight needs to be complemented either by increasing the Maximum Take-Off Weight (MTOW) or by reducing the weight of another system. For this study, the MTOW is kept constant as changing MTOW will lead to an increase in the surface area of aerodynamic surfaces which will lead to an increase in the structural weight of the engine, hence leading to a snowball effect. For this reason, the MTOW is kept constant and the design payload is varied. So, a net increase in propulsion system weight will reduce the design payload of the aircraft.
- The third step is to calculate the DOC. The DOC is the cost that is directly dependent on the usage of the aircraft. For example fuel consumption, emissions, maintenance cost, etc.
- The next step is the calculation of the Indirect Operating Cost(IDOC). These costs are the indirect cost that airline has to incur but are not directly dependent on the length of the journey. The costs include landing fees, ground operations, marketing, etc.
- The fifth step is to calculate the total cost of having an airline operation and is dependent on DOC and IDOC.
- The sixth step is to calculate the Internal Rate of Return (IRR). IRR is used to analyze the average rate of return an investment gives over the lifetime of that investment. If the IRR is greater than zero, this means that the project is profitable. This will be explained thoroughly in the section 10.1.5

Each step and its calculation is explained thoroughly in the subsequent sections.

### 10.1.1. NEW DESIGN PAYLOAD

It has been explained in section 10.1 that MTOW has been kept constant, and hence, the design payload of the MTOW has been decreased in order to complement the net added

weight in the propulsion system. The reference values for the aircraft are given in the table 10.2. Equation 10.3 shows the MTOW of the reference aircraft. The MTOW has five components. First is the empty aircraft weight. It is the weight of an empty aircraft without the fuel, propulsion system, and cargo. The second component of weight is the fuel weight. The fuel weight depends on the range of the aircraft and the calculation is given in appendix B. For this research, the design range of 5000 km is chosen [74]. Hence, the fuel consumption is dependent on the range of the aircraft. The third component of the MTOW is the propulsion system. For a turbofan engine, the propulsion system weight mainly includes the weight of the engine, piping, and nacelle. The fourth component is the Design payload which, like the fuel, depends on the range. If the range is low then more payloads can be taken as fuel weight has been reduced. The fifth component of the weight is the Tank weight. In an aircraft powered by kerosene, the tank weight is not usually considered a separate category as it is part of the empty aircraft weight. However, for a hydrogen-powered aircraft, the tank weight is high because of cryogenic requirements and a high volume of hydrogen. Hence, it has been considered in this study.

$$\text{MTOW} = \left( \begin{array}{l} \text{Empty Aircraft Weight} + \text{Fuel Weight} + \text{Propulsion} \\ \text{System Weight} + \text{Design Payload} + \text{Tank Weight} \end{array} \right) \quad (10.1)$$

Equation 10.2 shows the mathematical formula to calculate the Design Payload of the SOFC-GT hybrid-powered aircraft. The empty aircraft weight will stay the same as no modifications have been done to the aircraft. The fuel weight will reduce because of the increase in efficiency and as a result, the total amount of fuel required for the whole journey will also reduce, hence reducing the tank weight as well. In the end, the Propulsion system weight will increase which will depend on the size or power of the fuel cell. If the increase in propulsion system weight cannot be complemented by the reduction in tank and fuel weight then the new design payload will decrease, eventually leading to a decrease in the total revenue.

$$\text{Design Payload}_{New} = \text{MTOW}_{Ref} - \left( \begin{array}{l} \text{Empty Aircraft Weight}_{Ref} + \\ \text{Fuel Weight}_{New} + \\ \text{Propulsion System Weight}_{New} + \\ \text{Tank Weight}_{New} \end{array} \right) \quad (10.2)$$

### 10.1.2. DIRECT OPERATING COST

The Direct Operating Cost or DOC is a cost that is directly related to the cost of the operation of the aircraft. For example, the cost of fuel, maintenance, crew, emissions, etc are dependent directly on the usage of the aircraft and comes under the DOC. If aircraft are used, for example, for longer flights, then the fuel and maintenance costs will increase but the other costs like landing fees and ground operations, which are part of IDOC, will still be the same. Figure 10.2 gives an overview of the DOC of the aircraft and is explained below.

- **Total Standing Charges:** Total Standing Charges is basically the fixed cost of the aircraft operation which needs to be paid whether an aircraft is used or not. It has multiple components and is defined below:

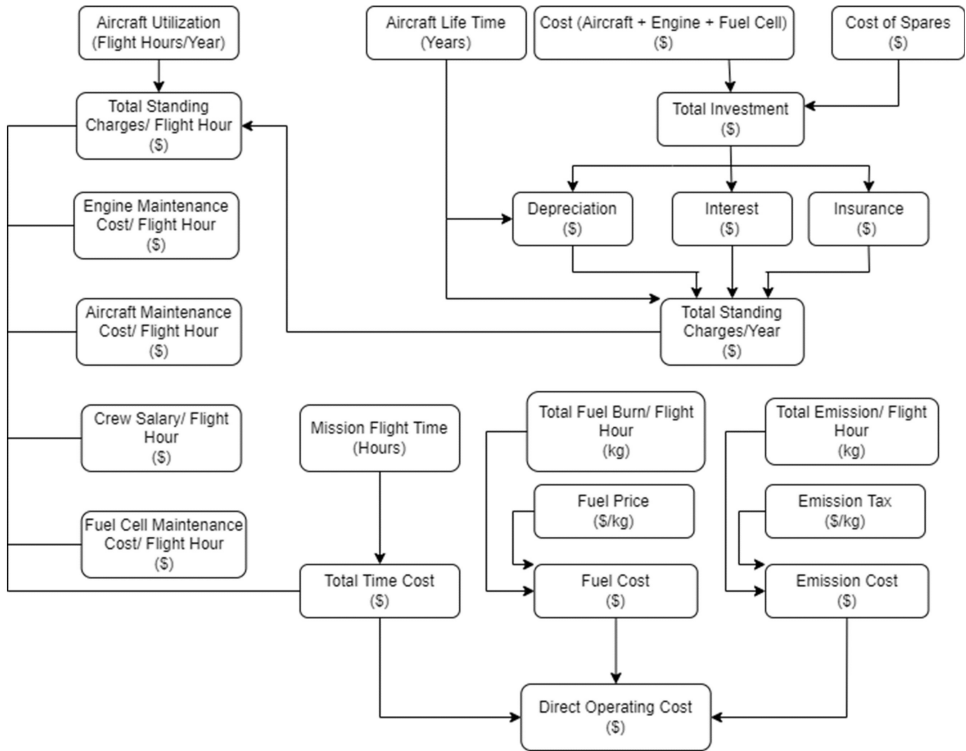


Figure 10.2: Direct Operating Cost Overview for the aircraft (Adapted from [75])

1. **Total Investment:** Total Investment of the aircraft is the total capital, over the lifetime of the aircraft, that the airline has to incur. It is dependent on the initial cost of the aircraft, engine, and fuel cell, and the cost of spare and is given in the equation

$$\text{Total Investment} = \left( \begin{array}{l} [C_a * (1 + SP_a)] + [C_e * (1 + SP_e)] + \\ [C_{fc} * (1 + SP_{fc})] \end{array} \right) \quad (10.3)$$

where

$C_a$ = Initial Cost of Aircraft, \$

$SP_a$ = Fraction of spare parts to the cost of aircraft, %

$C_e$ = Initial Cost of Engine, \$

$SP_e$ = Fraction of spare parts to the cost of engine, %

$C_{fc}$ = Initial Cost of Fuel Cell, \$

$SP_{fc}$ = Fraction of spare parts to the cost of fuel cell, %

It should also be noted that the lifetime of the fuel cell and the engine is not the same. The lifetime of an engine is approximately 66000 hrs compared to

the 40000 for a fuel cell as given in table 10.2. Hence, for the whole lifetime of the aircraft, there would be a need for one complete fuel cell and another fuel cell whose 65% life will be over. Hence, this requirement of more than 1 fuel cell has been accounted for in the initial cost of the fuel cell.

2. *Depreciation:* Depreciation is basically the reduction in the real value of an asset over its lifetime. Every machine has a lifetime and as the machine approaches the end of its lifetime, the value of that machine reduces in real currency. It depends on the total investment of the aircraft and the lifetime of the aircraft. The total depreciation of the aircraft per year is calculated using equation 10.4. The total investment of the aircraft is basically the initial cost of the aircraft and propulsion system along with the cost of spare parts required over the lifetime of the year. The depreciation percentage is calculated using the equation 10.5 and is dependent on the lifetime of the aircraft and the residual value of the aircraft left at the end of the lifetime of the aircraft. The data values like the lifetime, initial cost, etc have been taken [75] and are given in table 10.2.

$$\frac{\text{Depreciation}}{\text{year}} = \text{Total Investment} * \text{Depreciation in percentage} \quad (10.4)$$

$$\text{Depreciation}(\%) = \frac{[100 - \text{Residual left at the end of lifetime}]}{\text{Lifetime of the aircraft}} \quad (10.5)$$

3. *Interest:* The second fixed cost is the interest that the airline has to pay for the debt it has taken in order to buy the aircraft and the spare parts. It has been assumed that all the financing of the aircraft is done using debt and not equity. The amount of interest paid per year is calculated using the equation 10.6 and is dependent on the total investment and the interest rate. The interest rate depends highly on the country from which the debt has been issued. However, for this study, it is considered to be 5.5% [75].

$$\text{Interest/year} = \text{Total Investment} * \text{Interest Rate} \quad (10.6)$$

4. *Insurance:* Just like Interest, Insurance is also a cost that an airline has to pay in order to ensure the whole aircraft in case of an uncertain situation like accidents or crashes which may occur. Even though aircraft are one of the most reliable machines but there is always a minute probability of things not going according to plan. Hence, insurance is required. It is calculated using the equation 10.7 and the insurance rate is taken as 0.5% of the total investment[75].

$$\frac{\text{Insurance}}{\text{year}} = \text{Total Investment} * \text{Insurance Rate} \quad (10.7)$$

The addition of all the costs presented above forms the total standing charges and is given in equation 10.8. It should be noted that total standing charges will be

lower for the reference engine when compared SOFC-GT hybrid. This is because of the increase in the initial cost of the aircraft and the increase in the number of spare parts during the lifetime of the aircraft.

$$\frac{\text{Total Standing Charges}}{\text{year}} = \left( \frac{\text{Depreciation/year} + \text{Interest/year} + \text{Insurance/year}}{\text{year}} \right) \quad (10.8)$$

- **Engine Maintenance Cost:** The engine maintenance cost is a variable cost and depends directly on the usage of the engines. This is the cost which includes the servicing of the engine, oil changing, and inspection of the engine for security and reliability purposes. The engine is the key part of an aircraft and hence has to be inspected before every flight as well as thorough maintenance is required after a particular amount of flight hours. The data for engine maintenance costs vary per airline and is dependent on how they service their engines. If the airline has its own facility then the costs are usually lower compared to third-party maintenance services. The data for this cost has been taken [75] from and is given in table 10.2.
- **Aircraft Maintenance Cost:** Similar to engine maintenance, the aircraft also needs to be serviced before a flight, and thorough maintenance is required after a specific amount of flight hours. The maintenance usually consists of inspection of actuators for control surfaces, landing gears, and load-bearing structures. The data for this cost has been taken from [75] and is given in table 10.2.
- **Fuel Cell Maintenance Cost:** For the SOFC-GT hybrid, the maintenance for SOFC and its sub-systems needs to be done in order to maintain the efficiency and reliability of the systems. The maintenance usually consists of inspection for micro-cracks in the structure, electrode and electrolyte along with the cleaning of pores to maintain the maximum TPB (Triple Phase Boundaries) as mentioned in section 2.1. The cost of maintenance of fuel cell is taken from [76] and is given in table 10.2.

$$\frac{\text{Fuel Cell Maintenance Cost}}{\text{hour}} = \frac{\text{Fuel Cell Cost} * \frac{\text{Maintenance cost}}{\text{year}}}{\frac{\text{Total flight hours}}{\text{year}}} \quad (10.9)$$

- **Crew Salary:** Another variable cost is the salary of the crew which includes the pilots and the flight attendants. It depends on the time of the mission and the frequency of the missions. The cost of crew salary is taken from [75] and given in table 10.2.
- **Fuel Cost:** Another variable and major cost to the airline is the fuel cost which is calculated using the equation 10.10 and the methodology is given in appendix B. The price of green hydrogen is currently very high and uncertain because of low production and high infrastructure cost for renewable energy. The reference price of \$ 6 per kg for comparison with the reference engine has been taken [77]. However, some industry experts hope to bring down the price to as much as \$ 2

per kg but the estimate is quite optimistic [77]. Hence, an analysis of different fuel prices has also been done.

$$\frac{\text{Fuel Cost}}{\text{hour}} = \text{Total Fuel Burn per hour} * \text{Fuel Price} \quad (10.10)$$

- **Emission Cost:** The emission cost includes the cost that an airline has to pay in the form of tax to the government for the emissions released by the aircraft during the mission. Currently, the tax is only on one type of emission, carbon emissions and there are multiple types of taxes. For example, CORSIA, which is a tax that airline has to pay for international flights, and EU-ETS tax which airlines have to pay if they operate within Europe [78]. However, hydrogen-powered aircraft do not have direct carbon emissions and hence, the airlines would not have to pay the carbon tax.

However, the hydrogen-powered aircraft does have other emissions like  $NO_x$  and water which also contribute to the radiative forcing, just like carbon emissions. Hence, in this study, a tax for  $NO_x$  and water will be considered in order to have a fair comparison between the reference and SOFC-GT hybrid engine. The emission cost will be calculated using the equation 10.11.

$$\text{Emission Cost} = \left( \begin{array}{l} NO_x \text{ emission/hour} * NO_x \text{ emission tax} + \\ \text{Water emission/hour} * \text{water emission tax} \end{array} \right) \quad (10.11)$$

The summation of all the costs presented above constitutes the Direct Operating Cost and will be used to calculate the total cost of the aircraft operation.

### 10.1.3. INDIRECT OPERATING COST

Indirect Operating Costs or IDOCs are the costs that are indirectly dependent on the operation of the aircraft. These costs include marketing and promotion, ground operations, airport fee, lounges, etc. The estimation of these costs is quite complicated because of a lot of variables and uncertainty which are highly dependent on the airlines. Hence, finding the data for these costs is a challenge. Hence, this cost has been estimated as a fraction of total cost rather than the summation of each component that comes under IDOC. As per the Federal Aviation Administration (FAA), the DOC of aircraft operation is approximately 48% of the total cost of the airline [81]. This means all the IDOC is about 52% of the total cost. For this study, an assumption of 50% for both DOC and IDOC has been taken. Hence, the IDOC becomes similar to DOC, which is easier to calculate and data is already available for the analysis of DOC.

One thing that must be noted here is that this approximation by FAA is for a jet fuel-powered engine. Hence, in order to calculate the IDOC, first, the calculation of DOC for a kerosene-powered engine is done and then used as an IDOC for the total cost analysis of a hydrogen-powered aircraft. The IDOC would be the same for a hydrogen-powered aircraft as all elements of costs are not dependent on the fuel which has been used by the aircraft. Hence, IDOC has been calculated using this methodology.

Sr. No.	Parameter	Unit	Value	Reference
1	Aircraft Cost	\$	80.8 * 1e6	[75]
2	Engine Cost	\$	16.8 * 1e6	[75]
3	SOFC Cost per kW	\$/kW	441.4	[76]
4	Heat Exchanger Cost per kW	\$/kW	190.3	[76]
5	Motor Cost per kW	\$/kW	53.6	[79]
6	Fuel Cell Compressor Cost per kW	\$/kW	11.3	[76]
7	Power Electronics Cost per kW	\$/kW	32	[76]
8	Aircraft Maintenance Cost per hour	\$/hour	617.5	[75]
9	Engine Maintenance Cost per hour	\$/hour	445	[75]
10	Fuel Cell Maintenance Cost per year	%	6	[76]
11	Flight Crew Cost per hour	\$/hour	190	[75]
12	Fuel Cell Miscellaneous Cost	%	12	[76]
13	Aircraft Spare Parts	%	10	[75]
14	Engine Spare Parts	%	30	[75]
15	Interest Rate	%	5.5	[75]
16	Insurance Rate	%	0.5	[75]
17	Residual left at the end of aircraft Life	%	10	[75]
18	Aircraft and engine life	year	20	[75]
19	Fuel Cell Life	hour	40000	[76]
20	Jet Fuel Cost per kg	\$/kg	0.65	[80]
21	Green Hydrogen Cost per kg	\$/kg	6	[77]
22	Flight hours per year	hour/year	3300	[75]
23	Maximum Take off Weight (MTOW)	kg	89000	[74]
24	Design Payload	kg	17670	[74]
25	Engine Weight	kg	2380	[63]
26	Flight Range	km	5000	[74]

Table 10.2: Values of parameters used for the calculation of IRR

#### 10.1.4. TOTAL COST

The total Cost of an airline operation is the summation of all the costs that the airline has to bear in order to run its operation and can be calculated by adding the DOC and IDOC which have been explained in section 10.1.2 and 10.1.3 respectively. For the reference engine, the total cost can be calculated by the method mentioned above and is given in equation 10.12.

$$\text{Total Cost}_{\text{Reference}} = \text{DOC} + \text{IDOC} \quad (10.12)$$

However, for the SOFC-GT hybrid-powered aircraft, this method cannot be used as it does not include the impact of the reduction in design payload when the fuel cell is added to the turbofan.

As mentioned in section 10.1.1, the new design payload capacity could be lower than the reference aircraft payload capacity and this will lead to a reduction in the number of

passengers that the aircraft can carry, eventually leading to a reduction in total revenue as it has been assumed that the price for a ticket for the passengers has not been increased. In order to calculate this reduction in revenue, the following methodology has been used.

- First, the total cost for the reference engine has been calculated by adding the DOC and IDOC. For this analysis, the Design payload, Design fuel load, and Design range have been considered.
- Second, a profit margin of 9% has been considered on top of the total cost to calculate the total revenue generated by the airline for a particular mission and operating condition [82]. Equation 10.13 shows the mathematical formula to calculate the revenue for the reference engine.

$$\text{Revenue} = \frac{\text{Total Cost} * (1 + \text{Profit Margin})}{100} \quad (10.13)$$

- The third step of the methodology is to calculate the revenue per kg of the design payload as shown in equation 10.14.

$$\frac{\text{Revenue}}{\text{kg}} = \frac{\text{Revenue}}{\text{Reference Design Payload}} \quad (10.14)$$

- Finally, the fourth step is to calculate the total reduction in revenue due to the reduction in payload and is given in equation 10.15. The calculation is straight forward as it directly depends on the change in design payload and the revenue per kg generated in the reference case.

$$\text{Revenue Reduction} = (M_{P_{Ref}} - M_{P_{New}}) * \frac{\text{Revenue}}{\text{kg}} \quad (10.15)$$

where

$M_{P_{Ref}}$  = Reference Design Payload, kg

$M_{P_{New}}$  = New Design Payload, kg

After the calculation of revenue reduction, the total cost for SOFC-GT hybrid-powered aircraft operation can be calculated and is given in equation 10.16. Unlike the reference aircraft, an additional cost, which is the loss in revenue, has to be considered as this cost will have to be incurred by the airlines.

$$\text{Total Cost}_{\text{SOFC-GT}} = \text{DOC}_{\text{SOFC-GT}} + \text{IDOC} + \text{Revenue Reduction} \quad (10.16)$$

### 10.1.5. INTERNAL RATE OF RETURN (IRR)

Internal Rate of Return or IRR is the average annual return on the investment over a specific period of time. It is the average rate of return at which the present value of future return is equal to the initial investment which has been made by the company. In simple words, if a company invests a sum of money in a project and gets the same amount of money back in future money in the form of returns over a period of time, the rate at which that money is coming back to the company is called the Internal Rate of Return. The IRR is calculated using the Net Present Value or NPV formula and in order to calculate IRR, NPV needs to be zero. NPV is given in equation 10.17.

$$NPV = -(\Delta\text{Investment}) + \sum_{k=1}^n \frac{\Delta\text{Total Cost}_k}{(1 + IRR)^k} \quad (10.17)$$

where

n= Total number of years

k= Particular year

$\Delta$  Investment= Initial Investment<sub>SOFC-GT</sub> – Initial Investment<sub>Ref</sub> , \$

$\Delta$ Total Cost<sub>k</sub>= Total Cost<sub>Ref</sub> – Total Cost<sub>SOFC-GT</sub>, \$

$\Delta$ Total Cost<sub>k</sub> is the profit that airlines will generate if they use a SOFC-GT hybrid over a turbofan engine.

Figure 10.3 shows the methodology to calculate the IRR and evaluate the profitability of the project.

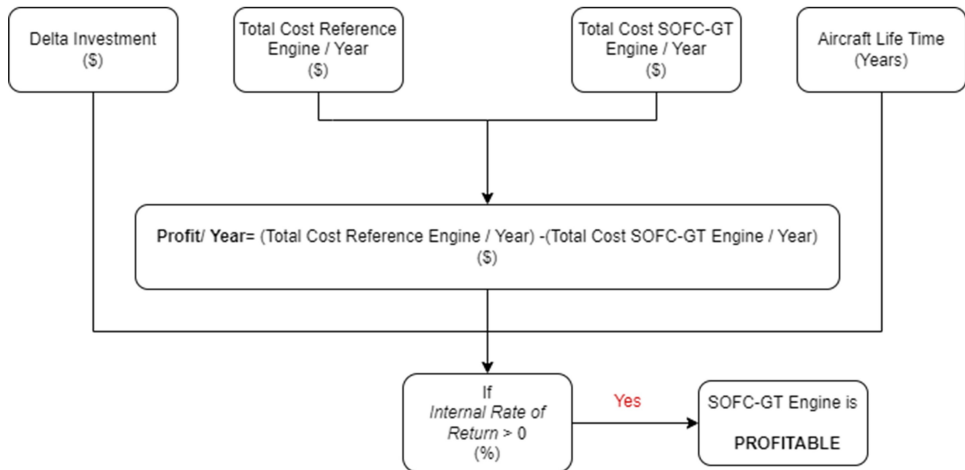


Figure 10.3: Methodology to calculate the Internal Rate of Return and evaluate the profitability of the SOFC-GT hybrid

If the IRR is positive, it means that for the given  $\Delta$ Total Cost or profit,  $\Delta$ initial investment and lifetime, the company will not lose money. However, if the IRR is negative, it means

that the company will lose money on its initial investment, and hence the investment is not profitable. A summary is given in table 10.3.

Sr. No.	Analysis	Result
1	$IRR < 0$	Unprofitable
2	$IRR > 0$	Profitable
3	$IRR = 0$	Breakeven

Table 10.3: Summary of the impact of IRR and WACC on overall profitability and Feasibility of the project

It should be noted that the IRR does not account for external factors which impact the profitability of a project. These factors include inflation, cost of capital, etc which are not in the control of the company. In this research, inflation has not been considered in order to keep the analysis simple. The cost of capital has been considered in the form of interest rate.

### 10.1.6. ASSUMPTIONS FOR ECONOMIC ANALYSIS

This section talks about the assumptions that have been taken for the economic study and they are given below.

- The reference aircraft chosen for this study is Airbus A321.
- Engine life is assumed to be similar to the life of the aircraft i.e. 20 years.
- The fuel weight has been calculated using the cruise (Off-Design condition) flight time. For other conditions like Take-off (Design condition), Top of climb, and approach, a factor has been included to account for the fuel consumption. The calculation is given in the appendix B
- The engine weight is kept constant for all the analysis. The propulsion system weight is changing but the turbofan weight is kept constant for all the engines, whether its SOFC-GT hybrid or reference engine.
- The fuel price is assumed to be the same for the whole lifetime of the aircraft. The price of fuel may vary but the assumed price for analysis is the average of the price for the lifetime of the aircraft.
- Interest and insurance rates are assumed to be constant for the whole lifetime of the aircraft.
- Inflation has not been included in this analysis.
- Engine price for CFM-56-5A3 and the reference engine is assumed to be the same. Although the CFM-56-5A3 engine core is smaller, due to the increase in the fan size, the price will increase. In order to simplify the calculation, the price is assumed to be constant.
- The increase in fuel cell cost with fuel cell power is assumed to be linear.

## 10.2. ECONOMIC ANALYSIS RESULTS

This section discusses the results of economic analysis based on the methodology given in section 10.1. Two types of analysis has been done and they are as follow:

- **Economic Analysis without Emissions:** The first type of economic analysis has been done without including the emissions tax. This is because of no tax on emissions like  $NO_x$  and  $H_2O$  has yet been implemented by the governments.

The analysis concludes that the commercially available fuel cell is currently not feasible due to higher mass and presents the value of required specific power for which the SOFC-GT hybrid would be economically feasible. Also, the benefit of increasing the power output of fuel cell in terms of fuel cost is not enough to compensate for the increase in investment and other related costs.

This analysis shows that increasing the fuel prices decreases the required specific power of the fuel cell. In the end, the sensitivity analysis is done which shows that the impact of aircraft parameters is much higher on the overall economics of the aircraft. However, the sensitivity to aircraft parameters is decreasing as fuel cell power output is increased.

- **Economic Analysis with Emissions:** The second type of analysis includes the different scenarios of emission tax and shows the impact of emissions tax on the overall economics of the aircraft.

The analysis concludes that even after including the highest amount of tax, the SOFC-GT hybrid is not feasible for the commercially available fuel cell. Also, the required fuel cell specific power is decreasing as emission tax is increased and the system is becoming feasible at lower fuel prices compared to the no emission tax case.

In the end, the sensitivity analysis showed that increasing the tax reduces the sensitivity of both, aircraft and fuel cell parameters.

### 10.2.1. RESULTS (WITHOUT EMISSIONS)

This section presents the result for economic analysis without emission tax. Figure 10.4 shows the change in total investment and fuel cell cost as the fuel cell power is increased. It can be seen that as the fuel cell power is increased, the cost of fuel cell increases linearly as well based on the costs for different fuel cell parts as presented in 10.2. As more power is needed from the fuel cell, the number of SOFC stacks required increases along with the size of the balance of the plant and hence the costs.

As a consequence of the increase in fuel cell cost, the total lifetime investment of an aircraft increases as well. The cost of turbofan and aircraft are kept constant while the fuel cell cost is changing with power. The total lifetime and fuel cell cost for CFM 56 - 5A3 engine integrated with the fuel cell which is producing higher thrust as explained in section 8.3.1 has also increased as shown in the figure as well. It should be noted that the data has been extrapolated for the fuel cell power output of 5 and 6 MW in order to show the comparison between the reference engine and the CFM-56-5A3 engine integrated with the fuel cell to provide the higher thrust.

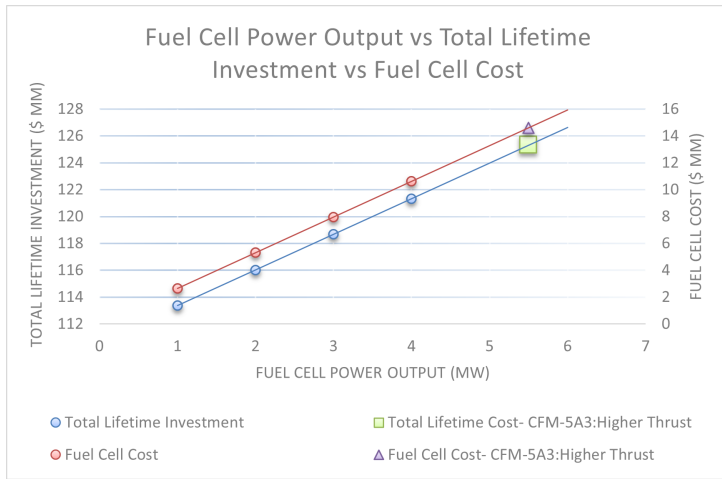


Figure 10.4: Change in fuel cell power vs total lifetime investment vs fuel cell cost

### 10.2.2. RESULT 1

***SOFC-GT hybrid is not feasible for the current values of fuel cell-specific power***

Sr. No.	Parameter	Unit	Value	Reference
1	SOFC Specific Power	kW/kg	0.275	[83]
2	Heat Exchanger Specific Power	kW/kg	8.853	[83]
3	Motor Power to Weight Ratio	kW/kg	5.900	[84]
4	Hydrogen Gravimetric Efficiency	%	64	[85]

Table 10.4: Values of parameters used for the calculation of fuel cell weight

As per the analysis, the SOFC-GT hybrid is not economically feasible for the commercially available fuel cell system. The specific power of the different parts of the fuel cell system is given in table 10.4 and the total specific power of the fuel cell is calculated to be 0.253 kW/kg. As can be seen that the biggest contributor to the weight is the SOFC and this is precisely because the commercially available SOFC are not designed for transportation or aviation in general but for stationary applications. Hence, the specific power is very low as weight is not a big constraint in the stationary application.

Table 10.5 shows the results of the analysis for 1 MW power output and it can be seen that the  $\frac{\Delta DOC}{hour}$ , as given in 10.18, is positive, which means that the economic benefit from the reduction in fuel consumption is higher than the increase in the standing charges and maintenance cost per hour. However, the  $\frac{\Delta TotalCost}{hour}$  is negative which means that even though the  $\frac{\Delta DOC}{hour}$  is positive, the revenue reduction because of the decrease in design payload is much higher. This is the reason that the Internal Rate of Return cannot be calculated as there is no benefit of adding the fuel cell and hence the return is not possible. It should be noted that the price of green hydrogen is \$ 6/kg and no emissions have

Sr. No.	Parameter	Unit	Value
1	$\Delta DOC$	\$/hour	253.5
2	$\Delta$ Total Cost	\$/hour	-7527
3	Internal Rate of Return	%	-

Table 10.5: Result of the Economic Analysis for commercially available fuel cell-specific power for 1 MW power output

been considered for this analysis and the Indirect Operating Cost (IDOC) is the same for both reference and SOFC-GT hybrid.

$$\frac{\Delta DOC}{hour} = \frac{DOC_{Reference}}{hour} - \frac{DOC_{SOFC-GT}}{hour} \quad (10.18)$$

$$\frac{\Delta Total Cost}{hour} = \frac{Total Cost_{Reference}}{hour} - \frac{Total Cost_{SOFC-GT}}{hour} \quad (10.19)$$

### 10.2.3. RESULT 2

***The required specific power to break even for initial investment is increasing as fuel cell power output is increasing***

As mentioned in section 10.2.2, the reduction in TSFC and the subsequent fuel and tank weight does not complement the weight added to the system. Hence, an analysis has been done in order to calculate the specific power of the complete fuel cell system for which the SOFC-GT hybrid break-even over the lifetime of the aircraft. Figure 10.5 shows the specific power required for given fuel cell power. It is shown in the figure that as the fuel cell power is increasing, the required minimum specific power is increasing as well. **For example, in the case of 1 MW fuel cell power output, the specific power required is 2.3 kW/kg compared to 2.88 kW/kg for 4 MW power output.** It means that the benefit that the airline gets in terms of fuel cost reduction by adding a higher power fuel cell is less than the increase in the standing cost, maintenance cost, and revenue reduction. It should also be noted that the emission tax has not been included in this specific analysis and the results with emission tax will be presented in the later sections.

However, the CFM 56-5A3 engine integrated with a fuel cell and producing the same thrust as CFM 56-5B1, has a higher required specific power compared to the CFM 56-5B1. As per the CFM 56-5B1, the required specific power should be around 3.15 kW/kg (as per the extrapolated data) but the required specific power for CFM 56-5A3 is 3.52 kW/kg. This is because of the higher TSFC of CFM 56-5A3 integrated with fuel cell compared to the CFM 56-5B1 as mentioned in section 8.3.1. Hence, it needs a higher specific power to compensate for the increase in fuel consumption.

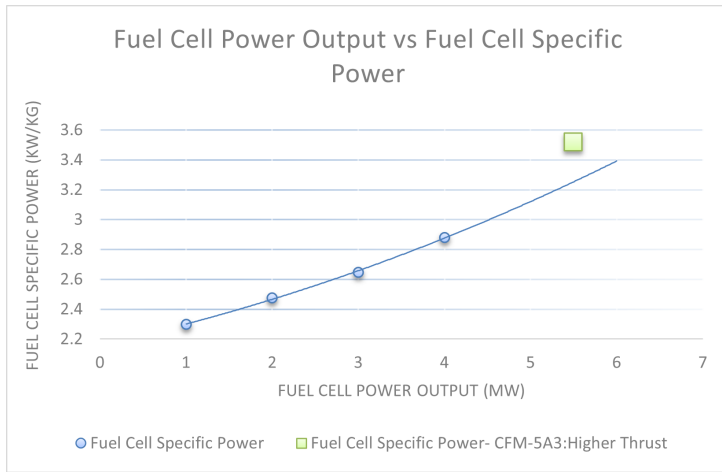


Figure 10.5: Change in required specific power as fuel cell power is changed

### 10.2.4. RESULT 3

***The Internal Rate of Return from propulsion system perspective is decreasing as fuel cell power output is increasing***

As mentioned in section 10.2.2, the required specific power will increase if the fuel cell power is increased and this is because the propulsion system efficiency increase does not complement the increase in weight and investment. This does not mean that the DOC is reducing when the fuel cell is added. As shown on the y-axis of figure 10.6, the percentage reduction in DOC is increasing as the fuel cell power is increased. However, the Internal Rate of Return for DOC or IRR-DOC is decreasing as shown on the secondary axis.

The IRR-DOC is not the same as the IRR mentioned in section 10.1.5 and figure 10.3. The IRR-DOC is the internal rate of return calculated based upon only the Direct Operating Cost and not the total cost incurred by the airline and is shown in equation 10.20. IRR-DOC is the IRR from the propulsion system’s perspective and not the whole aircraft’s perspective. It shows the impact of adding the fuel cell on the performance and economics of the engine, not the whole aircraft. Hence, IRR-DOC does not include the impact of the reduction in design payload in the case of the addition of fuel cell and .

$$NPV = -(\Delta\text{Investment}) + \sum_{k=1}^n \frac{\Delta\text{DOC}_k}{(1 + IRR)^k} \tag{10.20}$$

where

n= Total number of years

k= Particular year

$\Delta$  Investment= Initial Investment<sub>SOFC-GT</sub> – Initial Investment<sub>Ref</sub> , \$

As can be seen from the secondary axis of figure 10.6, the IRR-DOC is reducing as fuel cell power is increasing. This means that even though adding the fuel cell does have a benefit in terms of DOC but the capital cost and other related costs because of the addition of fuel cells cannot be counteracted by the reduction in fuel cost.

It should also be noted again that IRR-DOC is independent of the specific power or weight of the system as it only focuses on the propulsion system, not the whole aircraft. Along with this, the reduction in DOC and IRR-DOC for the CFM 56 -5A3 is lower and it is expected because of the lower efficiency as explained above.

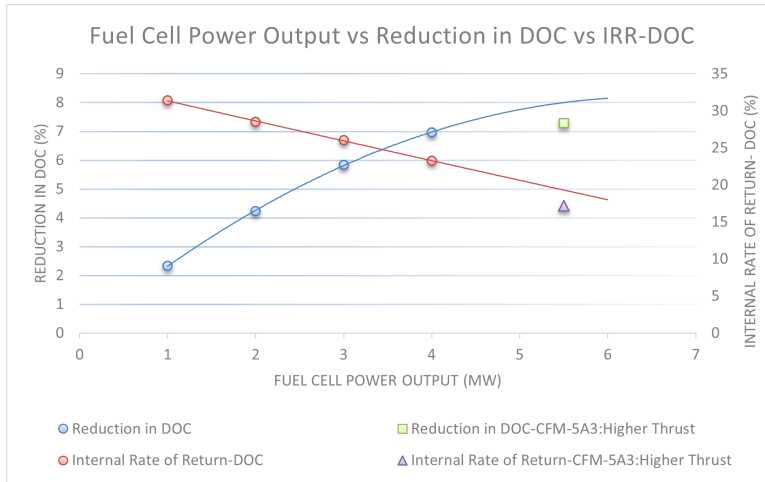


Figure 10.6: Reduction in Direct Operating Costs and the change in Internal Rate of Return for Direct Operating Costs as fuel cell power is changed

### 10.2.5. RESULT 4

#### ***Increase in fuel price decreases required specific power to break-even the initial investment***

It has been mentioned in section 10.1 that the reference price for green hydrogen is \$ 6/kg. But as green hydrogen production is still in the nascent stages, there might be a deviation in fuel prices when the production is starting to rise. Industry experts believe that the price of hydrogen in the year 2030 would be around \$ 6/kg while the European Union believes that the price could be as low as \$ 2/kg [77]. Also, hydrogen prices vary drastically from country to country because of their dependence on the initial capital cost of renewable energy. Hence, an analysis of different fuel prices has also been done in this study to account for the future uncertainty in fuel prices.

Figure 10.7 shows the change in required specific power at which the SOFC-GT hybrid would break even as fuel price is increased. It can be clearly seen that the required specific power is reducing and the reason for it is the higher reduction in DOC for the

SOFC-GT hybrid. The reduction in fuel is the same for all the different fuel prices as the operating conditions are fixed but the increase in fuel price makes the fuel a bigger part of the DOC as well as the total cost. Hence, the reduction in fuel will then have a higher impact on the DOC and the total cost. This means that the reduction in DOC can compensate for the reduction in revenue due to payload decrease which will eventually lead to the project being profitable at lower specific power or in other words, higher propulsion system weight.

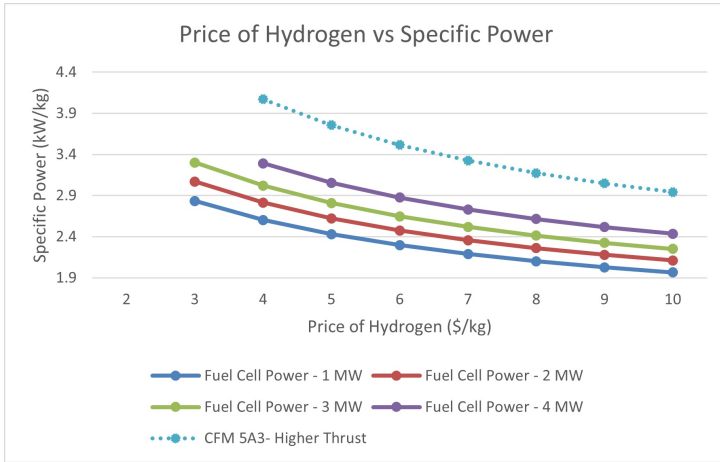


Figure 10.7: Change in required specific power as the fuel price is increased

It should also be noted that figure 10.7 does not present the values of specific power at the fuel price of \$ 2/kg for all the different fuel cell power outputs and \$ 3/kg for the fuel cell power output of 4 MW. This is because the cost benefit at the lower fuel prices cannot compensate for the increased investment and other costs and hence, the IRR is negative, meaning the system is not feasible

**10.2.6. ECONOMICS SENSITIVITY ANALYSIS (WITHOUT EMISSIONS)**

This section talks about the sensitivity analysis that has been done in order to understand the impact of different parameters on the required specific power for 1 MW and 4 MW fuel cell power output to break even. The analysis has been shown in figure 10.8. The sensitivity coefficient shown in the figure is given in equation 10.21.

$$\text{Sensitivity Coefficient} = \left( \frac{\text{Specific Power}_{NEW} - \text{Specific Power}_{REF}}{\text{Specific Power}_{REF}} \right) * 100 \quad (10.21)$$

where

Specific Power<sub>NEW</sub>= Required Specific Power when the given parameter is increased by 1%, kW/kg

specific power<sub>REF</sub>= Required Specific Power for the reference case, kW/kg

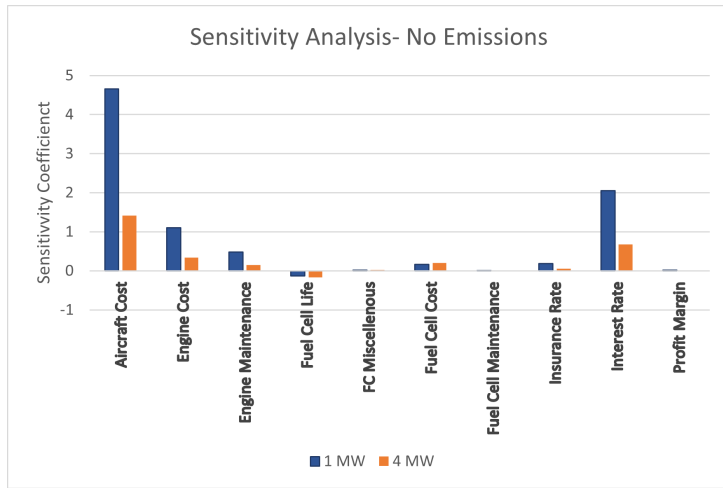


Figure 10.8: Sensitivity Analysis of required Specific Power for a 1 MW and 4 MW fuel cell power output in order to breakeven (IRR=0)

The sensitivity Coefficient shows the % change in the required specific power when the given parameter is increased by 1%. For example, when the parameter 'Aircraft Cost' is increased by 1% from the reference case, the required specific power for 1 MW and 4 MW fuel cell power output increased by 4.66% and 1.41% respectively. This is because of the increase in the standing charges which will lead to an increase in the Direct Operating Cost(DOC) and hence, will require a higher specific power to breakeven. It can also be seen that the sensitivity coefficient is lower for the 4 MW power output, which means that the increase in aircraft cost will have a lower impact on specific power. This is because of the increase of overall investment due to FC cost, maintenance, and the subsequent increase in insurance and interest cost along with the reduction in fuel consumption, which reduces the contribution of aircraft cost in the overall impact and hence its impact when it is increased. This is true for each parameter that has been included in the study. For example, in the case of an interest rate increase, the impact on 4 MW system is lower because of the lower contribution to the overall cost and hence the impact of increasing it is also lower.

Similar to aircraft cost, when engine cost and fuel cell cost have increased, the required specific power has increased by 1.1% and 0.164% for 1 MW power output and the reason is the same as given above for the aircraft cost. The engine cost is higher than the fuel cell cost as given in table 10.2 and hence the specific power is more sensitive to engine cost.

The same reasoning can be applied to engine and fuel cell maintenance, interest rate, and insurance rates. However, increasing the fuel cell life leads to a sensitivity coefficient of -0.13% and -0.166% for 1 MW and 4 MW power output respectively. This means that increasing the fuel cell life will decrease the required specific power and it is because of the decrease in the initial total capital as fuel cell life has increased. Also, the coefficient is more negative for 4 MW power output and the reason is similar as given above. Higher fuel cell power output means the contribution of fuel cell in total cost is higher and hence

if fuel cell life increases then its will have a higher impact as well.

*It can be understood very well from the figure 10.8 that the required specific power is more sensitive to changes in aircraft parameters rather than the change in fuel cell parameters. This means that even if the fuel cell cost and fuel cell maintenance increase by 10%, the specific power needs to be increased from 2.297 kW/kg to 2.335 kW/kg and 2.3 kW/kg respectively for 1 MW power output. While on the other hand, by increasing the aircraft cost and engine cost by 10%, the specific power needs to be increased to 3.37 kW/kg and 2.55 kW/kg. Hence, it can be concluded that from an economics perspective, more research should be focused on how to minimize the change in aircraft when the fuel cell is added to the turbofan than the change in the fuel cell itself as the impact of change is fuel cell on overall economics is comparatively low.*

### 10.2.7. RESULTS (WITH EMISSIONS)

This section discusses the results of economic analysis with emissions calculated in section 9. As mentioned, there are primarily two types of emissions from hydrogen, Nitrogen Oxides ( $NO_x$ ) and Water/Steam ( $H_2O$ ), has been included in this study and three scenarios have been considered as given in table 10.6. There is currently no tax on water emissions but water does have a greenhouse effect as mentioned in section 9. Hence, in order to include the impact of water, it has been calculated using the emission tax on  $CO_2$ . For the current scenario, the  $CO_2$  tax is \$30/tonne which is \$0.03/kg as given in [78]. As per figure 9.1, at the altitude of 11 km, which is similar to the cruise condition for the aircraft considered in this study, the Global Warming Potential or GWP of water is 40% off  $CO_2$ . Hence, the water tax for the current scenario is assumed to be 40% of  $CO_2$  tax for the current scenario, which is \$0.012/kg.

Sr. No.	Scenario	Nitrogen Oxide ( $NO_x$ ) Tax \$/kg	Water/Steam ( $H_2O$ ) Tax \$/kg
1	Current Scenario	5.43	0.012
2	Near Future Scenario (5-7 years in future)	22.625	0.05
3	Future Scenario (15-20 years in future)	90.5	0.2

Table 10.6: Different scenarios for emission tax considered in this study

On the other hand, for  $NO_x$  emissions, the tax for the current scenario has been taken [86]. Different governments all around the world have implemented different taxes for  $NO_x$  but as per the report, the tax of \$5.43/kg by the Swedish Government has been able to reduce the  $NO_x$  emission in the country. Other places like France and USA which have lower taxes are not able to reduce  $NO_x$  emissions with these tax rates.

In order to calculate the emissions for near-future scenario, the  $CO_2$  tax has been considered from the report by PricewaterhouseCoopers [87] which mentions the tax of \$125/tonne by the year 2030, and hence, the water tax has been calculated using the same methodology given above. The  $NO_x$  tax has been increased by same proportion

as the  $CO_2$  tax. For future scenario, which would be 15-20 years, the author took an educated guess that the  $CO_2$  tax may be around \$500/tonne and the water and emission tax has been calculated proportionally as mentioned in table 10.6.

### 10.2.8. RESULT 5

***SOFC-GT hybrid is not feasible for the current values of fuel cell-specific power even after considering the emission tax***

Even after including the emissions for the future scenarios, the SOFC-GT hybrid is not economically viable as per the analysis done by the author. Table 10.7 shows the  $\Delta DOC$ ,  $\Delta$ Total Cost and Internal Rate of Return for different scenarios which has been explained above. As can be seen,  $\Delta DOC$  is increasing as the tax is increased because the SOFC-GT hybrid is more sustainable and hence, increasing the tax will decrease the Direct Operating Cost.

However, the total cost of SOFC-GT hybrid-based aircraft is also increasing and this is because of the increase in the revenue loss by the airline when the fuel cell is integrated. As mentioned in section 10.1, the payload has been decreased in order to compensate the weight of the fuel cell, and hence, the revenue of the airline will decrease. The revenue has been calculated using the reference engine and when the cost of emission is added to the reference engine, the revenue per kg of payload increases. This is the reason when the fuel cell is added and the payload is decreased, the revenue reduction increases, and hence the total cost of adding the fuel cell increased with an increase in emission tax.

Sr. No.	Parameter	Unit	Current Scenario	Near Future Scenario	Future Scenario
1	$\Delta DOC$	\$/hour	260.91	284.4	376.94
2	$\Delta$ Total Cost	\$/hour	-7570	-7705.1	-8238.4
3	Internal Rate of Return	%	-	-	-

Table 10.7: Result of the Economic Analysis for commercially available fuel cell specific power for 1 MW power output with the inclusion of emission analysis

### 10.2.9. RESULT 6

***The required specific power to break even is decreasing as emission tax is increasing***

Figure 10.9 shows the change in required specific power as fuel cell power is increased for reference engine and CFM-56-5A3 engine integrated with fuel cell for all scenarios of emission tax. It can be seen that the required specific power is decreasing and the reason for it is the decrease in DOC because of lower emissions by the SOFC-GT hybrid. However, the decrease is higher as the fuel cell power output is increased. For example, for the future scenario, the required specific power decreased by 8.83%, 9.11%, and 9.68% for 1 MW, 4 MW, and CFM-56-5A3. The reduction in specific power is because

of the exponential decrease in  $NO_x$  emissions as fuel cell power is increasing as shown in figure 9.5. It should be noted that the price of hydrogen in this analysis is \$6/kg, which is the reference for this study.

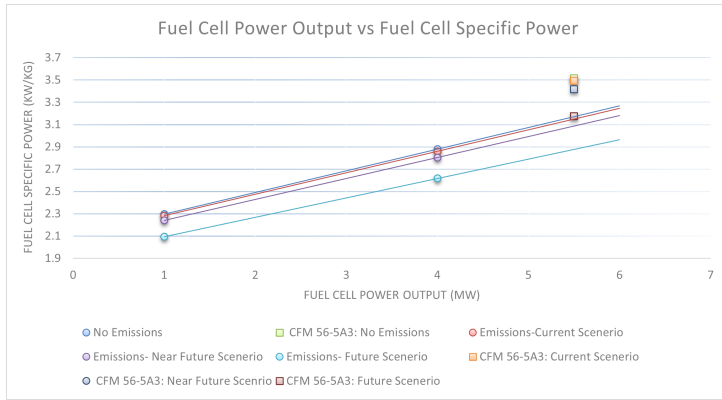


Figure 10.9: Change in fuel cell-specific power as fuel cell power output is increased when emission tax is included

10.2.10. RESULT 7

*The SOFC-GT hybrid is becoming feasible at lower fuel prices as emissions tax is increasing*

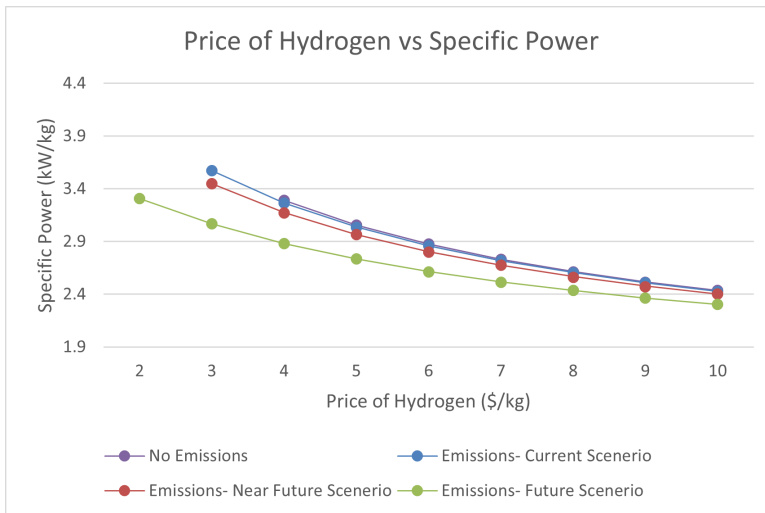


Figure 10.10: Change in required specific power as fuel price is increased when emission tax is included for 4 MW power output

Section 10.2.5 discusses that the SOFC-GT hybrid is not feasible for \$2/kg and \$3/kg for fuel cell power output for 4 MW when emissions are not included in the analysis. However, with the inclusion of emissions, the SOFC-GT hybrid is becoming feasible at lower fuel prices as can be seen from figure 10.10. Figure shows that for the current and near-future scenarios, the SOFC-GT hybrid with fuel cell power output of 4MW is feasible for \$3/kg of fuel price, and for the future scenario, the fuel price could go to \$2/kg, or even below that as well. This is because of the compensation of revenue reduction due to increase in fuel cell mass by the reduction in emission tax. This signifies that if the European Union's optimistic goal of decreasing hydrogen prices to \$2/kg is achieved, even the fuel cell power output of 4 MW is possible with the specific power of 3.3 kW/kg.

### 10.2.11. ECONOMIC SENSITIVITY ANALYSIS (WITH EMISSIONS)

This section talks about the sensitivity analysis that has been done in order to understand the impact of different parameters on the required specific power for 1 MW power output to break even for different emission scenarios. The analysis has been shown in figure 10.8. The sensitivity coefficient shown in the figure is given in equation 10.21. It is evident from the figure that as the emission tax is increased, the impact of parameters like aircraft cost, engine cost, interest rate, which negatively impact the economics, is decreasing. This is primarily because of an increase in the contribution of emission tax to the total cost of flying and hence, increasing these costs will have a lower impact on the overall economics and required specific power. This has been explained thoroughly in section 10.2.6.

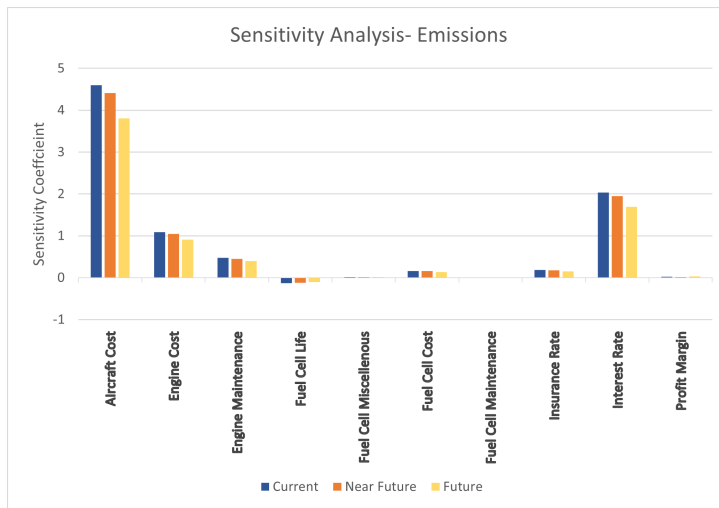


Figure 10.11: Sensitivity Analysis of required Specific Power for a 1 MW fuel cell power output in order to breakeven (IRR=0) for different emission scenarios

However, the sensitivity coefficient is increasing (becoming more positive) for fuel cell life as emission tax is increased. For example, for the no emission case, the sensitivity coefficient is -0.13% compared to -0.1% for the future scenarios. This means that the

impact of fuel cell life is reducing as emission tax is increased. The reason is the same as for other parameters which is the increase in the contribution of emission tax to the total cost which has decreased the impact of other parameters.

*Nevertheless, it can be concluded that increasing emission tax exponentially does not have a major impact on the sensitivity of parameters included in this study.* For example, increasing the emission tax, both  $H_2O$  and  $NO_x$  by 1666.6% from the current scenario to the future scenario only decreased the sensitivity coefficient by 17.40% and 16.74% for Aircraft Cost and interest rate, respectively. The impact of this decrease would have significance on the overall economics but the change is smaller.

Therefore, the emission tax does not have much impact on the economy and required specific power of the SOFC-GT hybrid run aircraft but the environmental impact will reduce which is the moral and social responsibility of any company and government working for the betterment of society.



# 11

## CONCLUSIONS, LIMITATIONS, CONTRIBUTIONS & RECOMMENDATIONS

This section talks about the summary of the whole research project and presents the answer to all the research questions that have been formulated in order to achieve the research objectives. In the end, the recommendations for future work have also been presented in order to take the project further and improve results.

### 11.1. RESEARCH PROJECT SUMMARY

Section 1 talks about the current scenario of engine emissions and thrust specific fuel consumption and its trend over the years which proves that the gas turbine technology is maturing. Hence, there is a need for new disruptive innovations in the propulsion sector in order to achieve ACARE 2050 goals. But if the disruptive technologies which are proposed like Boundary Layer Ingestion(BLI), Turbo-electric propulsion, and Distributed Propulsion(DP) were to be implemented in a Boeing 737-800 aircraft, it will reduce the fuel burn by between 7-12% [13], which will not be sufficient for the industry emission reduction targets. Hence, the author believes that along with the technologies which have been proposed, other concepts should also be investigated which could increase efficiency and one of those concepts or technology could be the fuel cell. But fuel cell, due to their low TRL and low specific power could not be used alone for commercial aircraft. Although, there is a possibility of using a hybrid concept called SOFC-GT, which has been discussed thoroughly in section 2.

Section 3 gives a detailed explanation of multiple concepts researched in the past for ground and aerospace applications which shows that the SOFC-GT hybrid has the capability to reach an electrical efficiency of more than 60% and an integrated system efficiency of 85%. Along with this, the concept does not disregard the gas turbine technology, which has been developed over the decades and achieved an engineering feat

when it comes to eliminating inefficiencies. On the contrary, it is complementary to gas turbine technology and provides more scope for improvement. Hence, the author believes that this concept should be explored more and after a thorough analysis of multiple types of research, the author has identified many research gaps which have been presented in section 4. The main research gap is *the impact of adding the fuel cell to a gas turbine on thrust-specific fuel consumption, emissions, and economics*. Based on these research questions, multiple research questions and objectives have been formulated in order to answer the main question:

***“Is it technically and economically feasible to develop a SOFC-GT based hybrid propulsion system running on hydrogen for a commercial aircraft?”***

In order to answer these questions, mathematical models have been developed for fuel cell, gas turbine, and SOFC-GT hybrid are given in section 5, 6 and 7 respectively. The validation and verification of these models has also been presented in their respective sections. Section 8 discusses the technical results and also presents a new comparison methodology developed by the author in order to do a fair comparison between the reference engine and SOFC-GT hybrid. Sensitivity analysis has also been done which shows the impact of change in different parameters on the thermodynamic efficiency of the SOFC-GT hybrid. After the discussion on technical results, emission analysis has been done and section 9 discusses the emission methodology, Verification, and results of the emission analysis.

After the technical analysis, the economic analysis has been done, which is the second part of this thesis and is given in section 10. A methodology has been developed by the author for this analysis, given in section 10.1 and the results have been discussed. Two types of scenarios has been considered in the economic analysis, one being the no emissions case and the second being the analysis with emissions. In the analysis of emissions, three scenarios for taxes have been considered, current, near future, and future, as explained in table 10.6. In the end, sensitivity analysis for multiple parameters for both scenarios, economic analysis with and without emissions, has been done.

The answers to all the research questions are given below.

## 11.2. CONCLUSION

This section discusses the answers to all the research questions presented in section 4. The questions are as follows.

1. ***What is the difference in steady-state performance for the SOFC based hybrid propulsion system compared to a conventional Gas Turbine propulsion system? What is the impact of adding the fuel cell on gas turbine parameters?***

- TSFC increased for Design (Sea Level Static) condition when the fuel cell is added to the engine. The TSFC increased by 0.21% and 1.35% for 1 MW and 4 MW fuel cell power output. This is because of the decrease in mass flow rate of the engine, which reduced the propulsive efficiency, and hence the total

efficiency. This is the reason that a new methodology to keep the Specific Thrust of the reference engine and SOFC-GT hybrid has been implemented in order to have a fair comparison.

- The Thrust Specific Fuel Consumption (TSFC) for the SOFC-GT hybrid is lower for both Design and Off-Design (Cruise) conditions when compared to conventional Gas Turbine, given the Specific Thrust of both the engines is the same. For example, TSFC has been reduced by 1.8% and 6.03% for Design and Off-Design conditions when 1 MW fuel cell power output.

The TSFC reduction has increased from 6.03% for 1 MW fuel cell power output to 19.89% for 4 MW in Off-Design conditions. The reasons for this reduction are higher efficiency of the fuel cell, the addition of waste heat from the fuel cell to gas turbine, and a decrease in transmission loss.

- The core mass flow rate of the gas turbine is reducing as the bypass ratio of the engine is increasing. This is because the fraction of power is coming from the fuel cell and hence, the core size needs to be reduced in order to reduce the core power loss. This will lead to an increase in propulsive efficiency, and hence total efficiency, as more air is bypassing the core and the core weight will also reduce. The reduction in core mass flow rate is 3.55% and 13.8% for 1 MW and 4 MW power output for Design condition. *It should be noted that the total mass flow rate entering the SOFC-GT is similar to the reference case which means that the physical size of the fan and overall engine will stay the same.*

- The TIT for Off-Design condition is decreasing because of the reduction in gas power required from the core as the fuel cell is complementing the part of gas power. The TIT has decreased by 5.10% and 17.63%, a substantial decrease, for 1 MW and 4 MW power output respectively.

*Increasing the fuel cell power output decreases the thermodynamic efficiency of the standalone gas turbine as TIT is decreasing. But the overall thermodynamic efficiency of the complete propulsion system increases.*

- The cooling air requirement has decreased by 13.56% and 85.4% for the fuel cell power output of 4 MW for Design and Off-Design condition, respectively considering the active cooling mechanism. For the former, the reason for the reduction is an absolute decrease in mass flow rate due to a decrease in core size. For the latter, the cooling air reduction is higher because of the decrease in TIT along with the decrease in core size. Reduction in cooling air will increase total efficiency as a higher fraction of air is passing through the combustor.

**2. Does the improvement in performance complement the added weight? If not, how much improvement is needed in the specific power of the Fuel Cell?**

- No, the improvement in performance does not complement the added weight for the commercially available fuel cell specific power. The weight reduction in fuel and tank weight for 1 MW power output is 277.5 kg for one engine for the whole mission of Airbus A321. While the weight added to the one engine is 3952.6 kg leading to a net weight increase of 3675.10 kg for one engine. Hence, the SOFC-GT hybrid is not feasible for the current values of fuel cell-specific power.
- No amount of improvement in the SOFC-GT hybrid performance from the TSFC perspective can complement the weight of the fuel cell system for the current value of fuel cell-specific power. This is because the total mass of fuel consumed during the journey is less than the weight added to the propulsion system.

3. ***What is the reduction in emissions, mainly  $NO_x$  & Water, for the SOFC-GT hybrid when compared to a conventional Gas Turbine propulsion system based upon the correlation method? (0 D emission Analysis)***

**$NO_x$  Emissions**

- The  $NO_x$  emissions are decreasing as fuel cell power output is increasing. The emissions have decreased by 29.11% and 78.05% for 1 MW and 4 MW fuel cell power respectively during Off-Design condition. This decrease is because of the decrease in fuel flow in the combustor leading to a lower equivalence ratio. It should be noted that the correlation model used in this study can only be used for Off-Design conditions due to the constraints of the relation.
- Fuel Cell does not have any  $NO_x$  emissions as the maximum temperature inside the fuel cell is 1200 K. Hence, increasing the fuel cell power output will reduce the  $NO_x$  emission.
- Increase in the power output will increase the temperature of the mixture (air + fuel cell byproducts) entering the combustor, which will increase the  $NO_x$  emissions. The temperature of the mixture entering the combustor has increased by 4.55% and 6.20% for Design and Off-Design condition respectively, for 4 MW power output. However, overall emissions are decreasing, hence concluding that the emissions are most sensitive to fuel flow, and an increase in temperature of the mixture entering the combustor does not have much impact.
- Phenomena like the addition of steam and reduction in  $O_2$  concentration due to a fraction of air being used by fuel cells, are not included in this study. Both of these phenomena will reduce the  $NO_x$  emissions even further than given in this study. More sophisticated models are needed to quantify these

effects, which were out of the scope of this study.

### *H<sub>2</sub>O Emissions*

- *H<sub>2</sub>O* emissions are also reducing as the fuel flow rate is decreasing when fuel cell power is increased. *H<sub>2</sub>O* emissions depend directly on the mass of fuel used in the propulsion system. For example, the emissions decreased by 6% and 19.9% for 1 MW and 4 MW power output respectively.
- Reduction in altitude will reduce the Global Warming Potential of the *NO<sub>x</sub>* and *H<sub>2</sub>O* emissions.

#### 4. *Does the improvement in performance complement the increase in fuel cell-related Costs? If not, how much improvement is needed in fuel cell-specific power to achieve feasibility?*

- The specific power needed to break even from an economic perspective at the fuel price of \$6/kg for 1 MW fuel cell power output is **2.3 kW/kg** compared to the commercially available specific power of 0.253 kW/kg. It should also be noted that NASA has already patented a SOFC for Aerospace applications with the specific power of 2.5 kW/kg [27].
- The required specific power to break even is increasing with the increase in fuel cell power output. The required specific power increased by 24.98% when the fuel cell power output is increased from 1 MW to 4 MW. This means that the benefit in fuel reduction by increasing the fuel cell power is not compensating for the increase in investment and decrease in revenue due to the payload decrease that the airline has to incur. Hence, the required specific power is increasing.
- The required specific power to break even is decreasing if fuel price is increased and vice versa. The specific power decreased by 30.60% when the fuel price increased from \$3/kg to \$10/kg for 1 MW power output. This is because the increase in fuel price increased the reduction in operating cost, hence the weight of the fuel cell system can be increased as revenue reduction can be compensated by the reduction in fuel price.
- If only an aircraft engine is considered, the addition of a higher power fuel cell is not compensating for the increase in initial investment and other costs like maintenance, interest, etc.
- The SOFC-GT hybrid is not feasible for the fuel price of \$2/kg as the benefit of decreasing fuel consumption is not enough to complement the increase in

investment and other related fuel cell-related costs.

- The SOFC-GT hybrid will be **most suitable for medium-range or long-range flights** compared to short-range flights as the benefit from fuel cost and emissions tax would be higher for medium and long-range missions.

5. *Does an introduction of  $NO_x$  and Water emission tax makes the propulsion system feasible for the current values of fuel cell-specific power? If not, how much improvement is needed in the specific power of the Fuel Cell?*

- Three different scenarios for emissions are considered, given in table 10.6, and the introduction of emission cost for  $NO_x$  and  $H_2O$  does not make the propulsion system feasible or attractive. The addition of emission tax has a lower contribution to the total cost when compared to revenue reduction due to a decrease in payload when the fuel cell is added.
- The increase in tax does reduce the required specific power to breakeven as the part of revenue reduction can be compensated by the reduction in emission cost. The required specific power decreased by 0.64%, 2.54%, and 8.83% for current, near future, and the future scenario for 1 MW fuel cell power output.

6. *Can a Gas turbine be downsized while keeping the maximum thrust of the engine similar to the reference case? What is the difference in performance, from both technical and economic perspectives, for the downsized engine when compared to the reference engine integrated with a fuel cell?*

**Technical Analysis**

- Yes, the gas turbine can be downsized while keeping the thrust requirements similar to the reference case. For this study, the CFM-56-5A3 engine has been used as a downsized engine which has a sea-level thrust of 118 kN. The engine will be integrated with a fuel cell to provide 133.6 kN of thrust, similar to the reference case.
- The fuel cell power required for the downsized engine is 5.5 MW because of the high power requirements during the maximum take-off conditions.
- The TSFC for the downsized engine reduced by 7.2% and 23.25% for Design and Off-Design conditions respectively when compared to the reference case.
- The reduction in TSFC is low when compared to the reference engine integrated with 5.5 MW of fuel cell. The expected reduction for the reference

engine is 9.08% and 24.25% compared to 7.29% and 23.25% for Design and Off-Design condition respectively. This is because of the lower TIT and OPR for the downsized engine which reduced the thermodynamic efficiency of the propulsion system. The data is given in table 8.1.

- The fuel cell power required is high and that is because of the high power requirement during the maximum power takeoff condition. Fuel cell power addition along with the increase in TIT would be a better solution than the fuel cell addition alone as with the same TIT as reference engine, the fuel cell power output of only 1.25 MW is required. With this hybrid approach, the compressor and turbine can still remain the same, which will reduce the complexity but the TIT will increase, meaning a more sophisticated material and cooling system will still be required.

### Economic Analysis

- The specific power required to breakeven is higher for downsized engines compared to the reference engine with a fuel cells. This is because of the higher fuel consumption for the downsized engine. Hence, higher specific power is needed to compensate for the fuel cell and is increased by 8.05% compared to reference engine integrated with the same fuel cell power output.

## 7. Which parameters of fuel cell and gas turbine have the major impact on the performance of the propulsion system? (Sensitivity Analysis)

### Technical Sensitivity Analysis

- The SOFC-GT hybrid is most sensitive to TIT and OPR for 1 MW power output, followed by outlet temperature of SOFC byproducts ( $T_{FCout}$ ). The sensitivity coefficient, which is defined as the % change in thermodynamic efficiency when the concerned parameter is changed by 1%, is 0.275%, 0.0485 % and 0.0238% respectively for 1 MW power output.
- Increasing the fuel cell power output decreases the sensitivity of the SOFC-GT hybrid to gas turbine parameters like TIT and OPR. This is because of the increase in the contribution of gas power by the fuel cell at higher power outputs. The coefficient decreased from 0.275% to 0.242% when fuel cell power output increased from 1 MW to 4 MW.

Along with this,  $T_{FCout}$  is becoming more important than OPR as fuel cell power output is increased because of the similar reasons given above.

- Inlet temperature of SOFC inlet ( $T_{FCin}$ ) has a negative impact on the propulsion system as increasing the  $T_{FCin}$  leads to the increase in mass flow rate required to adhere to the maximum fuel cell temperature constraint. This

increase in mass flow rate leads to higher fuel cell compressor work which reduces the gas power. It should be noted that increasing  $T_{FCin}$  will increase the fuel cell efficiency but the benefit is not enough to compensate for the increase in compressor work.

- Fuel cell parameters like fuel utilization and current have negligible impact, even at higher fuel cell power output.

### **Economics Sensitivity Analysis (No Emissions)**

- The system is most sensitive to changes in aircraft parameters like aircraft cost and interest rate compared to fuel cell parameters like fuel cell life, maintenance, etc. Among all the fuel cell parameters, fuel cell cost has the most impact on the system. For example, the sensitivity coefficient for aircraft cost, interest rate and fuel cell cost is 4.66%, 2.06% and 0.165% respectively for 1 MW power output.
- The sensitivity to all aircraft economic parameters is decreasing at higher fuel cell power because of the increase in the contribution of fuel cell in total cost and reduction in fuel consumption. The sensitivity coefficient for aircraft cost decreased from 4.66% for 1 MW power output to 1.41% for 4 MW power output.
- Sensitivity Analysis shows that the change in engine and aircraft cost needs to be minimized when the fuel cell is added from an economics perspective. An increase in fuel cell-related cost does not impact the economics as much as aircraft parameters, even for higher fuel cell power.

### **Economics Sensitivity Analysis (With Emissions)**

- Increasing the emission tax reduces the sensitivity for all parameters as the contribution of tax in total cost increases. The sensitivity coefficient for aircraft cost decreased from 4.66% for no emission case to 3.80% for future emission scenario (1 MW power output).
- The impact of emissions tax, even for future scenario i.e. the  $CO_2$  and  $NO_x$  tax of \$0.5/kg and \$90.5/kg respectively, is low on all the economic parameters. Hence, emissions have a low impact on the economics of the SOFC-GT hybrid.

### 11.3. LIMITATIONS

This section presents the limitations for the research done in this study. The research done in this project is a feasibility study and the aim of the study was to do a broad analysis rather than a detailed component level or conceptual design. Hence, the research has some limitations and they are as follows.

- The fuel cell model used in this study are 0D models and hence, there are multiple factors which has not been included in this study like:
  - Starting of the SOFC
  - Area considerations for the complete fuel cell
  - A heat exchanger model which can analyze both, Design and Off-Design conditions.

These factors will have a negative impact on the feasibility of the system as there may be requirements for changes in the operation in order to adhere to multiple constraints, leading to a decrease in efficiency, increase in complexity, weight, and costs.

- The fuel used for the analysis is hydrogen and no changes have been assumed in the engine.

However, multiple changes need to be made like changing fuel injectors, fuel heat exchangers, compressors, and other auxiliary systems which will have an impact on the cost and weight.

- SOFC is a low TRL technology when compared to other fuel cells like PEM. Hence, the technology needs more research and time to be able to become a reliable technology for Aerospace applications.

The increase in reliability may require sophisticated materials and robust auxiliary systems, leading to an increase in cost and complexity, leading to a negative impact on feasibility.

- The impact of the addition of weight on the TSFC because of fuel cell has not been analyzed in this study. The analysis has only been done from an economic perspective.

Nevertheless, an increase in weight will lead to an increase in drag and the thrust requirement if the payload had to be kept constant. But because of the scope of this study, this analysis has not been done.

- The reference engine used in this study is CFM-56-5B1, which is not among the latest generation of engines. Hence, the benefit shown in the TSFC and emissions would be lower for the current or future generations of engines. This is because of the modern engine usually has higher propulsive efficiency and hence, the relative increase due to fuel cell would be lower.

However, the trend for TSFC, core size, and cooling air reduction along with emissions would be the same.

- The  $NO_x$  emission model used in this study is based on the correlation and hence, does not analyze all the phenomena which will act in changing the emissions.
- The economic model developed uses multiple assumptions like:
  - No inflation
  - Financing through debt rather than a combination of debt and equity.
  - Linear pricing model.

The removal of these assumptions will lead to a reduction in required specific power compared to the results presented in this study. However, because of the complexity of the economic model and the scope of this study, these assumptions had to be considered.

#### 11.4. SCIENTIFIC CONTRIBUTION

This section presents the scientific contribution of this research project are as follows:

- **Impact of the addition of fuel cell on turbofan:** The study concludes that adding the fuel cell to turbofan will not provide the complete benefit of fuel cell and even leads to a drop in performance during the Design or Seal Level Static condition. The results show engine parameters like BPR, FPR, and cooling air requirements need to be changed in order to achieve the maximum benefit of the integrated system. Along with this, the impact of adding the fuel cell to a downsized engine has also been evaluated.

Past research has shown the impact of adding the fuel cell on the thermodynamic efficiency. But changing the parameters is important for a fair comparison as concluded by this study.

- **Required fuel cell specific power:** The research shows the required fuel cell specific power for different assumptions and conditions along with the impact of increasing the fuel cell power on the required specific power from an economics perspective.

Past research has only focused on the technical aspect of SOFC-GT hybrid, thermodynamic efficiency to be precise, but the addition of the weight of SOFC has a significant impact on the overall feasibility of the system as concluded in this research.

- **Methodology:** Multiple methodologies have been developed or optimized in this research. These methodologies can be used later on by other researchers to either complement this research or for the research on their own. The methodologies are as follows:

- Methodology to analyze the integrated system for constant Specific Thrust and at their most optimum point.

- Methodology to check the economic feasibility and calculate the required Specific Thrust of the complete fuel cell. This methodology has been adapted [75] but multiple changes for SOFC-GT hybrid and economic feasibility have been done.
- **Most important parameters:** Three different types of sensitivity analysis have been done in this study namely, technical, economics with emissions, and economics without emissions. The study presents the most important parameters to be studied from both, technical and economic perspectives, based upon the size of fuel cell added.

This will help the researchers in focusing future research on a conceptual design by keeping the impact of these parameters on the overall system.

## 11.5. RECOMMENDATIONS

Based upon the results above, the author will give the following recommendations.

### Future Analysis Recommendations

- An analysis can be done where the electrical power requirement of the aircraft is being completed by the fuel cell along with the part of power going into the shaft. It will eliminate the requirement of the whole bleed system along with the generator, hence reducing cost and weight.
- A Multidisciplinary Design Optimization can be developed where gas turbine and fuel cell parameters can be used as design variables in order to find the most optimum SOFC-GT hybrid propulsion system from TSFC and emissions perspective.
- An analysis for different propulsion system architectures like distributed propulsion and turbo-electric propulsion can also be done. The electrical power required to run the fans can be provided by the fuel cell.
- An analysis for different alternative fuels like methanol blended with hydrogen can be done. The SOFC would require reform in this case which will make the system heavier, costlier, and less efficient but a feasibility study can be done.
- An analysis for Proton Exchange Membrane or PEM fuel cell integrated with gas turbine can also be done where a high-pressure air from LPC can be used to run the PEM fuel cell. However, the PEM fuel cell is not as efficient as SOFC, and the heat output of the PEM fuel cell is not very high, the specific power is currently 10 times higher than the commercially available SOFC.

### Fuel Cell Model Recommendations

- One-dimensional Solid Oxide Fuel Cell model with area dependence can be used in order to better understand the rate of reactions, change in temperature and voltage along with concentrations along the fuel channel inside the fuel cell. It will help in maintaining the constraints.

- A more sophisticated heat exchanger model can be used to analyze the real exchange in heat between fuel cell byproducts and inlets of the fuel cell.
- Heat loss to surroundings can be considered in order to understand the impact of a fuel cell on its surroundings, especially if the fuel cell is placed in the fuselage.

#### **SOFC-GT Hybrid Model Recommendations**

- Gearbox can be considered for transferring power from the motor to the shaft.
- Cooling for a motor can be considered.
- Pressure loss during mixing of fuel cell byproducts and HPC air can be considered.
- A more thorough analysis of the impact of the reduction in core size or mass flow rate on the compressor and turbine efficiencies and static margins can be done.

#### **Emission Model Recommendations**

- A more sophisticated model can be used in order to calculate the emission at maximum take-off conditions.
- A more sophisticated model can be used to calculate the impact of steam addition and reduction in  $O_2$  concentration in the flow.
- A model to calculate the Global Warming Potential at different altitudes for  $NO_x$  and  $H_2O$  emissions can be implemented to better understand the impact and tax implications of these emissions.

#### **Economic Model Recommendations**

- Inflation can be considered for future study.
- A variable pricing model for fuel cell, engine, and aircraft cost can be considered.
- A variable pricing model for fuel price can be considered as well based upon the predictions of future price of the fuel in each year.
- Weighted Average Cost of Capital or WACC can be used in order to analyze the feasibility of an investment rather than using the debt as the medium to pay for aircraft.
- The Indirect Direct Operating Cost can be calculated by using the data from airlines.
- A model can be used to calculate the weight of the engine which incorporates the changes made to the engine when the fuel cell is added.

# BIBLIOGRAPHY

- [1] European Commission. *Reducing emissions from aviation*. Feb. 2017. URL: [https://ec.europa.eu/clima/policies/transport/aviation\\_en#tab-0-0](https://ec.europa.eu/clima/policies/transport/aviation_en#tab-0-0).
- [2] Department for Business, Energy & Industrial Strategy. *Greenhouse gas reporting: conversion factors 2019*. July 2020. URL: <https://www.gov.uk/government/publications/greenhouse-gas-reporting-conversion-factors-2019>.
- [3] International Civil Aviation Organization (ICAO). *Future of Aviation*. URL: <https://www.icao.int/Meetings/FutureOfAviation/Pages/default.aspx>.
- [4] Toru Hasegawa, Sijia Chen, and Lan Duong. *Effects of Novel Coronavirus (COVID-19) on Civil Aviation: Economic Impact Analysis*. Report. Aug. 2021. URL: [https://www.icao.int/sustainability/Documents/Covid-19/ICAO\\_coronavirus\\_Econ\\_Impact.pdf](https://www.icao.int/sustainability/Documents/Covid-19/ICAO_coronavirus_Econ_Impact.pdf).
- [5] U.S. Department of Energy. *Combined Heat and Power Technology Fact Sheet Series*. July 2016. URL: <https://www.energy.gov/sites/prod/files/2016/09/f33/CHP-Gas%5C%20Turbine.pdf>.
- [6] GE Aviation. *The GE9X Engine Explore The World's Largest Jet Engine*. 2019. URL: [https://www.ge.com/news/sites/default/files/2020-09/ge9x\\_engine\\_infographic.pdf](https://www.ge.com/news/sites/default/files/2020-09/ge9x_engine_infographic.pdf).
- [7] Jens Flottau. *Airbus Bids Adieu to A340, Postpones A350 Delivery*. Nov. 2011. URL: <https://aviationweek.com/airbus-bids-adieu-a340-postpones-a350-delivery>.
- [8] "A review of gas turbine engine with inter-stage turbine burner". In: *Progress in Aerospace Sciences* 121 (2020), p. 100695. ISSN: 0376-0421. URL: <https://doi.org/10.1016/j.paerosci.2020.100695>.
- [9] Kousuke Nishida, Toshimi Takagi, and Shinichi Kinoshita. "Analysis of entropy generation and exergy loss during combustion". In: *Proceedings of the Combustion Institute* 29.1 (2002), pp. 869–874. URL: [https://doi.org/10.1016/S1540-7489\(02\)80111-0](https://doi.org/10.1016/S1540-7489(02)80111-0).
- [10] Elena De la Rosa Blanco, Cesare Hall, and D Crichton. "Challenges in the silent aircraft engine design". In: *45th AIAA aerospace sciences meeting and exhibit*. 2007, p. 454. URL: <https://doi.org/10.2514/6.2007-454>.
- [11] Ralph Jansen et al. "Overview of NASA electrified aircraft propulsion (EAP) research for large subsonic transports". In: *53rd AIAA/SAE/ASEE Joint Propulsion Conference*. 2017, p. 4701. URL: <https://doi.org/10.2514/6.2017-4701>.
- [12] James L Felder. "NASA electric propulsion system studies". In: (2015). URL: [Avialable%20at%20https://ntrs.nasa.gov/citations/20160009274](https://ntrs.nasa.gov/citations/20160009274).

- [13] Jason Welstead and James L Felder. “Conceptual design of a single-aisle turboelectric commercial transport with fuselage boundary layer ingestion”. In: *54th AIAA aerospace sciences meeting*. 2016, p. 1027. URL: <https://doi.org/10.2514/6.2016-1027>.
- [14] Alan H Epstein and Steven M O’Flarity. “Considerations for reducing aviation’s CO<sub>2</sub> with aircraft electric propulsion”. In: *Journal of Propulsion and Power* 35.3 (2019), pp. 572–582. URL: <https://doi.org/10.2514/1.B37015>.
- [15] Meherwan P Boyce. *Gas turbine engineering handbook*. Elsevier, 2011. URL: <https://www.elsevier.com/books/gas-turbine-engineering-handbook/boyce/978-0-12-383842-1>.
- [16] Francesco S Mastropierro et al. “Modeling Geared Turbofan and Open Rotor Engine Performance for Year-2050 Long-Range and Short-Range Aircraft”. In: *Journal of Engineering for Gas Turbines and Power* 142.4 (2020). URL: <https://doi.org/10.1115/1.4045077>.
- [17] Scott W Ashcraft et al. “Review of propulsion technologies for N+ 3 subsonic vehicle concepts”. In: (2011). URL: <https://www.semanticscholar.org/paper/Review-of-Propulsion-Technologies-for-N%5C%2B3-Subsonic-Ashcraft-Padr%5C%C3%5C%B3n/c910510a90004b75506a0c5a781600b2df1e4ee0>.
- [18] Office of Energy Efficiency and Renewable Energy. *Comparison of Fuel Cell Technologies*. URL: <https://www.energy.gov/eere/fuelcells/comparison-fuel-cell-technologies>.
- [19] Haoyu Fang. “Challenges with the Ultimate Energy Density with Li-ion Batteries”. In: *IOP Conference Series: Earth and Environmental Science*. Vol. 781. 4. IOP Publishing, 2021, p. 042023. URL: <https://doi.org/10.1088/1755-1315/781/4/042023>.
- [20] UDL Intellectual Property. *Sky’s the limit — battery technologies for commercial electric air travel*. URL: <https://www.lexology.com/library/detail.aspx?g=efc951c8-6805-44e8-a729-3d98a75f9265>.
- [21] VS Kolosnitsyn and EV Karaseva. “Lithium-sulfur batteries: Problems and solutions”. In: *Russian Journal of Electrochemistry* 44.5 (2008), pp. 506–509. URL: <https://doi.org/10.1134/S1023193508050029>.
- [22] *GE90 Commercial Aircraft Engine*. URL: <https://www.geaviation.com/commercial-engines/ge90-engine>.
- [23] Dr. Frank Anton. *eAircraft: Hybrid-elektrische Antriebe für Luftfahrzeuge*. Sept. 2019. URL: [https://www.bbaa.de/fileadmin/user\\_upload/02-preis/02-02-preistraeger/newsletter-2019/02-2019-09/02\\_Siemens\\_Anton.pdf](https://www.bbaa.de/fileadmin/user_upload/02-preis/02-02-preistraeger/newsletter-2019/02-2019-09/02_Siemens_Anton.pdf).
- [24] Jens Palsson, Azra Selimovic, and Lars Sjunnesson. “Combined solid oxide fuel cell and gas turbine systems for efficient power and heat generation”. In: *Journal of power sources* 86.1-2 (2000), pp. 442–448. URL: [https://doi.org/10.1016/S0378-7753\(99\)00464-4](https://doi.org/10.1016/S0378-7753(99)00464-4).

- [25] Daniel F Waters, Lucas M Pratt, and Christopher P Cadou. “Gas Turbine/Solid Oxide Fuel Cell Hybrids for Aircraft Propulsion and Power”. In: *Journal of Propulsion and Power* (2021), pp. 1–14. URL: <https://doi.org/10.2514/1.B38026>.
- [26] Toyota. *Outline of the Mirai*. Nov. 2014. URL: [https://www.toyota-europe.com/download/cms/euen/Toyota%5C%20Mirai%5C%20FCV\\_Posters\\_LR\\_tcm-11-564265.pdf](https://www.toyota-europe.com/download/cms/euen/Toyota%5C%20Mirai%5C%20FCV_Posters_LR_tcm-11-564265.pdf).
- [27] National Aeronautics & Space Administration. *High Power Density Solid Oxide Fuel Cell*. URL: <https://ntrs-prod.s3.amazonaws.com/t2p/prod/t2media/tops/pdf/LEW-TOPS-120.pdf>.
- [28] Toshiaki Yamaguchi et al. “Evaluation of extruded cathode honeycomb monolith-supported SOFC under rapid start-up operation”. In: *Electrochimica Acta* 54.5 (2009), pp. 1478–1482. URL: <https://doi.org/10.1016/j.electacta.2008.09.029>.
- [29] Sakurambo. *Solid oxide fuel cell*. Oct. 2007. URL: [https://commons.wikimedia.org/wiki/File:Solid\\_oxide\\_fuel\\_cell.svg](https://commons.wikimedia.org/wiki/File:Solid_oxide_fuel_cell.svg).
- [30] Valentina Zaccaria. “SOFC degradation model for cyber-physical simulations and control of fuel cell gas turbine hybrid systems”. PhD thesis. University of Genoa, Apr. 2017. URL: <https://doi.org/10.13140/RG.2.2.35420.39046>.
- [31] James Larminie, Andrew Dicks, and Maurice S McDonald. *Fuel cell systems explained*. Vol. 2. J. Wiley Chichester, UK, 2003. URL: <https://doi.org/10.1002/9781118706992>.
- [32] Vinay Bhat. *Activation energy*. May 2006. URL: [https://commons.wikimedia.org/wiki/File:Activation\\_energy.svg](https://commons.wikimedia.org/wiki/File:Activation_energy.svg).
- [33] Joshua E Freeh, Joseph W Pratt, and Jacob Brouwer. “Development of a solid-oxide fuel cell/gas turbine hybrid system model for aerospace applications”. In: *Turbo Expo: Power for Land, Sea, and Air*. Vol. 41723. 2004, pp. 371–379. URL: <https://doi.org/10.1115/GT2004-53616>.
- [34] Stephanie Seidler et al. “Pressurized solid oxide fuel cells: Experimental studies and modeling”. In: *Journal of Power Sources* 196.17 (2011), pp. 7195–7202. URL: <https://doi.org/10.1016/j.jpowsour.2010.09.100>.
- [35] Daniel F Waters and Christopher P Cadou. “Engine-integrated solid oxide fuel cells for efficient electrical power generation on aircraft”. In: *Journal of Power Sources* 284 (2015), pp. 588–605. URL: <https://doi.org/10.2514/6.2014-1313>.
- [36] Ji Hye Yi and Tong Seop Kim. “Effects of fuel utilization on performance of SOFC/gas turbine combined power generation systems”. In: *Journal of Mechanical Science and Technology* 31.6 (2017), pp. 3091–3100. URL: <https://doi.org/10.1007/s12206-017-0553-y>.
- [37] Fuelcell.co.uk. *Molten Carbonate Fuel Cells (MCFC)*. URL: <http://www.fuelcell.co.uk/molten-carbonate-fuel-cells/>.
- [38] Hypoint. *Technical White paper*. URL: <https://docsend.com/view/t9aw2mk>.
- [39] Pacific Northwest National Laboratory. *Solid Oxide Fuel Cell (SOFC) Technology for Greener Airplanes*. 2010. URL: [https://www.energy.gov/sites/prod/files/2014/03/f12/aircraft\\_9\\_chick.pdf](https://www.energy.gov/sites/prod/files/2014/03/f12/aircraft_9_chick.pdf).

- [40] OC Onar and A Khaligh. *Alternative Energy in Power Electronics*. 2015. URL: <https://www.sciencedirect.com/book/9780124167148/alternative-energy-in-power-electronics>.
- [41] Olivier Bethoux. *Hydrogen fuel cell road vehicles: state of the art and perspective*. 2020. URL: <https://doi.org/10.3390/en13215843>.
- [42] Fandi Ning et al. “Flexible and lightweight fuel cell with high specific power density”. In: *ACS nano* 11.6 (2017), pp. 5982–5991. URL: <https://doi.org/10.1021/acsnano.7b01880>.
- [43] AF Massardo and F Lubelli. “Internal reforming solid oxide fuel cell-gas turbine combined cycles (IRSOFC-GT): Part A—Cell model and cycle thermodynamic analysis”. In: *J. Eng. Gas Turbines Power* 122.1 (2000), pp. 27–35. URL: <https://doi.org/10.1115/1.483187>.
- [44] Stefano Campanari. “Full load and part-load performance prediction for integrated SOFC and microturbine systems”. In: *J. Eng. Gas Turbines Power* 122.2 (2000), pp. 239–246. URL: <https://doi.org/10.1115/1.483201>.
- [45] SH Chan, HK Ho, and Y Tian. “Multi-level modeling of SOFC–gas turbine hybrid system”. In: *International Journal of Hydrogen Energy* 28.8 (2003), pp. 889–900. URL: [https://doi.org/10.1016/S0360-3199\(02\)00160-X](https://doi.org/10.1016/S0360-3199(02)00160-X).
- [46] F Calise et al. “Simulation and exergy analysis of a hybrid solid oxide fuel cell (SOFC)–gas turbine system”. In: *Energy* 31.15 (2006), pp. 3278–3299. URL: <https://doi.org/10.1016/j.energy.2006.03.006>.
- [47] P Costamagna, L Magistri, and AF Massardo. “Design and part-load performance of a hybrid system based on a solid oxide fuel cell reactor and a micro gas turbine”. In: *Journal of Power Sources* 96.2 (2001), pp. 352–368. URL: [https://doi.org/10.1016/S0378-7753\(00\)00668-6](https://doi.org/10.1016/S0378-7753(00)00668-6).
- [48] Yousef Haseli, Ibrahim Dincer, and GF Naterer. “Thermodynamic modeling of a gas turbine cycle combined with a solid oxide fuel cell”. In: *International Journal of hydrogen energy* 33.20 (2008), pp. 5811–5822. URL: <https://doi.org/10.1016/j.ijhydene.2008.05.036>.
- [49] Michael M Whiston et al. “Exergy and economic comparison between kW-scale hybrid and stand-alone solid oxide fuel cell systems”. In: *Journal of Power Sources* 353 (2017), pp. 152–166. URL: <https://doi.org/10.1016/j.jpowsour.2017.03.113>.
- [50] Christopher J Steffen Jr, Joshua E Freeh, and Louis M Larosiliere. “Solid oxide fuel cell/gas turbine hybrid cycle technology for auxiliary aerospace power”. In: *Turbo Expo: Power for Land, Sea, and Air*. Vol. 47284. 2005, pp. 253–260. URL: <https://doi.org/10.1115/GT2005-68619>.
- [51] Nicholas K Borer et al. “Design and Performance of a Hybrid-Electric Fuel Cell Flight Demonstration Concept”. In: *2018 Aviation Technology, Integration, and Operations Conference*. 2018, p. 3357. URL: <https://doi.org/10.2514/6.2018-3357>.

- [52] Tina Stoia, Shailesh Atreya, and Patrick O'Neil. "A Highly Efficient Solid Oxide Fuel Cell Power System for an All-Electric Commuter Airplane Flight Demonstrator". In: *54th AIAA Aerospace Sciences Meeting*. 2016, p. 1024. URL: <https://doi.org/10.2514/6.2016-1024>.
- [53] Keiichi Okai et al. "Effects of Fuel Type on Aircraft Electric Propulsion with SOFC/GT Hybrid Core". In: *53rd AIAA/SAE/ASEE joint propulsion conference*. 2017, p. 4957. URL: <https://doi.org/10.2514/6.2017-4957>.
- [54] Shaimaa Seyam, Ibrahim Dincer, and Martin Agelin-Chaab. "Novel hybrid aircraft propulsion systems using hydrogen, methane, methanol, ethanol and dimethyl ether as alternative fuels". In: *Energy Conversion and Management* 238 (2021), p. 114172. URL: <https://doi.org/10.1016/j.enconman.2021.114172>.
- [55] Patricia Aguiar, CS Adjiman, and Nigel P Brandon. "Anode-supported intermediate temperature direct internal reforming solid oxide fuel cell. I: model-based steady-state performance". In: *Journal of power sources* 138.1-2 (2004), pp. 120–136. URL: <https://doi.org/10.1016/j.jpowsour.2004.06.040>.
- [56] Eric S Hendricks and Justin S Gray. "p-cycle: A tool for efficient optimization of gas turbine engine cycles". In: *Aerospace* 6.8 (2019), p. 87. URL: <https://doi.org/10.3390/aerospace6080087>.
- [57] Southwest Research Institute. *Numerical Propulsion System Simulation (NPSS)*. Sept. 2021. URL: <https://www.swri.org/consortia/numerical-propulsion-system-simulation-npss>.
- [58] SH Chan, XJ Chen, and KA Khor. "An electrolyte model for ceramic oxygen generator and solid oxide fuel cell". In: *Journal of power sources* 111.2 (2002), pp. 320–328. URL: <https://doi.org/10.1115/1.4044696>.
- [59] Ying-Wei Kang et al. "A reduced 1D dynamic model of a planar direct internal reforming solid oxide fuel cell for system research". In: *Journal of Power Sources* 188.1 (2009), pp. 170–176. URL: <https://doi.org/10.1016/j.jpowsour.2008.11.073>.
- [60] Daniel F Waters, Lucas M Pratt, and Christopher P Cadou. "Gas Turbine/Solid Oxide Fuel Cell Hybrids for Aircraft Propulsion and Power". In: *Journal of Propulsion and Power* 37.3 (2021), pp. 349–361. URL: <https://doi.org/10.2514/1.B38026>.
- [61] Ramesh K Shah and Dusan P Sekulic. *Fundamentals of heat exchanger design*. John Wiley & Sons, 2003. URL: <https://doi.org/10.1002/9780470172605>.
- [62] NLR-Royal Netherlands Aerospace Centre. *Gas turbine simulation program*. URL: <https://www.gspteam.com/>.
- [63] Wikimedia Foundation. *CFM International CFM56*. Dec. 2021. URL: [https://en.wikipedia.org/wiki/CFM\\_International\\_CFM56](https://en.wikipedia.org/wiki/CFM_International_CFM56).

- [64] Wikimedia Commons. *File:Turbofan operation.svg* — Wikimedia Commons, the free media repository. [Online; accessed 21-March-2022]. 2022. URL: [https://commons.wikimedia.org/w/index.php?title=File:Turbofan\\_operation.svg&oldid=621387874%7D](https://commons.wikimedia.org/w/index.php?title=File:Turbofan_operation.svg&oldid=621387874%7D).
- [65] Nathan Meier. *Nate Meier's jet*. Sept. 2021. URL: <https://www.jet-engine.net/>.
- [66] International Civil Aviation Organization (ICAO). *ICAO aircraft engine emissions databank*. URL: <https://www.easa.europa.eu/domains/environment/icao-aircraft-engine-emissions-databank>.
- [67] Donato Aquaro and MJATE Pieve. "High temperature heat exchangers for power plants: Performance of advanced metallic recuperators". In: *Applied Thermal Engineering* 27.2-3 (2007), pp. 389–400. URL: [Avialable%20at%20https://doi.org/10.1016/j.applthermaleng.2006.07.030](https://doi.org/10.1016/j.applthermaleng.2006.07.030).
- [68] Cheryl L Bowman, James L Felder, and Ty V Marien. "Turbo-and hybrid-electrified aircraft propulsion concepts for commercial transport". In: *2018 AIAA/IEEE Electric Aircraft Technologies Symposium (EATS)*. IEEE. 2018, pp. 1–8. URL: <https://doi.org/10.2514/6.2018-4984>.
- [69] *Brayton cycle - pv - TS diagram*. URL: <https://www.nuclear-power.com/nuclear-engineering/thermodynamics/thermodynamic-cycles/brayton-cycle-gas-turbine-engine/brayton-cycle-pv-ts-diagram/>.
- [70] Abhijit Guha. "Optimum fan pressure ratio for bypass engines with separate or mixed exhaust streams". In: *Journal of Propulsion and Power* 17.5 (2001), pp. 1117–1122. URL: <https://doi.org/10.2514/2.5852>.
- [71] Fredrik Svensson, Anders Hasselrot, and Jana Moldanova. "Reduced environmental impact by lowered cruise altitude for liquid hydrogen-fuelled aircraft". In: *Aerospace Science and Technology* 8.4 (2004), pp. 307–320. URL: <https://doi.org/10.1016/j.ast.2004.02.004>.
- [72] Cecil Marek, Timothy Smith, and Krishna Kundu. "Low emission hydrogen combustors for gas turbines using lean direct injection". In: *41st AIAA/ASME/SAE/ASEE joint propulsion conference & exhibit*. 2005, p. 3776. URL: <https://doi.org/10.2514/6.2005-3776>.
- [73] Rui Xue et al. "Effect of steam addition on the flow field and NOx emissions for Jet-A in an aircraft combustor". In: *International Journal of Turbo & Jet-Engines* 33.4 (2016), pp. 381–393. URL: <https://doi.org/10.1515/tjj-2015-0041>.
- [74] Lloyd R Jenkinson et al. *Civil jet aircraft design*. Vol. 338. Arnold London, UK, 1999. URL: <https://doi.org/10.2514/4.473500>.
- [75] D Nalianda Karumbaiah. "Impact of environmental taxation policies on civil aviation—a techno-economic environmental risk assessment". In: (2012). URL: <http://dspace.lib.cranfield.ac.uk/handle/1826/8355>.

- [76] Battelle Memorial Institute. *Manufacturing Cost Analysis of 100 and 250 kW Fuel Cell Systems for Primary Power and Combined Heat and Power Applications*. 2016. URL: [https://www.energy.gov/sites/prod/files/2018/02/f49/fcto\\_battelle\\_mfg\\_cost\\_analysis\\_100\\_250kw\\_pp\\_chp\\_fc\\_systems\\_jan2017.pdf](https://www.energy.gov/sites/prod/files/2018/02/f49/fcto_battelle_mfg_cost_analysis_100_250kw_pp_chp_fc_systems_jan2017.pdf).
- [77] Isla Binnie. *EU reaches for hydrogen stars as economics shift*. Nov. 2021. URL: <https://www.reuters.com/business/sustainable-business/green-hydrogen-already-competitive-with-polluting-alternative-eus-von-der-leyen-2021-11-29/>.
- [78] European Commission. *Reducing emissions from aviation*. URL: [https://ec.europa.eu/clima/eu-action/transport-emissions/reducing-emissions-aviation\\_en](https://ec.europa.eu/clima/eu-action/transport-emissions/reducing-emissions-aviation_en).
- [79] Machine Design. *Latest developments in Superconducting Motors | Machine Design*. URL: <https://www.machinedesign.com/motors-drives/article/21828530/latest-developments-in-superconducting-motors>.
- [80] FlightDeckFriend. *How much does jet fuel cost?: The price of jet A1*. Jan. 2021. URL: <https://www.flightdeckfriend.com/ask-a-pilot/how-much-does-jet-fuel-cost/>.
- [81] Federal Aviation Agency. URL: [https://www.faa.gov/regulations\\_policies/policy\\_guidance/benefit\\_cost/media/econ-value-section-4-op-costs.pdf](https://www.faa.gov/regulations_policies/policy_guidance/benefit_cost/media/econ-value-section-4-op-costs.pdf).
- [82] Scott McCartney. *How much of your \$355 ticket is profit for airlines?* Feb. 2018. URL: <https://www.wsj.com/articles/how-much-of-your-355-ticket-is-profit-for-airlines-1518618600>.
- [83] Robert Tornabene et al. "Development of parametric mass and volume models for an aerospace SOFC/gas turbine hybrid system". In: *Turbo expo: power for land, sea, and air*. Vol. 47284. 2005, pp. 135–144. URL: <https://doi.org/10.1115/GT2005-68334>.
- [84] Siemens AG. URL: [https://www.bbaa.de/fileadmin/user\\_upload/02-preis/02-02-preistraeger/newsletter-2019/02-2019-09/02\\_Siemens\\_Anton.pdf](https://www.bbaa.de/fileadmin/user_upload/02-preis/02-02-preistraeger/newsletter-2019/02-2019-09/02_Siemens_Anton.pdf).
- [85] Christopher Winnefeld et al. "Modelling and designing cryogenic hydrogen tanks for future aircraft applications". In: *Energies* 11.1 (2018), p. 105. URL: <https://doi.org/10.3390/en11010105>.
- [86] *Environmental economics*. Apr. 2001. URL: <https://ec.europa.eu/environment/enveco/taxation/>.
- [87] PricewaterhouseCoopers. *Green deal monitor 4 - national or European Taxation of CO2 emissions?* URL: <https://www.pwc.nl/en/topics/sustainability/green-deal-monitor/green-deal-monitor-4.html>.



# A

## SOFC-GT HYBRID RESULTS (TECHNICAL ANALYSIS)

This section discusses the results for each station inside the turbofan when the fuel cell is added. Figure [A.1](#) shows the nomenclature and the station numbers for the SOFC-GT hybrid. It can be seen that fuel cell and motor has been added to the turbofan which led to the introduction of two new station numbers. Station 31 and 32 represents the entry and exit of the air and byproducts from the fuel cell respectively.

Table [A.2](#) and fig:SData for each station for Off-Design condition (Reference Engine) shows the data for each station presented in figure [A.1](#) for Design and Off-Design condition respectively. For station number 31 and 32, there is no result as there is no fuel cell.

Table [A.4](#) and [A.5](#) shows the data for station numbers for Design and Off-Design condition respectively when 1 MW of fuel cell power output. It should be noted that Static Pressure, Mach Number and Area has not been included as fuel cell area has not been considered in this study. The conceptual design of fuel cell is out of the scope of this study and hence, this data has not been used.

It can be seen that a fraction of air is going into the fuel cell at station 31 and byproducts are coming at a higher temperature from station 32. The mass of flow has also increased as the fuel is added to the fuel cell. The pressure remains eventhough there is a 10% pressure loss inside the fuel cell because of the fuel cell compressor as explained in section [5](#). It should also be noted that the temperature of the mixture at station 33, which is just before the combustion chamber, is higher than temperature at station 3 because of the addition of heat from the fuel cell. The temperature is even higher for Off Design condition as given in table [A.5](#) because of higher fraction of fuel cell byproducts.

Similar results can also be seen from table [A.6](#) and [A.7](#) shows the data for station numbers for Design and Off-Design condition respectively when 4 MW of fuel cell power output. The mass flow going into the fuel cell has increased and so does the temperature of station 33 because of the same reason presented above.

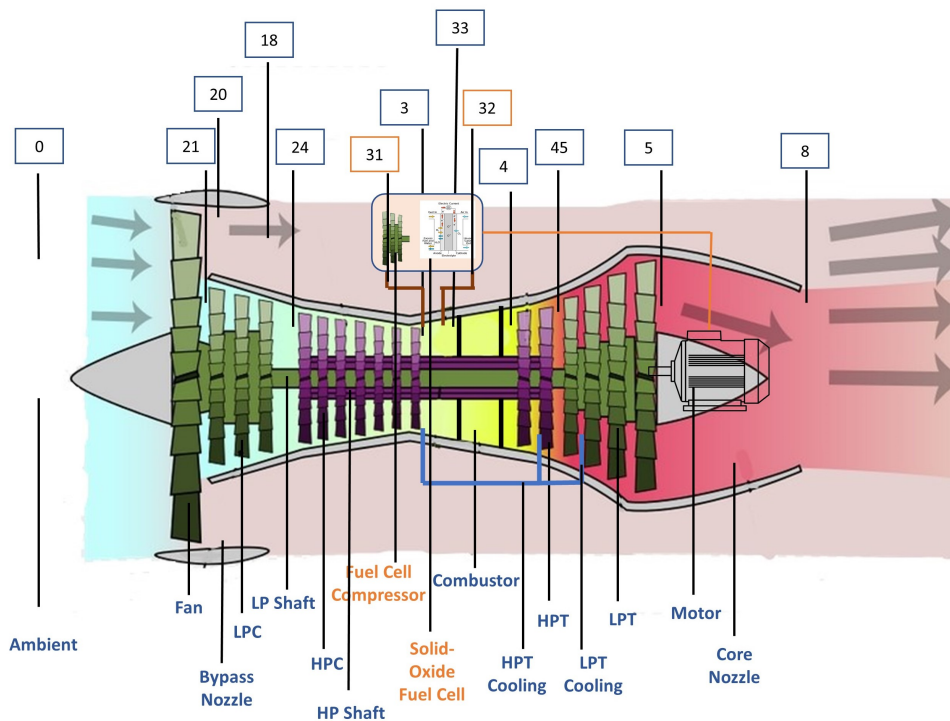


Figure A.1: SOFC-GT hybrid nomenclature and station numbers (Adapted from [64])

Station	Mass (kg/s)	Total Pressure (kPa)	Static Pressure (kPa)	Total Temperature (K)	Enthalpy (kJ/kg)	Mach No.	Area (m <sup>2</sup> )
0	396.80	97.72	97.72	286.17	-16.37	0.001	-
20	337.58	175.71	152.77	346.25	44.06	0.45	1.28
21	59.22	175.71	164.37	346.25	44.06	0.31	0.31
24	59.22	366.74	343.81	439.23	138.23	0.31	0.17
3	59.22	2904.31	2790.28	841.31	565.03	0.24	0.04
31	-	-	-	-	-	-	-
32	-	-	-	-	-	-	-
33	49.86	2904.31	2734.33	841.31	565.03	0.30	0.03
4	50.37	2747.48	2729.13	1722.37	559.32	0.10	0.12
45	59.73	817.97	769.73	1284.21	137.00	0.31	0.14
5	59.73	141.45	126.43	889.15	-357.82	0.41	0.51
8	59.73	139.93	97.71	889.15	-357.82	0.75	0.35
18	335.89	173.10	97.71	346.25	44.06	0.94	0.90

Figure A.2: Data for each station for Design condition (Reference Engine)

Station	Mass (kg/s)	Total Pressure (kPa)	Static Pressure (kPa)	Total Temperature (K)	Enthalpy (kJ/kg)	Mach No.	Area (m <sup>2</sup> )
0	144.04	33.03	21.66	244.46	-58.23	0.80	-
20	122.64	58.72	50.99	294.81	-7.69	0.45	1.28
21	21.39	58.72	54.95	294.81	-7.69	0.31	0.31
24	21.39	112.42	104.09	369.64	67.66	0.33	0.17
3	21.39	1069.11	1032.99	756.99	472.40	0.23	0.04
31	-	-	-	-	-	-	-
32	-	-	-	-	-	-	-
33	20.37	1069.11	999.24	756.99	472.40	0.32	0.03
4	20.51	1011.38	1004.77	1403.73	469.14	0.10	0.12
45	21.53	268.06	252.53	1056.92	67.22	0.30	0.14
5	21.53	42.26	37.01	707.97	-345.66	0.45	0.51
8	21.53	41.81	22.30	707.97	-345.66	1.00	0.35
18	122.03	57.84	30.55	294.81	-7.69	1.00	0.90

Figure A.3: Data for each station for Off-Design condition (Reference Engine)

Station	Mass (kg/s)	Total Pressure (kPa)	Static Pressure (kPa)	Total Temperature (K)	Enthalpy (kJ/kg)	Mach No.	Area (m <sup>2</sup> )
0	396.82	97.72	97.72	286.17	-16.37	0.00	-
20	339.73	173.76	151.07	345.01	42.82	0.45	1.30
21	57.10	173.76	162.54	345.01	42.82	0.31	0.30
24	57.10	366.74	343.81	439.22	138.22	0.31	0.16
3	57.10	2904.31	2790.28	841.29	565.01	0.24	0.04
31	2.12	2904.31	-	841.29	565.01	-	-
32	2.14	2904.31	-	974	125.60	-	-
33	48.06	2904.31	2734.33	847.8	565.01	0.30	0.02
4	48.56	2747.48	2729.14	1722.42	540.02	0.10	0.11
45	57.60	819.30	770.99	1284.91	120.76	0.31	0.13
5	57.60	147.24	131.62	897.05	-366.10	0.41	0.47
8	57.60	145.67	97.71	897.05	-366.10	0.79	0.32
18	338.03	171.17	97.71	345.01	42.82	0.93	0.91

Figure A.4: Data for each station for Design condition (1 MW fuel cell power output)

Station	Mass (kg/s)	Total Pressure (kPa)	Static Pressure (kPa)	Total Temperature (K)	Enthalpy (kJ/kg)	Mach No.	Area (m <sup>2</sup> )
0	145.19	33.03	21.66	244.46	-58.23	0.80	-
20	124.38	58.53	50.81	294.53	-7.97	0.45	1.30
21	20.81	58.53	54.75	294.53	-7.97	0.31	0.30
24	20.81	121.91	114.08	374.75	72.83	0.31	0.16
3	20.81	1067.42	1031.06	746.90	461.42	0.23	0.04
31	2.34	1067.42	-	746.90	461.42	-	-
32	2.36	1067.42	-	888.52	62.24	-	-
33	20.15	1067.42	1005.97	764.3	461.42	0.30	0.02
4	20.26	1009.78	1003.21	1331.20	412.31	0.10	0.11
45	20.94	266.09	250.99	1003.86	27.81	0.30	0.13
5	20.94	43.90	38.70	674.07	-358.09	0.43	0.47
8	20.94	43.43	23.14	674.07	-358.09	1.00	0.32
18	123.76	57.66	30.45	294.53	-7.97	1.00	0.91

Figure A.5: Data for each station for Off-Design condition (1 MW fuel cell power output)

Station	Mass (kg/s)	Total Pressure (kPa)	Static Pressure (kPa)	Total Temperature (K)	Enthalpy (kJ/kg)	Mach No.	Area (m <sup>2</sup> )
0	396.78	97.72	97.72	286.17	-16.37	0.00	-
20	345.78	169.86	147.67	342.51	40.29	0.45	1.35
21	51.00	169.86	158.89	342.51	40.29	0.31	0.27
24	51.00	366.74	343.81	439.20	138.20	0.31	0.14
3	51.00	2904.31	2790.28	841.25	564.97	0.24	0.03
31	8.48	2904.31	-	841.25	564.97	-	-
32	8.55	2904.31	-	974.12	124.80	-	-
33	42.98	2904.31	2734.33	879.62	564.97	0.30	0.02
4	43.39	2747.48	2729.15	1722.44	472.88	0.10	0.10
45	51.47	824.01	775.45	1287.23	64.39	0.31	0.12
5	51.47	165.03	147.55	919.99	-399.91	0.41	0.38
8	51.47	163.27	97.72	919.99	-399.91	0.90	0.25
18	344.05	167.33	97.72	342.51	40.29	0.91	0.95

Figure A.6: Data for each station for Design condition (4 MW fuel cell power output)

Station	Mass (kg/s)	Total Pressure (kPa)	Static Pressure (kPa)	Total Temperature (K)	Enthalpy (kJ/kg)	Mach No.	Area (m <sup>2</sup> )
0	148.41	33.03	21.66	244.46	-58.23	0.80	-
20	129.94	58.85	51.03	295.32	-7.17	0.46	1.35
21	18.47	58.85	55.29	295.32	-7.17	0.30	0.27
24	18.47	159.53	153.34	404.01	102.44	0.24	0.14
3	18.47	1015.12	978.18	729.15	442.19	0.23	0.03
31	9.39	1015.12	-	729.15	442.19	-	-
32	9.46	1015.12	-	871.71	43.27	-	-
33	18.39	1015.12	987.81	805.05	442.19	0.20	0.02
4	18.44	960.31	954.13	1155.43	236.35	0.10	0.10
45	18.58	255.27	241.79	873.27	-99.82	0.29	0.12
5	18.58	46.39	41.28	589.11	-423.81	0.42	0.38
8	18.58	45.89	24.39	589.11	-423.81	1.00	0.25
18	129.29	57.97	30.62	295.32	-7.17	1.00	0.95

Figure A.7: Data for each station for Off-Design condition (4 MW fuel cell power output)



# B

## FUEL WEIGHT CALCULATION (ECONOMIC ANALYSIS)

The appendix discusses the calculations for fuel weight which has been used in the Economic Analysis study. The study requires two types of fuel weight, one is the fuel weight per hour or the total fuel burn per hour as given in equation 10.10 and total fuel weight for the whole journey of the mission, as given in equations 10.3 and 10.2. The fuel burn per hour is given in equation B.1. The mass of fuel burn in Off-Design condition per second is taken directly from the technical analysis. A factor of 2 has also been included as Airbus A321 has two engines.

$$\frac{\text{Fuel Burn}}{\text{hour}} = 2 * \left( \frac{\text{Mass of fuel in Off-Design}}{\text{sec}} \right) * 3600 \quad (\text{B.1})$$

Equation B.2 shows the total fuel that aircraft carries during the mission. This includes the stock fuel as well which means that the aircraft has to carry a one hour flying worth of fuel along with the fuel for journey as per government regulations. The parameter  $\alpha$  includes the stock fuel and the fuel for different conditions like Take-off (Design condition), Top of climb and Approach. The value of the parameter is 0.2. It is calculated using the 1 hour worth of fuel along with other requirements mentioned above. Equation B.3 shows the calculation for flight time used in the equation B.2. The flight range is 5000 km [74] and flight speed at the given altitude is calculated to be 237 m/s or 853 km/hr.

$$\text{Total Fuel} = \frac{\text{Fuel Burn}}{\text{hour}} * \text{Flight time} * \alpha \quad (\text{B.2})$$

$$\text{Flight Time} = \frac{\text{Flight Range}}{\text{Flight speed}} \quad (\text{B.3})$$